UNBIASED EXPRESSION PROFILING IDENTIFIES A NOVEL NOTCH SIGNALING TARGET RND1 AS REGULATOR OF ANGIOGENESIS

Jing Du

Submitted in partial fulfillment of the
requirements for the degree of
Doctor of Philosophy
in the Graduate School of Arts and Sciences

COLUMBIA UNIVERSITY

2019

Abstract

Unbiased Expression Profiling Identifies A Novel Notch Signaling Target Rnd1 As Regulator Of Angiogenesis

Jing Du

Notch signaling controls normal and pathological angiogenesis through transcriptional regulation of a wide network of target genes. Despite intensive studies of the endothelial Notch function, a comprehensive list of Notch-regulated genes, especially direct transcriptional targets, has not been assembled in endothelial cells (ECs). Here we uncovered novel EC Notch targets that are rapidly regulated by Notch signaling using several unbiased *in vivo* and *in vitro* screening approaches that captured genes regulated within 6 hours or less of Notch signal activation. We used a gamma-secretase inhibitor in neonates to profile Notch targets in the brain endothelium using the RiboTag technique, allowing for isolation of endothelial specific mRNA from a complex tissue without disrupting cell-cell contact. We used two types of primary cultured endothelial cells to define ligand-specific Notch targets by tethered-ligand stimulation. The identified Notch targets were validated by determining their regulation within one to two hours of EGTA-mediated Notch activation. By comparing significantly regulated genes in each of the screens, we assembled a comprehensive database of potential Notch targets in endothelial cells. Of particular interest, we uncovered G protein pathway related genes as potential novel Notch targets. We focused on a novel candidate target passing selection criteria after all screens, a small GTPase RND1.

RND1(Rho GTPase1) regulates cytoskeleton arrangement through Rho and Ras signaling. *RND1* was validated as an endothelial Notch target in multiple endothelial cell types. In Human Umbilical Vein Endothelial Cells (HUVECs) we established angiogenic activity for RND1 that included regulation of cell migration towards VEGF and function in sprouting angiogenesis. We established that Notch and RND1 suppressed Ras activation but had no effects on Rho activation in HUVECs. These results demonstrate that RND1 expression is regulated by Notch signaling in endothelium and suggest that RND1 functions downstream of Notch in sprouting angiogenesis, revealing an unexplored role of endothelial Notch in regulating G protein pathways.

Table of Contents

List of Tables

List of Figures

Acknowledgements

I am grateful to a number of people who have helped, supported, and inspired me throughout my PhD Study. First of all, I would like to express my immense gratitude to my advisor and mentor, Dr. Jan Kitajewski, for the instruction, encouragement, and support during my study. You also have always been a role model for me in almost every aspect of my life and academics. I have developed into a better and more independent investigator through your training.

I am grateful to the members of my thesis committee: Dr. Peter Canoll, Dr. Iva Greenwald, Dr. Carrie Shawber, and Dr. Peter Sims for the support, detailed comments and constructive suggestions to this dissertation. It is potentially intimidating to have present one's work to such learned an accomplished individual, but you were always as friendly as you were incisive.

I would also like to thank the Cell Biology & Pathobiology Graduate program for giving me the opportunity to be here at Columbia University. I would like to give my special thanks to Dr. Ron Liem and Zaia Sivo, for providing the most educational and enjoyable environment that a student could possibly have. I would like to express my gratitude to the Physiology & Biophysics program in University of Illinois at Chicago, thank you all for being a second home in my PhD studies。

I am indebted to Dr. Bhairavi Swaminathan for being such an incredible partner on this project. You have devoted enormous time and effort to both bench work and in silicon analysis for this project, helped me in understanding the bioinformatic analysis, and assisted me in thesis writing. I would also like to thank Dr. Seock Won Youn for your

help with the functional analysis that greatly contributed to the development of the project. Dr. Reyhaan Chaudhri, thank you for your efforts in developing the tethered ligand assay.

This project cannot be done without the help from collaborators. I would like to thank Dr. Peter Sims, Dr. Huijuan Feng and Dr. Chaolin Zhang for your tremendous help and advice in the data analysis. I am grateful to Dr. Peter Canoll and the Canoll lab for graciously training me with the RiboTag IP technique, and I am truly benefited from your knowledge and guidance. Dr. Sarah Lutz, thank you for your help and instruction on brain dissection. I would also like to thank Dr. Henar Cuervo, for your generous help with tissue sectioning and your invaluable advice on this project. Dr. Raphael Kopan, thank you for the insights and advices that contributed significantly to the project.

I cannot thank you enough, my dear Kitajewski lab members, past and present, for your friendship, support and insight. I would like to give a special thank you to Dr. Naiche Adler for your tremendous help and advice on writing work. I would also like to thank members from Dr. Henar Cuervo lab and Dr. Dan Shaye lab, for being a huge support.

Lastly, my deepest gratitude goes to my family and friends for the love and care. Thank you, Brian Mao, for being both an incredible lab mate and an incredible friend. I am so grateful to have you accompanied on this long journey. Thank you, Di Yang, my beloved fiancé, I cannot accomplish all this without your love, care and support. Thank you, Dad and Mom, for always being proud and supportive of me. Words cannot express my gratefulness for all the sacrifice you have made to get to me where I am today. Thank you so much, I love you!

Chapter 1 Introduction

1.1 Angiogenesis

1.1.1 Mechanisms of blood vessel growth

The circulatory system develops by two distinct processes: vasculogenesis and angiogenesis. Vasculogenesis refers to the de novo formation of blood vessels, which occurs during early embryonic development when endothelial precursors differentiate and assemble into a primitive vascular labyrinth of small capillaries (Risau & Flamme, 1995). The vascular plexus then expands through a process referred to as angiogenesis and remodels into a highly organized vascular network composed of arteries, capillaries, and veins (Udan, Culver, & Dickinson, 2013). Angiogenesis is initiated when endothelial cells lining formed vessels are activated by pro-angiogenic signals. Local degradation of extracellular matrix allows "budding" of the activated endothelial cells from the existing vessels. These budding cells, called tip cells, lead new angiogenic sprouts and probe the environment for guidance cues. Following tip cells, stalk cells undergo proliferation and lumenization to support elongation of the angiogenic sprouts. Finally, the sprouts recruit mural cells such as pericytes and vascular smooth muscle cells, which serve to stabilize the newly formed vessel. This establishes a vascular network capable of delivering nutrients and oxygen through blood flow.

1.1.2 Anti-angiogenic therapy

Angiogenesis plays important role not only in mammalian embryogenesis, but also in physiological blood vessel formation after birth such as in menstrual cycle, pregnancy and wound healing(Carmeliet, 2003; Zygmunt, Herr, Munstedt, Lang, & Liang, 2003). Moreover, angiogenesis plays an important pathological role in diseases such as tumor growth, tumor metastasis, and retinopathies, which has stimulated intensive studies in anti-angiogenic therapy over the past decades(Mittal, Ebos, & Rini, 2014). Though there are a growing numbers of anti-angiogenic drugs, current anti-angiogenic therapies are often accompanied by side effects and drug resistance(Potente, Gerhardt, & Carmeliet, 2011). Development of improved anti-angiogenic therapies requires a deeper understanding of the molecular mechanisms controlling angiogenesis, identification of novel targets, and advances in new technologies.

1.2 Notch signaling pathway

1.2.1 Overview of the Notch signaling pathway

Notch signaling is an evolutionarily conserved pathway that is involved in cell fate determination and differentiation. Notch genes were originally discovered in *Drosophila melanogaster*, where mosaic loss of function mutations result in notches in the wing margins (Mohr, 1919). Notch signaling often controls binary cell-fate decisions between

cells that are initially equivalent, a process known as lateral inhibition. In *C. elegans*, for example, the Notch family member LIN-12 mediates interactions between two equivalent progenitor cells to induce one cell to adopt anchor cell (AC) and the other to adopt ventral uterine precursor cell (VU) cell fate(Greenwald, Sternberg, & Horvitz, 1983).

Mammals have four Notch genes, NOTCH1, NOTCH2, NOTCH3, and NOTCH4, which act as transmembrane receptors. Notch proteins are normally cleaved in the Golgi prior Site-1 (S1) by a furin-like convertase to membrane insertion, and appear at the cell surface as heterodimers consisting of N-terminal EGF-like repeats and LNR repeats non-covalently bound to the C-terminal heterodimerization (HD) region, transmembrane domain, and Notch intracellular domain (NICD) (Hambleton et al., 2004). NICD contains a RAM domain, seven ankyrin repeats (ANK), a transcription activation domain (TAD) and PEST domain. Notch ligands are also single-pass transmembrane proteins. Five Notch ligands in mammals are divided into two classes, the Delta-like-class ligands Delta-like1, Delta-like3, and Delta-like4 (abbreviated DLL1, DLL3, and DLL4) and Jagged-class ligands Jagged1 and Jagged2 (abbreviated JAG1 and JAG2)(Shawber & Kitajewski, 2004) (Figure 1-1). Notch ligands share a conserved degenerate EGF-like repeat, the DSL domain, which is required for ligand binding to Notch, followed by an EGF-like repeats. Notch EGF-like repeats 11 and 12 and the DSL domain of ligands are necessary for Notch interaction with all ligands (Kangsamaksin et al., 2015) .

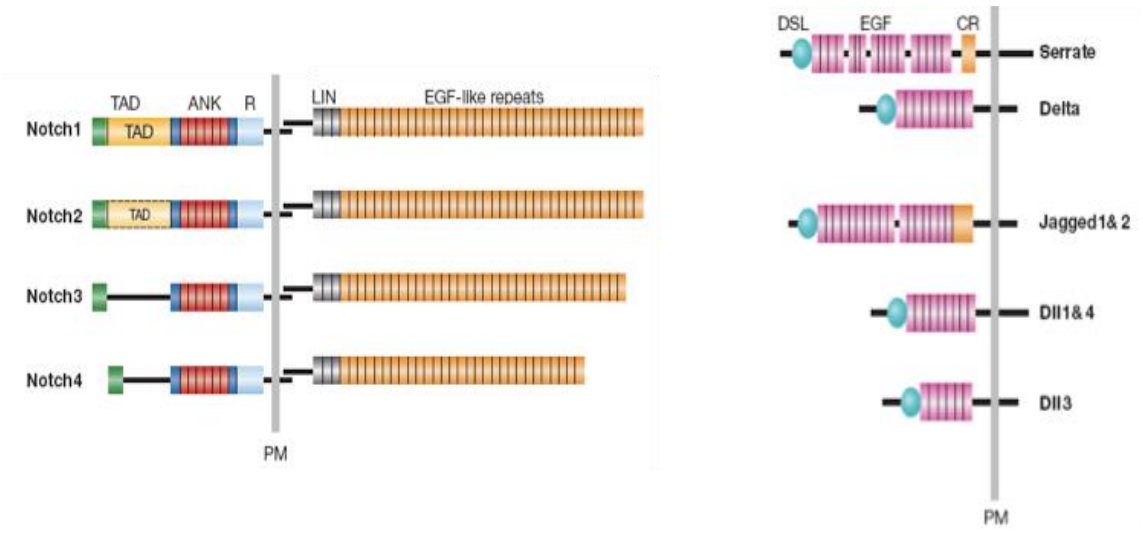

Figure 1-1. Mammalian Notch receptors and ligands

(Figure from Bray, 2006(Bray, 2006)) All Notch proteins (Notch1-4) are structurally similar. The extracellular domain of Notch contains multiple EGF like repeats and cysteine-rich LIN-12/Notch repeats. Following the transmembrane domains, the Notch intracellular domain (NICD) contains a RAM domain, seven ankyrin repeats (ANK), a transcription activation domain (TAD) and PEST domain. Notch ligands are divided into Delta-like and Jagged classes. Notch ligands share the DSL domain, which is required for ligand binding to Notch, and the EGF-like repeats. Jagged have 16 EGF-like repeats , and DLLs contain 8 or fewer. The Jagged proteins have additional cysteine-rich region, but the Delta-like protein do not(Kangsamaksin et al., 2015).

1.2.2 Signaling cascade and primary downstream targets of Notch

Notch proteins are cleaved in the Golgi at site 1 (S1) by a furin-like convertase to generate a non-covalently associated heterodimer at the cell surface. Notch signaling is initiated when a membrane-bound Notch ligand binds to a Notch protein's extracellular domain presented on the membrane of an adjacent cell, allowing successive cleavages by ADAM

metalloproteases at extracellular cleavage site 2 (S2) and by γ-secretase at intramembrane cleavage site 3 (S3). The S3 cleavage event releases the NICD that translocate to the nucleus. NICD heterodimerizes with the DNA binding protein CSL (also known as RBPJ, CBF1, RBPjκ, Su(H), Lag-1). Activated NICD displaces co-repressors off CSL and subsequently recruits co-activators such as Mastermind-like, SKIP, and histone acetyltransferases (HATs) to form a fully functional transcriptional activation complex that activates transcription of genes containing RBP-J binding sites (Borggrefe & Oswald, 2009; Fiuza & Arias, 2007).

Hairy and Enhancer-of-split-related (HES) basic helix-loop-helix (bHLH) transcription factors such as grl and Her in zebrafish, or Hey and Hes in mammals, represent the initially identified effectors of Notch signals during development, these have been referred to as "canonical Notch targets" (Iso, Kedes, & Hamamori, 2003). Hes and Hey are transcriptional repressors, and can suppress expression of downstream target genes such as tissue-specific transcriptional activators. Thus, these genes directly affect cell fate decisions as primary Notch effectors(Fischer, Schumacher, Maier, Sendtner, & Gessler, 2004) (Figure 1-2). Several lines of evidence have suggested these genes are direct Notch targets, that is, they are bound directly by NICD complexes which regulate their expression. For example, the promoters of *Hes1, Hes5* and *Hes7* as well as *Hey1, Hey2* and can be activated by a constitutive active form of Notch1 and in co-culture experiments with Notch-ligand expressing cells, these genes were elevated in the presence of cycloheximide, an inhibitor of protein synthesis, to exclude secondary effects, reviewed in (Borggrefe &

Oswald, 2009). Therefore, in mammals, *Hey* and *Hes* are the best characterized primary Notch targets.

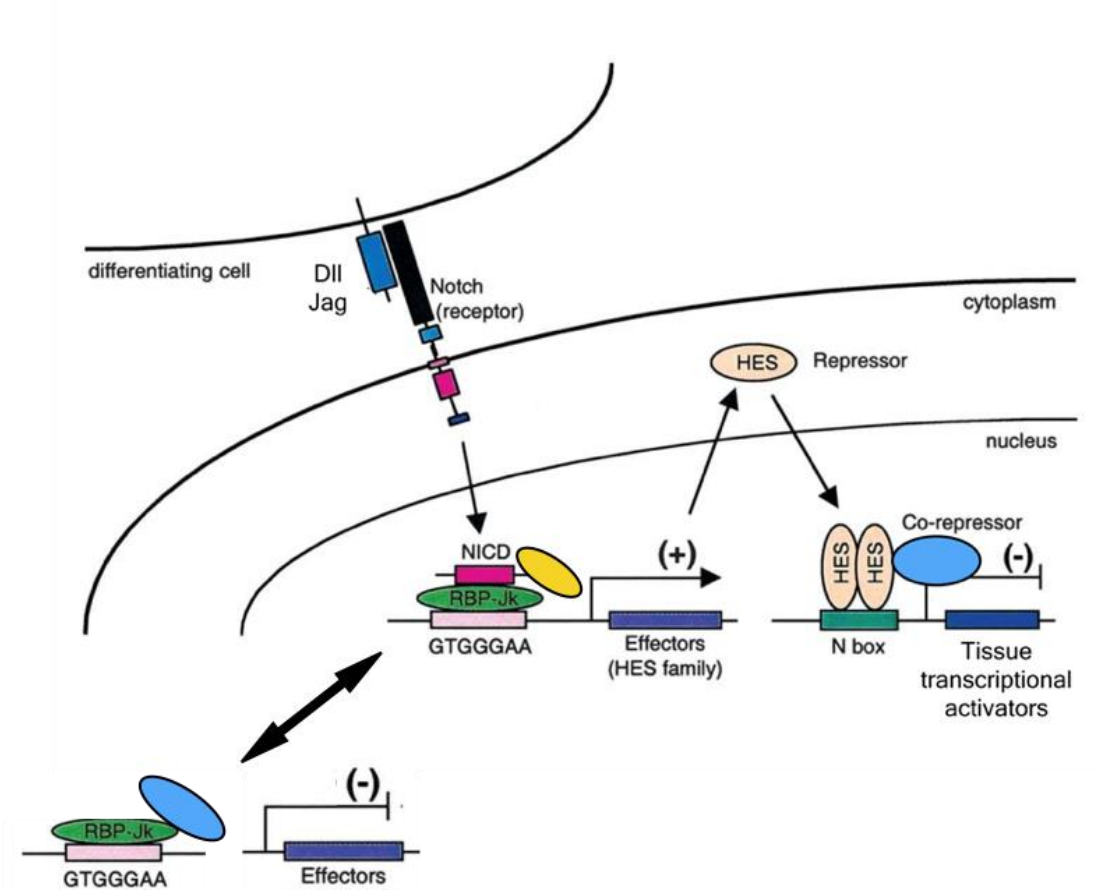

Figure 1-2. Notch signaling cascade

(Figure adapted from Iso, 2003(Iso, Kedes, et al., 2003)) The ligand binding to receptor induces cleavage events that free the Notch intracellular domain (NICD). NICD translocates to the nucleus, where it forms a complex with RBPJ protein, replacing co-repressor (CoR) complex (blue) with co-activator complex (yellow) and leading to activation of Notch direct target, with HES used here as an example. HES is a basic helix-loop-helix (bHLH) transcriptional repressor, and suppresses expression of downstream target genes.

Multiple other Notch targets have been identified as primary Notch targets. The transcription factor *GATA3*(Fang et al., 2007), a master regulator for T cell development

has been shown as a direct Notch target gene. In cancer cells, multiple genes such as *C-myc* (Fang et al., 2007; Palomero, Lim, et al., 2006; Wang et al., 2014; Weng et al., 2006) and cyclinD1(Ronchini & Capobianco, 2001) have been implicated as direct Notch targets. The targets were identified through a variety of screening approaches in immortalized cell lines such as T-ALL (T-cell Acute Lymphoblasts Leukemia) cells, and we will review and discuss those approaches in the last section of Chapter I.

1.3 Notch signaling in angiogenesis

1.3.1 Function of Notch signaling in vessel formation

Notch has been shown to play critical role in angiogenesis by regulating the fate of endothelial cells during this process. In mice, deficiency in a variety of Notch signaling components, including *Notch1, Notch1* and *Notch4, Jagged1, Dll1, Dll4, Hey1/Hey2*, and presenilin genes, *PS1* and *PS2*, results in embryonic lethality with vascular remodeling defects(Iso, Hamamori, & Kedes, 2003). In human, mutations in the *JAG1* and *NOTCH3* genes cause the autosomal dominant disorders Alagille syndrome and CADASIL, respectively, which present with abnormal vascular phenotypes. Mutations in the NOTCH1 receptor are associated with several types of cardiac disease(Penton, Leonard, & Spinner, 2012).

1.3.2 Notch effectors in endothelial cells

Notch plays an important role in regulating endothelial cell behaviors. Aside from the best-characterized primary Notch targets *HEY* and *HES*, a fairly limited description of other primary Notch targets have been defined in endothelial cells. *NRARP*, a direct Notch target, has been shown to coordinate endothelial Notch and Wnt signaling to control vessel density in angiogenesis (Lamar et al., 2001; Phng et al., 2009). EphrinB2 has been shown as direct Notch target that regulates arterial-venous differentiation (Iso et al., 2006). In quiescent endothelial cells, alarmin interleukin-33 (*IL*-33) was identified as direct target of Notch signaling (Sundlisaeter et al., 2012). *Slug*, a snail family protein, was shown as a direct Notch target in endothelial cells and regulate the endothelial-to-mesenchymal transition (EMT) (Niessen et al., 2008).

In endothelial cells, an important group of Notch effectors that have been well studied are VEGF receptors. Notch signaling inhibits *KDR* gene expression (VEGFR2) via HEY2 induction, and induces *FLT1* expression (VEGFR1) through unknown mechanisms. (Funahashi et al., 2010; Harrington et al., 2008; Suchting et al., 2007; Taylor, 2002). In cultured endothelial cells when Notch is constitutively activated, the Notch/CSL complex binds the VEGFR3 promoter and activates its transcription, leading to a higher level of VEGFR3 (*FLT4* gene) and increasing responsiveness to VEGF-C (Shawber et al., 2007).

1.3.3 Tip/Stalk cell model

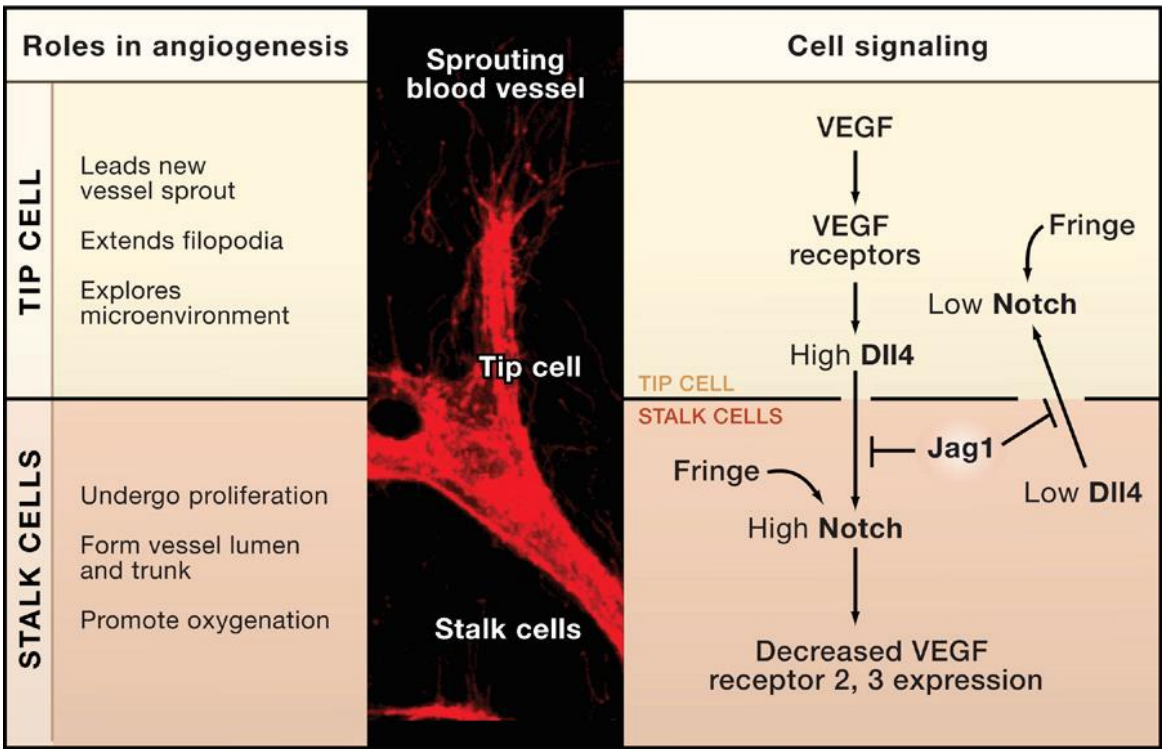

Figure 1-3. Tip/Stalk cell selection in sprouting angiogenesis

(Figure from Suchting, 2009)(Suchting & Eichmann, 2009) A sprouting blood vessel is composed of a tip cell and stalk cells. VEGF induces expression of Dll4 in tip cells, which activates Notch in the stalk cells to reduce VEGF receptor expression level. In the stalk cells, the glycosyltransferase Fringe modifies Notch to enhance Dll4-Notch signaling, but to reduce Jag1-Notch signaling. Stalk cell express low level of Dll4. Fringe modification allows Jag1 to antagonize Dll4-Notch signaling from stalk cell to tip cell.

Current models of angiogenesis center on the interplay between tip and stalk cells, two endothelial cell fates that can rapidly interchange during the process of angiogenesis. Determination of tip cell versus stalk cell fate occurs through Notch signaling and Vascular Endothelial Growth Factor (VEGF) signaling (Figure 1-3). Hypoxia triggers the release of angiogenic factors, the best characterized of which is VEGFA. VEGFA activates quiescent endothelial cells in preexisting vessels by interacting with VEGF receptor 2 (VEGFR2) on the cell, and induces expression of Notch ligand Dll4 in activated cells. These cells become

tip cells, with chemotactic filopodial extensions, and are highly migratory towards environmental cues such as VEGFA. Dll4 in tip cells binds to Notch in adjacent cells and activates Notch signaling in adjacent endothelial cells. Notch signaling then suppresses tip cell fate in neighboring cells by regulating expression of VEGF receptors, including downregulation of VEGFR2, which plays a primary role in endothelial cell activation and migration, and upregulation of soluble variant of VEGFR-1, a high affinity, low activity receptor in endothelial cells that can act as a competitive inhibitor of VEGFA/VEGFR2 interaction. The net result is that Notch signaling in the tip cell decreases sensitivity to VEGF-A in adjacent endothelial cells, which adopt a distinct cell fate to become the stalk cells that proliferate, lumenize and form the body of the sprout (Tung, Tattersall, & Kitajewski, 2012). This model is supported by the phenotypes of endothelial loss of Dll4 or inhibition of Notch-Dll4 interaction, which result in de-repression of tip cell fate and excess sprouting(Hellstrom et al., 2007; Kangsamaksin et al., 2015; Lobov et al., 2007).

The role of Jag1 remains more controversial and elusive. Loss of Jag1 or inhibition of Notch-Jag1 interaction produces hypo-sprouting phenotype; that is reduced angiogenic sprouting. This has been interpreted as opposite roles of Jag1 and Dll4 in angiogenesis(Benedito et al., 2009; Kangsamaksin et al., 2015). It has been suggested that Jag1 enhances angiogenesis by antagonizing the effects of Dll4-mediated Notch signaling during sprouting angiogenesis. Unlike Dll4, which is primarily expressed in tip cells, Jag1 is strongly expressed in stalk cells and can antagonize Dll4-Notch signaling to maintain an activate tip cell phenotype that is responsive to VEGF(Benedito et al., 2009; Suchting & Eichmann, 2009). The antagonistic interaction between Dll4 and Jagged1 in endothelial

cells is mediated by glucosaminyl transferases of the Fringe family, which regulates posttranslational modification of Notch [38]. Fringe modification promotes Notch activation by Dll4 and reduces Notch activation by Jag1, thereby enabling Jag1 to antagonize Dll4-Notch activation through competitive binding activity(Benedito et al., 2009; LeBon, Lee, Sprinzak, Jafar-Nejad, & Elowitz, 2014). Other studies have showed that JAG-specific $N1_{10-24}$ decoy, reduced the mRNA levels of Notch targets *HEY1, HEYL, HES1*, suggesting Jag1 is an activating ligand. Jagged inhibition has been shown to reduce angiogenesis while also reducing Notch signaling using Jagged-specific Notch decoy, suggesting that Jagged-Notch may promote Notch signaling in a manner that is pro-angiogenic(Kangsamaksin et al., 2015).

Some studies have offered important revisions to this classical tip/stalk model. For instance, tip and stalk cell identities may shift between neighboring cells in a dynamic fashion, suggesting that in stalk cells, Notch-mediated suppression of tip cell fate and VEGF responsiveness is unstable and frequently overcome (Jakobsson et al., 2010). It's been reported that deacetylase SIRT1 acts as an intrinsic negative regulator of Notch in stalk cells(Guarani et al., 2011). Additionally, evidence indicated that multiple cells constitute the tip of developing blood vessels, suggesting a non-binary Notch signaling scenario between tip and stalk cells (Pelton, Wright, Leitges, & Bautch, 2014).

1.4 Unbiased screening studies of Notch targets

1.4.1 Unbiased screening studies in ECs

In endothelial cells, multiple primary Notch targets such as *HEY, HES, NRARP*, EphrinB2, and *FLT4* as well as non-direct effectors, including VEGFRs have been defined to play important roles mediating the function of Notch in angiogenesis. Those studies provide valuable insights of the regulatory mechanism of Notch in endothelial cells, leading to establishment of elegant models such as the role of Notch in regulation of tip/stalk cell selection during sprouting angiogenesis.

However, most of the studies on EC Notch targets were carried out on a gene-by-gene basis. Very limited insights have been gained of the EC Notch regulation networks through global, unbiased screening studies. Harrington LS et al. performed a cDNA microarray-based screening study in HUVECs with retroviral-mediated Dll4 overexpression (OE) (Harrington et al., 2008). This type of study compares steady-state level changes in Notch target gene expression to control. Data from the screens indicated that Dll4 down-regulates VEGFR2*(KDR)*, and up-regulates VEGFR1(*FLT1*) and sVEGFR1 (s*FLT1*). While this provided important insights into the network of Dll4-Notch regulation, the method of study did not allow identification of primary/direct response genes following Dll4-Notch activation. Another limitation of the study is that retroviral-mediated ligand OE can lead to both Notch activation and potential cis-inhibition of Notch, and thus was not the most physiological relevant approach of Notch activation.

1.4.2 Unbiased screening studies in other cell types

A number of studies have utilized different approaches to profile Notch targets in T-acute lymphoblastic leukemia(T-ALL) cell lines and other cancers cells.

The ability to identify direct Notch transcriptional targets was greatly facilitated by the establishment of the chromatin immunoprecipitation (ChIP) assay coupled with next generation sequencing (ChIP-Seq). The development of ChIP-grade anti-Notch and anti-RBPJ antibodies provided the ability to verify the direct interaction between the Notch complex and endogenous target gene loci. Most of the ChIP or ChIP-seq studies have been limited to T-ALL and other cancers where Notch is constitutively active (Palomero, McKenna, et al., 2006; Wang et al., 2011) or to immortalized cell culture systems where Notch activation was achieved (Castel et al., 2013; Krejci & Bray, 2007).

Recently, a new technique termed Split DamID (SpDamID) was developed by the Kopan group, allowing differentiation between monomeric and dimeric Notch binding sites(Hass et al., 2015). In this technique, DNA methylase (DAM) is split into two halves, and each halve is fused to one components of the Notch transcriptional complex. Methyltransferase activity is reconstituted at Notch complex formation sites, complex-bound DNA is methylated, and bound sites are detected via digestion with a methylation-sensitive enzyme DpnI. The technique was used in mK4 cells and successfully identified genomic sites bound by Notch monomer and dimer, as a complementary approach to ChIP-seq.

Despite revealing physical interaction between Notch/CSL and a target gene locus, an important limitation to ChIP and SpDamID is that Notch/CSL binding does not always indicate that a particular locus is expressed(Wang et al., 2011). Another limitation is that the short half-life of the active NICD has made it difficult to determine the genomic locations bound by endogenous Notch transcriptional complexes operating at physiological levels(Hass et al., 2015).

Another common approach for identifying direct and canonical Notch targets is via the use gamma secretase inhibitor (GSI), which provides a method for rapidly modulating Notch signaling. GSI inhibits the gamma secretase-dependent S3 cleavage that releases the Notch intracellular domain from the Notch extracellular domain. Cells treated with GSI causes reduction of NICD and accumulate a pool of membrane-tethered NOTCH. Upon washout of GSI, this pool of partially processed receptors is rapidly cleaved by gamma-secretase, allowing for precisely timed NOTCH activation(Bailis et al., 2013). A GSI washout assay in combination with RNA Seq or ChIP-Seq was used to profile Notch targets regarding T cell leukemia in several studies. Direct Notch target genes were identified as transcripts whose expression level rebound between 4 hours to 72 hours after GSI wash out and was insensitive to cycloheximide treatment(Liefke et al., 2010; Wang et al., 2014; Wang et al., 2011; Weng et al., 2006).

Despite being widely used to modulate Notch signaling, GSI is not a Notch-specific inhibitor and can target other signaling events. It is important to consider that the results

of the GSI-based screen could also be caused by its effect on other gamma-secretase substrates such as VEGFR1(Haapasalo & Kovacs, 2011).

Collectively, even though multiple approaches have been taken to identify target genes of Notch signaling, the majority of the studies were done in cancer cells and other immortalized cell lines and not physiologically relevant cells. In addition, each of those approaches has its limitations and one should not solely rely on a single screen, but utilize multiple approaches collectively to identify the common targets.

1.4.3 Techniques to profile cell-type specific gene expression *in vivo*

Most of the studies on Notch target identification *in vivo* were carried out on a gene-by-gene base, and the full repertoire of Notch target genes *in vivo* is poorly understood. Multiple components of the Notch signaling pathway were identified through classical forward genetic screens conducted in *Drosophila* (Artavanis-Tsakonas, Rand, & Lake, 1999; Bray, 2006) but these studies are difficult to be directly translate to mammalian endothelial cells. In mammals, genome-wide screening of genes in specific cell types *in vivo* have typically been performed through ChIP-Seq, RNA-Seq or Single-Cell RNA-Seq on isolated cells from the complex tissue. Those approaches face one major challenge: by physically isolating cells of interest from complex tissue, gene expression can change during experiments and hence the measured gene expression profile may not represent the gene expression profile when they were in an intact tissue. This is especially true in the

context of Notch signaling that relies on cell-cell contact, where physical disruption of tissue may alter the gene expression.

To overcome the limitation of physical cell isolation-based approaches, a recently developed approach was designed whereby an epitope-tagged ribosomal protein is expressed in a specific population of cells in the mouse. The epitope-tagged ribosomal protein incorporates into the ribosome in a cell type of interest. The ribosome, when incorporated into polysomes, can be affinity-purified from tissue lysate for mRNA extraction and analysis (detailed scheme will be discussed in Chapter 3). In one RiboTag model, a mouse line was made to conditionally express an EGFP-tagged rpL10a, a 60S ribosomal protein. However, the limitation of this system is that the Lox-Stop-Lox-EGFP-rpL10a cassette is inserted into the Rosa26 allele, so that protein is expressed from exogenous alleles and must compete with the endogenous rpL10a for ribosome occupancy(Zhou et al., 2013). The problem was solved with the creation of another knock-in mouse line termed RiboTag. RiboTag is a knock-in mouse line that express HA tagged rpL22 protein from the endogenous allele to replace the wildtype rpL22 by Cre-mediated recombination(Sanz et al., 2009).

RiboTag has several major advantages over other technologies that define expressed genes in specific mammalian cell types. First, the RiboTag approach provides the information that is closest to gene expression profile in an intact tissue, because changes gene expression or mRNA levels does not proceed after tissue lysis. Moreover, these methods allow analysis of the ‘translatome'—ribosome-associated mRNA— which represents

genes that are actively being translated and serves as a better predictor of the proteome than the transcriptome does.

The technique has been applied to multiple systems both *in vivo* and *in vitro*(Gonzalez et al., 2014; Lesiak, Brodsky, & Neumaier, 2015; Sanz et al., 2013; Sanz et al., 2009; Shigeoka et al., 2016). A recent study carried out a RiboTag based screens on mouse retinal ECs at different postnatal stages of angiogenesis. However, this system has not yet been used to profile specific signaling pathway in any tissues.

1.5 Summary, hypothesis and working strategy

Notch signaling controls developmental and physiological angiogenesis and contributes to pathological angiogenesis through regulation of target genes that then produce proteins that carry out elements of Notch function. Thus, identifying Notch downstream effectors and uncovering their roles in angiogenesis are critical to understanding regulatory mechanism of Notch in angiogenesis. Although many insights were provided of Notch targets by previous studies, the short list of established endothelial Notch targets, especially the primary target genes, does not account for the full range of Notch responses.

A comprehensive list of Notch effectors, especially the primary targets of Notch, has not been assembled in endothelial cells, nor do we know much about the functions of different Notch targets in angiogenesis. In addition, only very limited knowledge of Notch regulation landscape have been gleaned through unbiased *in vivo* screenings.

Thus, we hypothesized that novel endothelial Notch primary and/or rapid target genes will be uncovered using unbiased and physiologically relevant screening approaches. We therefore set out to establish a comprehensive understanding of genome-wide response of Notch using both *in vivo* and *in vitro* studies. Through combining these screens, we aim to identify high-confidence novel primary targets of Notch that are important in regulating endothelial behavior. The knowledge gained from those novel Notch targets will contribute to a better understanding of the transcriptional regulation mechanism of Notch signaling in angiogenesis. (Figure 1-4)

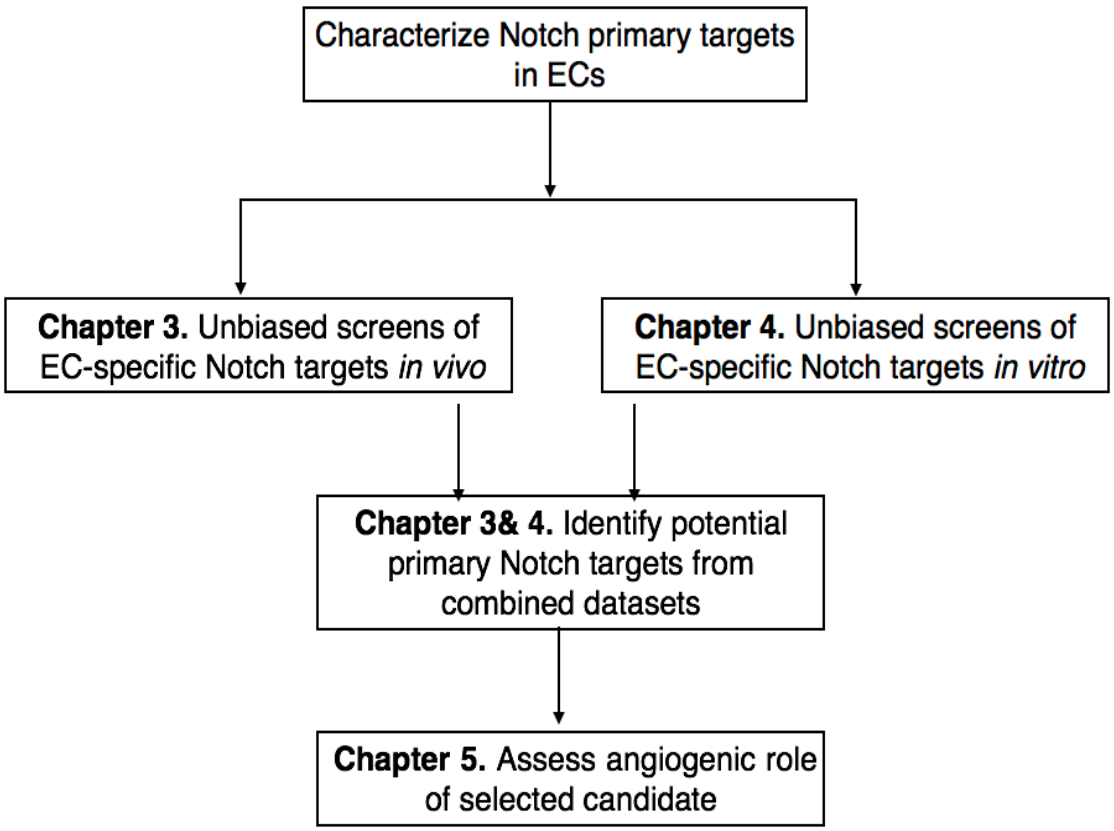

Figure 1-4. Project working strategy

Chapter 2 Materials and Methods

2.1 Cell culture

Primary cells and cell lines:

Human Umbilical Vein Endothelial Cells (HUVECs) were isolated from human umbilical cords following established protocols(Jaffe, Nachman, Becker, & Minick, 1973). The cells used in experimental replicates were isolated from different donors. Cells were grown in EGM^{TM}-2 Endothelial Cells Growth Media (Lonza) (every supplement from the bullet kit was added except for Hydrocortisone) on cell culture dish coated with rat tail type I collagen (Corning). The HUVEC cells used in experiments were passage five or lower.

Human Retina Microvasculature Endothelial Cells (HRECs) were purchased from Cell System. Cells were maintained on fibronectin (Sigma) coated plates (Millipore) and in EGM^{TM}-2 Endothelial Cells Growth Media (Lonza). Cells used for experiments were up to passage 8.

Human Dermal Microvasculature Endothelial Cells (HDECs) were purchased from American Type Culture Collection (ATCC). Cells were grown in EGM^{TM}-2MV Microvasculature Endothelial Cell Growth Media (Lonza) on rat tail type I collagen coated plate. Cells used in experiments were passage 5 or lower.

293T cells were acquired from ATCC and maintained in High Glucose DMEM (Gibco) with 10% Heat Inactivated- Fetal Bovine Serum (HI-FBS) and 1X antibiotics penicillin-streptomycin.

D551 human skin fibroblasts were purchased from ATCC and maintained in EMEM (Gibco) with 10% HI-FBS and 1X penicillin-streptomycin.

Mouse Lewis Lung Carcinoma (LLC) cell line was acquired from ATCC and maintained in High Glucose DMEM (Gibco) with 10% HI- FBS and 1X penicillin-streptomycin.

Lentivirus-mediated stable expression of constructs in primary cells

To perform stable knockdown and overexpression studies in primary cells, a lentiviral infection system was utilized. For lentiviral gene transfer, lentiviral vector pLKO.1 was used for shRNA knockdown and pCCL was utilized for overexpression studies. 293T cells were calcium phosphase mediated-transfected with the following combination of plasmids: 3 μg of pVSVG, 5μg of pMDLg/pRRE, 2.5μg of pRSV-Rev, and 10μg of pCCL/pLKO vector encoding genes of interest. Transfected 293T cells were allowed to produce lentivirus for 48 hours and the supernatant was collected, filtered through 0.45μm filter and then added onto the target primary cells. Single round of infection was performed. The primary cells were allowed to express shRNA or overexpression constructs for at least 48 hours before experiments. We have tested 5 different shRNAs to knockdown human Rnd1, all acquired from Sigma (TRCN0000047433-47437).

siRNA transfection for transient knockdown in primary cells

DharmaFECT™ Transfection system (Dharmacon) was utilized to perform transient knockdown based on the instruction manual. In separate tubes, SiRNA or DhamraFECT4 reagent were diluted with serum free media. After 5-minute incubation, siRNA and DharmaFECT4 reagents were mixed together followed by 20-minute incubation in room temperature. Reagents were mixed with antibiotic-free media and transfected into targets cell. Primary cells were incubated for 24-72 hours for RNA analysis, and 48-96 hours for protein analysis. Functional assays were performed in 48-72 hours. SiRNA used to knockdown human *RND1* in HUVECs is ON-TARGETplus siRNA from Dharmacon J-008929-05. Non-targeting control is D-001810-10-05. SiRNA was used at final concentration of 25nM for all the functional studies.

Tethered Ligand Assay (TLA)

Extracellular domains of human DLL4 fused to Fc (Final concentration 10μg/ml, 10171-H02H, Sin Biologicals Inc.), JAG1-Fc (Final concentration 40μg/ml, 11648-H02H, Sino Biologicals Inc.), or IgG-Fc control proteins (Final concentration 10μg/ml, 10702-HNAH, Sino Biologicals Inc.) was mixed with Fibronectin (Final concentration 10 μg/ml Sigma. Coating was performed by incubating plates with 100 μl/well of 24-well plate of the above proteins suspended in PBS at room temperature or at 4 ^{o}C overnight, then washing the plates with PBS prior to adding cells and media. Primary ECs were seeded into 80%-90% confluency on top of the coated plate. RNA was collected from the plate 6 hours after seeding the cells. For the experiments with HUVECs, each experiment consisted of cells from a different isolate (biological replicates), while the experiments from HRECs were

obtained from three frozen batches from a single commercially purchased vial Cell Systems (technical replicates).

EDTA/EGTA Notch activation assay

Primary ECs plated to 70% confluency were treated with Gamma Secretase Inhibitor (GSI) compound E (ALX-270-415-c250, Enzo Life Sciences) at 200nM O/N to inhibit endogenous Notch signaling. The following day, cells were washed with PBS 2X and were treated with 1xPBS supplemented with 10mM EGTA or EDTA for 15 minutes at 37ºC. After 15 minutes incubation, the PBS was replaced with fresh EGM2 (if cell detached, supernatant was collected, spin down, resuspended with fresh media and placed back to the same plate). Start time was established as the moment that EGTA was added, and RNA was collected at different time points from 30 minutes up to 4 hours. For the CpE treatment group, 500 nM of CpE were supplemented to PBS wash solution, EGTA treatment solution, as well as fresh EGM2 media after EGTA treatment. HRECs used in the RNA seq experiment were obtained from three frozen batches from a single commercially purchased vial Cell Systems (technical replicates).

Co-culture Notch reporter assay

HeLa cells were transfected with either pCRIII-JAG1-FLAG, pCRIII-Dll4-FLAG or pCRIII-GFP-FLAG. HUVECs were transfected with pGL3.11CSL-Luc(containing 11 repeats of a CSL-responsive element) and pGL3.Renilla-luc housekeeping plasmid. Lipofection was mediated using lipofectamine 2000 (Thermo Fisher Scientific) as per

manufacturer's instructions. 24 hours after Lipofection, two types of cells were co-cultured at 1:1 ratio in HUVEC media overnight. Cells were then lysed, and luciferase activity was measured using the Dual-Luciferase Reporter Assay System (Promega Corporation), as per manufactures' instructions.

MTT viability assay

HUVECs cells were plated at the same number among cell lines in triplicate in 96-well plates, and the viability of HUVECs were measured at 24, 48, 72, and 96 hour time point using MTT (3-(4,5-Dimethylthiazol-2-yl)-2,5-Diphenyltetrazolium Bromide) (Sigma). Briefly, at each time point, 100 μL of fresh medium were changed and 10 μL of 12mM MTT were added into each well. After 4 hours of incubation at 37 ^{o}C, 25 μL of medium were removed, and 50 μL of DMSO were added and mixed thoroughly. Following 10 minutes incubation at 37 ^{o}C , each sample was read absorbance at 570 nM with microplate reader.

EdU assay

HUVEC proliferation was measured using Click-iT EdU Imaging Kits (Invitrogen) following the manufacturer instruction. Briefly, cells were cultured with EdU working solution to get labeled. Cells were then fixed, permeabilized, and subjected to EdU detection and DNA staining. Imaging and quantification were performed using Celigo Imaging Cytometry (Nexcelom Biosciences). Data was presented as % of (EdU positive cells / by total DAPI positive cells).

Endothelial monolayer wounding (scratch) assay

HUVECs were seeded at confluency in 24-well plates. After incubation overnight, the confluent cell monolayer was scratched with 200 μl pipet tips across the diameter of each well. Floating cells were gently washed off with 1XPBS and fresh media were replaced. Pictures were taken at every 3 hours at 10X within the same area until the scratch was completely closed. Contrast between the cellular area and the scratch was enhanced, and the open wound area was measured by Image J as described in an established protocol (Kees Straatman, 2008).

Boyden chamber transwell migration assay

HUVECs were serum starved in starvation medium (EBM2 + 0.5%FBS) overnight. $1X10^5$ cells per well (24-well format) HUVECs were seeded in triplicate in collagen coated insert of 8 μm pore size transwell chamber (BD Falcon) with 400ul/well serum free media for 3 hours. Following starvation, 1.2 mL of serum free media supplemented with stimulant (50ng/ml hVEGFA from R&D 293-VE, 100ng/ml hSDF1 from R&D 350-NS-010, 1μM S1P from Enzo Life Sciences BML-SL140) was placed in the lower transwell chamber. Cells were allowed to migrate for 6 hours towards lower chamber stimulant, followed by fixation of the cells with 4%PFA for 15 minutes and 10 minutes incubation of 0.1% crystal violet to stain the cells. Cells from top of the membrane insert were wiped and cleaned with cotton swab and the migrated cells at the bottom of insert were imaged at 10X . Cell migration were measured by quantifying area covered by cells and dividing by total area of the image using ImageJ (3 different areas per well, 3 wells per sample).

Fibrin Beads Sprouting Assay (FIBA)

HUVEC cells were incubated with cytodex3 collagen-coated dextran bead at a ratio of 400 cells/bead for 4 hours in EGM-2 with gentle agitation every 20 minutes. The HUVEC coated beads were then placed on TC-treated dishes in EGM-2 media overnight. Following day, beads were washed with EGM 3X and embedded at a density of 150 beads/500ul within a fibrin clot composed of 3mg/mL fibrinogen (Sigma-Aldrich), 0.15 TIU/mL aprotinin (Sigma-Aldrich) and 0.625 U/mL thrombin (Sigma-Aldrich) in 24-well plate. Once the gel was polymerized, $1X10^5$ D551 fibroblast was resuspended in 1 ml EGM-2 media and were seeded on top of the gel for each well. Media was changed every other day and sprouting can be observed from day 2-day 3 until day 7. To quantify the assay, sprouts number and length were measured using 5 low power (5X) image from each well, for a total of between 50-100 beads per group.

G-Lisa RhoA and Ras activation assay

Assays were performed using RhoA (Cytoskeleton, BK124), and Ras (Cytoskeleton BK131) G-Lisa Activation Assay Kit. HUVECs were serum starved in EBM2 with 1% serum overnight and serum-free (EBM2) for additional 3 hours the following day. The cells were then stimulated with 100 ng/ml hEGF (Sigma-Aldrich E9644) to activate Ras for 5-10 minutes or 50 nM Thrombin (Enzyme Research Laboratories HT1002a) to activate RhoA for 2-5 minutes. Cell lysates were harvested and snap frozen. The lysates were added to plates containing RhoA/Ras GTP binding proteins linked to the wells. Inactive GDP-bound protein was washed out during washing steps and the active GTP-

bound form of RhoA/Ras was then detected with specific antibodies. G-Lisa assay was performed based on manufacture recommendations and signal is measured at 490 nm absorbance using microplate reader.

cDNA library creation and quantitative PCR

RNA was isolated from cultured cells using RNeasy Kit (Qiagen). RNA was reversed transcribed to cDNA using the Verso cDNA synthesis kit (Fischer Scientific), all according to manufacturer specifications. Quantitative Real Time PCR(qRT-PCR) was performed using SYBR Green master mix (Applied Biosystem) and primers specific to genes of interest (Table 2-1). Mean threshold cycle number (Ct) were determined of each gene and compared to the mean Ct of housekeeping gene beta actin.

Table 2-1. Primer sequence for qRT-PCR gene expression analysis

Gene Symbol	Species	Forward Primer (5'-3')	Reverse Primer (5'-3')
ACTB	Human/Mouse	CGAGGCCCAGAGCAAGAGAG	CTCGTAGATGGGCACAGTGTG
HEY1	Human	ATCTGCTAAGCTAGAAAAAGCCG	GTGCGCGTCAAAGTAACCT
HEY2	Human	GCCCGCCCTTGTCAGTATC	CCAGGGTCGGTAAGGTTTATTG
HES1	Human	CCTGTCATCCCCGTCTACAC	CACATGGAGTCCGCCGTAA
NRARP	Human	TCAACGTGAACTCGTTCGGG	ACTTCGCCTTGGTGATGAGAT
RND1	Human	CTATCCAGAGACCTATGTGCC	CGGACATTATCGTAGTAGGGAG
RND2	Human	TCCTGATTCTGATGCTGTGCTC	ATTGGGGCAGAACTCTTGAGTC
RND3	Human	GACAGTGTCCTCAAAAAGTGGAAA	CTGGCGTCTGCCTGTGATT
GUCY1B3	Human	ACGACCACCTTGCTACCATC	TGGATTTGTTGTGCCACTGT
RAPGEF5	Human	CTTAGTCATCTCCAAATCCCTCG	AGATCCCAAGTGTTCATTCCC
RGS4	Human	TTCATCTCAGTCCAGGCAAC	GGAATCCTTCTCCATCAGGTTG
ARHGEF17	Human	CCTGCCTTTCTCAAGTTCCTAG	GTCCTCAGGTGTATGCTTCAG
F2RL1	Human	GTGATTGGCAGTTTGGGTCT	CTGCATGGGATACACCACAG
ARHGAP24	Human	TTAGCCTCAACTCCTTTCATCC	CAGACGGTTCCCATATCTCTTC
Hey1	Mouse	GCGCGGACGAGAATGGAAA	TCAGGTGATCCACAGTCATCTG
Hey2	Mouse	AAGCGCCCTTGTGAGGAAAC	GGTAGTTGTCGGTGAATTGGAC
Hes1	Mouse	CCAGCCAGTGTCAACACG	AATGCCGGGAGCTATCTTTCT
Nrarp	Mouse	AAGCTGTTGGTCAAGTTCGGA	CGCACACCGAGGTAGTTGG
Rnd1	Mouse	CAGTTGGGCGCAGAAATCTAC	TGGGCTAGACTTGTTCAGACA

2.2 Mouse experiments

DAPT administration in postnatal animals

For postnatal studies, the RiboTag mouse was bred to the endothelial specific *Cdh5CreER^{T2}* driver line to obtain *Rpl22HA/HA;Cdh5CreER^{T2}* (RiboTagEC) mice. Cre recombination was induced through oral gavage of mother at P1(postnatal day1, the first day that a litter was discovered was considered postnatal day 0) , P2, P3 with 0.25mg

tamoxifen/kg body weight dissolved in corn oil. On P6-P8, 100mg/kg DAPT (N-[N-(3,5-Difluorophenacetyl-L-alanyl)]-S-phenylglycinet-ButylEster;Calbiochem,565770) dissolved in 10% ethanol and 90% corn oil was subcutaneously injected at 10 μl/g bodyweight. Control mice were injected with vehicle only. 6 hours after injection, treated mice were sacrificed for follow-up studies.

RiboTag studies

Mice were sacrificed with tissues quickly removed, weight and snap frozen in liquid nitrogen. Frozen tissue was placed in pre-chilled homogenizer containing Homogenizing Buffer+ (Homogenizing Buffer/HB: 10mM Tris pH8, 10mM Tris pH7, 50mM NaCl, 15mM $MgCl_2$, 1mM DTT, 0.5% Triton, 100 μg/ml Cyclohexamide; Homogenizing Buffer+: for every 1ml , supplemented HB with 12μl Superase Inhibitor (SUPERase-IN, Invitrogen AM2696), 12 μl turbo DNase (Invitrogen AM2238), and 10 μl Protease Inhibitor (Thermo Scientific 78430)) to create a 5% weight/volume homogenate using the homogenizer and G27 needles. Tissues such as heart and retina were homogenized using RNase-free stainless-steel beads kit (Green kit, Next Advance) and the bullet blender at a spin speed 6-8 for 30 seconds-1minute (Next advance).

After tissue was completely homogenized, sample is then centrifuged at 10,000 rpm for 10 minutes at 4 ^oC. The supernatant was collected and 1:200 anti- HA antibody (ab9118, Abcam) was added to the sample, which is then rotated at 4^oC for 4 hours. Prior to the end of incubation, Dyna Protein A magnetic beads (10001D, Invitrogen) were collected from stock solution (300μl of stock solution of beads/1ml supernatant) and were equilibrate in

Homogenizing Buffer for 1 hour at 4ºC. The antibody-homogenate sample was then transferred to the beads and rotated overnight in the cold room.

The following day, magnetic beads were collected from the sample and washed with wash buffer（Wash Buffer: for every 1ml, supplement HB with 6μl SUPERase inhibitor, 6μl turbo DNase, and 5μl Protease Inhibitor）, 3X 10 minutes at 4ºC. After final wash was removed, 300μl of RLT reagent supplemented with Beta-Mercaptoethanol (10μl/ml) from the Qiagen RNeasy mini prep kit was then added to the beads, incubate for 5minuts at RT and collected. The collection step was repeated once by adding another 300 μl of RLT buffer to the same beads, and followed by purifying RNA using Qiagen RNeasy mini kit.

Tumor studies

For tumor studies, the RiboTag mice were bred to *Cdh5CreER*^{T2} line and *DNMAML-GFP* flox mouse line (*DNMAML1-GFP* has a *loxP*-flanked transcriptional STOP cassette upstream of a *DNMAML1-GFP* fusion protein, from Warren Pear, University of Pennsylvania) to obtain *Cdh5CreERT2;Rpl22HA/HA;DNMAMLflox/+* mouse line. *Cdh5CreER*^{T2}*;Rpl22*$^{HA/HA}$ mice were used as control. At 5 weeks, mice were intraperitoneal injected with 100 μl of 20mg/ml tamoxifen dissolved in corn oil for 5 days in a row to induce Cre recombination. At 6 weeks, mice were subcutaneously implanted with 5X10^5 Mouse Lewis Lung Carcinoma (LLC) cells suspended in PBS in the lower left flank. Tumor growth was monitored by caliper measurement and was harvested at day 14.

Immunofluorescence Studies

Tissues were fixed in 4% PFA overnight, and dehydrated in 30% sucrose solution until tissues sank to the tube bottom before embedding into OCT and snap frozen in Isopentane mixed with dry ice. Frozen tissue was sectioned (5μm for tumor, 10 μm for brain) and stored in -20^{o}C. Slides were warmed in room temperature and post fixed in cold acetone for 3 minutes. A hydrophobic pen was used to circle around the tissue sections. The sections were then blocked for 1 hour at room temperature in the blocking solution containing 3% bovine serum albumin (BSA) and 2% serum from which species the secondary antibody was made. Then slides were incubated with primary antibody at 4^{o}C overnight followed by secondary antibody for 30 minutes. Slides were then mounted with VECTASHIELD mounting media containing DAPI.

2.3 RNA sequencing and statistics

RNA sequencing and data analysis

RNA quantity and integrity were measured by Bio-analyzer and TAPE station (Agilent) before RNA sequencing. The sequencing conditions for TLA HUVEC samples, RiboTag brain and tumor studies were ~30 million SE read depth with 100-base fragments on the TruSeq platform in the Sulzberger Columbia Genome Center. Conditions for Tethered ligand assay HREC samples and EGTA assay samples were ~30 million PE reads with 150 base-paired fragments using the services of Novogene corporation.

Raw reads from the HUVEC and HRECs were mapped to the Human database (ENSEMBL/GRCh38) using STAR (version 2.5.0a) and processed with Samtools (version 1.4.1). The counts obtained by FeatureCounts were analyzed by DESeq2 to identify differentially expressed genes.

Reads from IP-ribosomes were aligned with the mouse rRNA reads with Bowtie2 to remove the contamination of the ribosomal RNA reads from the mRNA reads. Next, these reads were mapped to the mouse transcriptome Mouse: (UCSC/mm10) using STAR aligner and processed with Samtools to generate bam files. The *bam* files were processed to obtain raw counts by FeatureCounts, that generated a table of counts for each gene in the genome. These raw counts were normalized and then tested for differential gene expression using DESeq2. The normalized counts were scaled to log scale and were used to generate the Principal Component Analysis (PCA) and the Volcano plots using DESeq2. PCA is a statistic procedure that uses an orthogonal transformation to summarize features and important patterns (Lever et al, 2017). Volcano plot is a type of scatter plot that is used to identify changes in large data sets. .

Statistics

Analysis and statistics of RNA-seq results will be discussed in details in the following chapters. For other experiments, unless otherwise noted, two-way Analysis of variance (ANOVA) with Bonferroni post-hoc analysis was performed on all quantified data to determine significant differences between groups. The statistical tests were analyzed in GraphPad Prism software. P values less than 0.05 were considered statistically

significant. If a p-value is less than 0.05 it is flagged with one star (*). If a p-value is less than 0.01 it is flagged with two stars (**). If a p-value is less than 0.001 it is flagged with three stars (***). Unless otherwise noted, experiments were repeated at least three times.

Chapter 3 An *in-vivo* screen for Notch regulated genes in the endothelium of mice using RiboTag technology

3.1 Strategy and Rationale

Little is known about the primary transcriptional events of Notch activation in endothelial cells, especially from an intact animal. One difficulty faced by previous studies of Notch signaling lies in the difficulty in achieving tight temporal control of Notch activation or inhibition by *in vivo* genetic tools, which can take many hours or even days to recombine and either build up or deplete relevant Notch modulatory proteins. This imprecision makes it difficult to resolve primary transcriptional events *in vivo*, because the transcriptional profile of Notch modulation will contain Notch targets, feedback inhibitors, downstream secondary and tertiary effectors, and signatures of broadly changed differentiation states. We have overcome these difficulties by using a small molecule pharmacological Notch inhibitor, DAPT, which rapidly and effectively downregulates Notch signaling in mice(Dovey et al., 2001). This approach reduces the specificity of transcriptional response due to non-Notch targets, but can be timed precisely and is effective in mice. We will address specificity concerns with experiments in subsequent chapters.

Most methods of mRNA isolation from a specific cell type (i.e. endothelial cells) in a complex tissue to study cell type specific gene regulatory events involve tissue digestion and disruption. We have optimized the use of the RiboTag technology to isolate

endothelial-specific transcriptional profiles without disrupting the cell-cell contacts critical for Notch signaling.

We hypothesize that Notch signaling activates transcription of critical known and unknown angiogenic effectors *in vivo* and that discovery of novel Notch effectors will elucidate the unknown mechanism(s) of Notch regulations in angiogenesis. We further hypothesize that by screening preferentially for genes that respond rapidly, within six hours of Notch inhibition, to Notch signaling in endothelium, we will enrich for direct Notch targets and effectors. Therefore, we carried out an *in vivo* unbiased screening of Notch signaling targets using the RiboTag technique, focusing on transcriptional events occurring rapidly after dosage with Notch inhibitor DAPT.

3.1.1 Neonatal brain as a model of angiogenesis

The vertebrate central nervous system (CNS) is comprised of the brain, spinal cord, and retina, which are heavily vascularized tissue, to meet oxygen and glucose demands. Vascularization in mouse starts with vessel formation in the mesenchyme ventral to the neural tube at around E7.5-8.5(Ruhrberg & Bautch, 2013). This is followed by sprouting angiogenesis that invades the CNS to form the CNS vessel network during embryonic development and postnatal stages (Tata, Ruhrberg, & Fantin, 2015). The most intensively studied CNS angiogenesis model has been the perinatal mouse retina, which has contributed vastly to our understanding of postnatal blood vessel growth in the CNS(Hofmann & Luisa Iruela-Arispe, 2007). The mouse embryonic brain, including

hindbrain and brain, has also been used to study CNS vascularization(Vasudevan, Long, Crandall, Rubenstein, & Bhide, 2008). Evidence suggests that the brain microvasculature undergoes extensive endothelial proliferation and branching for at least a month after birth (Harb, Whiteus, Freitas, & Grutzendler, 2013). More detailed examination of the brain microvasculature revealed that endothelial tip cells, new blood vessels, and perfused blood vessels are being actively formed in the P8 brain, especially the cortex (Walchli et al., 2015). We therefore chose to focus on the P8 brain as an understudied but actively angiogenic region to study the effects of Notch modulation on angiogenesis.

3.1.2 Isolation of endothelial-specific mRNA from whole tissues

The RiboTag method, developed by the McKnight lab (Sanz et al., 2009), allows isolation of cell type specific mRNA from a tissue of interest without cell disaggregation and flow sorting, minimizing the risk of alterations secondary to breaking cell-cell contacts, time-dependent gene expression patterns, and mRNA quality during physical or enzymatic separation of cells. The RiboTag model incorporates a conditionally-expressed epitope-tagged ribosomal protein that can be recombined with Cre recombinase in targeted cell types, and then used to immunoprecipitation (IP) polysomes of a cell type and the associated mRNA.

The RiboTag mouse carries a Rpl22 allele consisting of a LoxP-flanked wild type C-terminal exon 4 followed by an alternate C-terminal exon encoding a similar Rpl22 sequence, but with three copies of the hemagglutinin (HA) epitope inserted before the stop

codon. After Cre recombination in the cell type of interest, the LoxP-flanked wild type Rpl22 exon 4 is removed and the Rpl22HA protein is then specifically expressed and incorporated into ribosomal particles in the desired cell type. The target tissue is snap frozen to preserve its transcriptional state, homogenized, and then anti-HA antibodies are used to IP HA-tagged polysomes along with their bound mRNA. This procedure results in isolation of polysomes from the cell type of interest, out of the bulk homogenate. Ribosome-associated mRNA can then be extracted for RT-qPCR, microarray or RNA-Seq analysis. This technique has been used successfully in multiple systems both *in vivo* and *in vitro* (Gonzalez et al., 2014; Lesiak et al., 2015; Sanz et al., 2013; Sanz et al., 2009; Shigeoka et al., 2016), and has recently been extended to mouse retinal ECs at different postnatal stages of angiogenesis, providing insights on the *in vivo* transcriptional regulation of normal angiogenesis over developmental stages of the postnatal mouse retina (Jeong et al., 2017).

To target the P8 brain endothelium, we crossed the RiboTag mouse to a *Cdh5CreERT2* mouse, which expresses a tamoxifen-inducible Cre-recombinase (Cre-ERT2) under the regulation of the vascular endothelial cadherin promoter (VECad), and generated *Rpl22HA/HA, Cdh5CreERT2/+* mice, known as RiboTagEC mice. This schematic is illustrated in Figure 3-1.

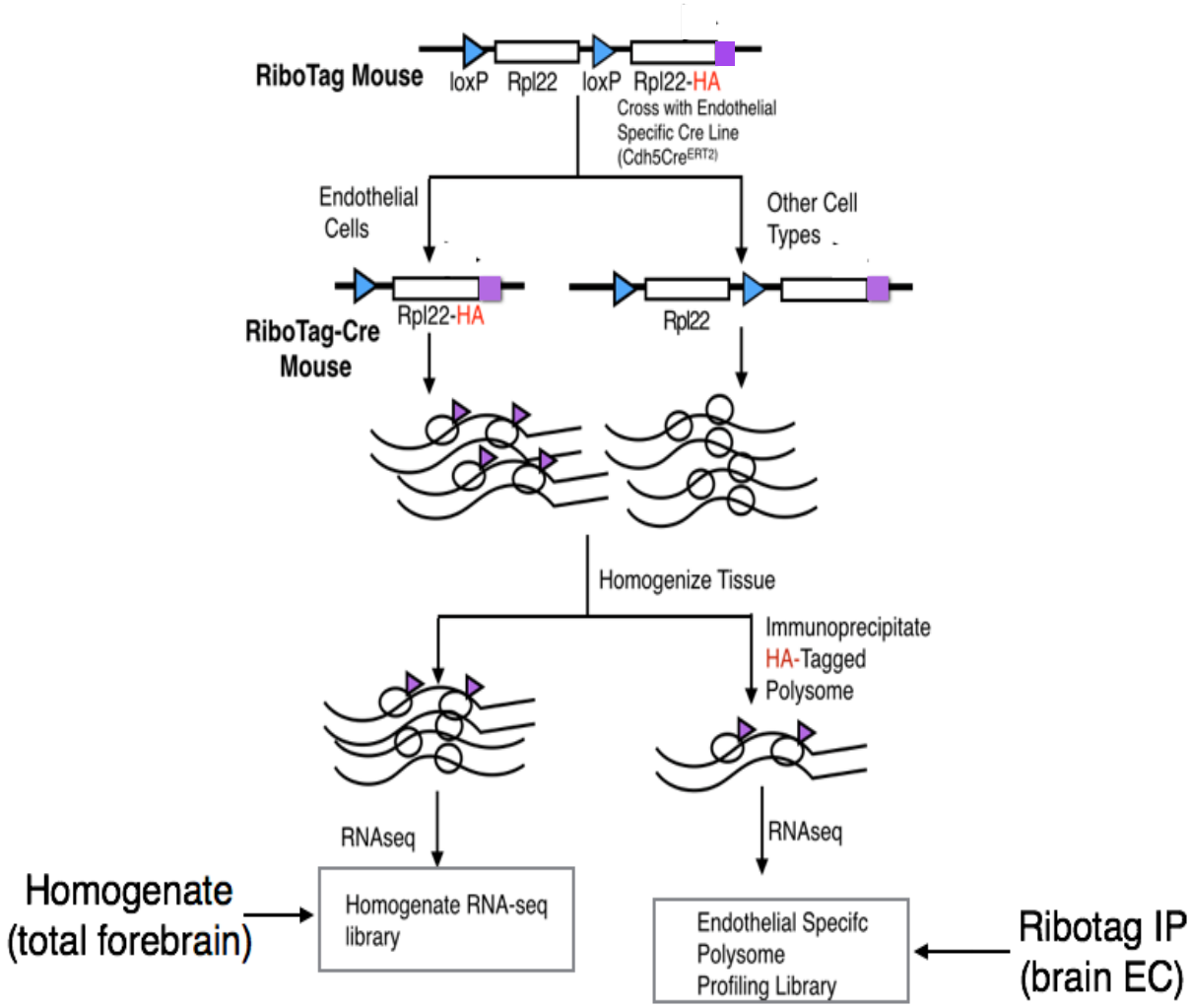

Figure 3-1. Schematic of the RiboTagEC mouse model and experimental workflow

(Figure adapted from Gonzalez, 2014)(Gonzalez et al., 2014) Tamoxifen-inducible recombination of the RiboTag allele using endothelial-specific Cdh5-creERT^2 led to expression of HA-tagged RpL22 ribosomal protein specifically in ECs. mRNA extracted from tissue homogenate were RNA-sequenced to build homogenate library (whole brain). Polysome-bound transcripts were IP from homogenate with anti-HA antibody, and was converted into polysome profiling library (EC-specific).

3.1.3 Modulation of Notch signaling *in vivo*

Modulation of Notch signaling by pharmacological inhibition via γ-secretase inhibitors (GSI) allows for a precise temporal control of Notch signaling *in vivo* (Bailis, Yashiro-Ohtani, & Pear, 2014). GSI inhibits the γ-secretase-dependent S3 cleavage that releases the Notch intracellular domain from the Notch extracellular domain and allows the intracellular domain to translocate to the nucleus and form a transcriptional complex (Figure 3-2). Administering GSI to postnatal mouse results in inhibition of Notch signaling and causes an increase in the number of tip cells and vascular sprouts in developing retinal vasculature, consistent with other Notch loss of function phenotypes (Ahmad et al., 2011; Benedito et al., 2009; Zarkada, Heinolainen, Makinen, Kubota, & Alitalo, 2015).

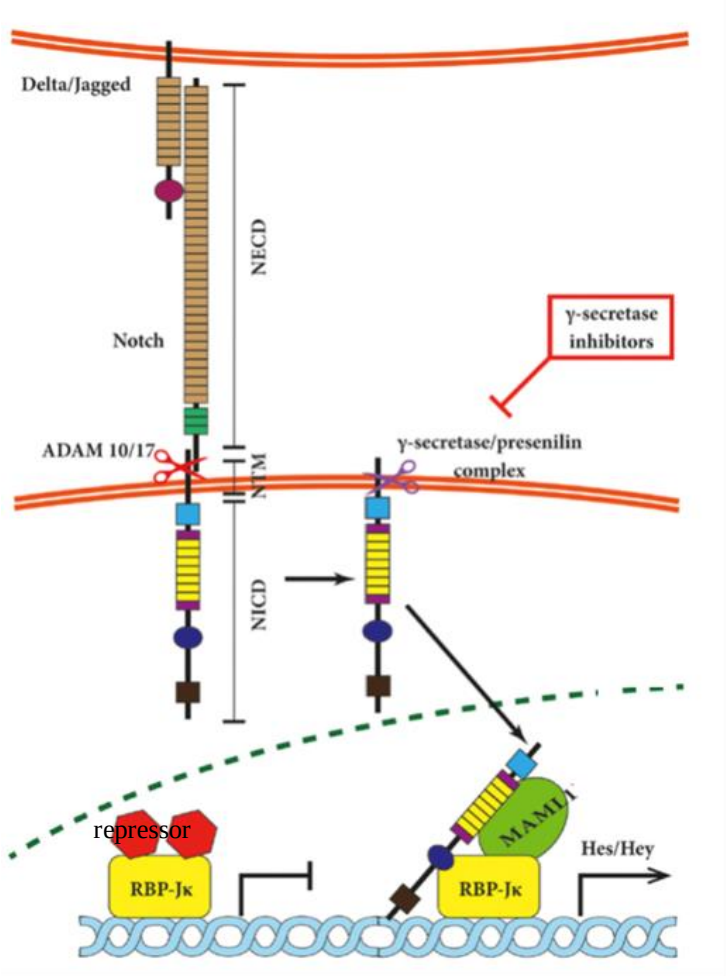

Figure 3-2. Schematic of Gamma secretase inhibitors (GSI) inhibition of Notch signaling

(Figure adapted from Teodorczyk and Schmidt, 2015)(Teodorczyk & Schmidt, 2014) The interaction between Notch ligand and receptors lead to S2 cleavage on the extracellular site by ADAM10 or ADAM17, followed by S3 cleavage by gamma-secretase-presenilin complex. The S3 cleavage give rise to NICD. GSIs have been widely used to inhibit Notch and are already in clinical trials.

In order to capture early transcriptional changes in ECs following Notch modulation, we administering the GSI N-[N-(3,5-difluorophenacetyl)-L-alanyl]-S-phenylglycine t-butylester (DAPT) to postnatal RiboTagEC mice, using previously established dosage

(Zarkada et al., 2015). With this system, we profiled the endothelial transcriptome from P8 brains, as well as selected other tissues for differentially expressed genes collected at earliest timepoints of Notch signaling inhibition after DAPT administration.

In summary, our strategy aimed at profiling the endothelial mRNA isolated from P8 brains from our RiboTagEC mouse model after GSI based inhibition of Notch signaling. By focusing on early timepoints after GSI treatment, we aimed to capture the early endothelial Notch transcriptional landscape during angiogenesis and identify novel Notch targets.

3.2 Analysis- Profiling Notch signaling using RiboTagEC system

3.2.1 Optimization of the RiboTagEC system

3.2.1.1 Rpl22HA expression was detected specifically and efficiently in endothelial cells

To induce Cre recombination in neonatal RiboTagEC mice the nursing females were gavaged with 250 mg/kg tamoxifen in oil at postnatal day (P) P1, P2 and P3. Recombination efficiency and tissue specificity of Rpl22HA expression was confirmed by sectioning the brains of P5 pups and immunostaining for HA and endothelial marker isolectin B4 (IB4) (Figure 3-3). These sections showed nearly complete overlap between

Rpl22HA and endothelium, demonstrating robust and specific expression of Rpl22HA in endothelial cells in mice brain.

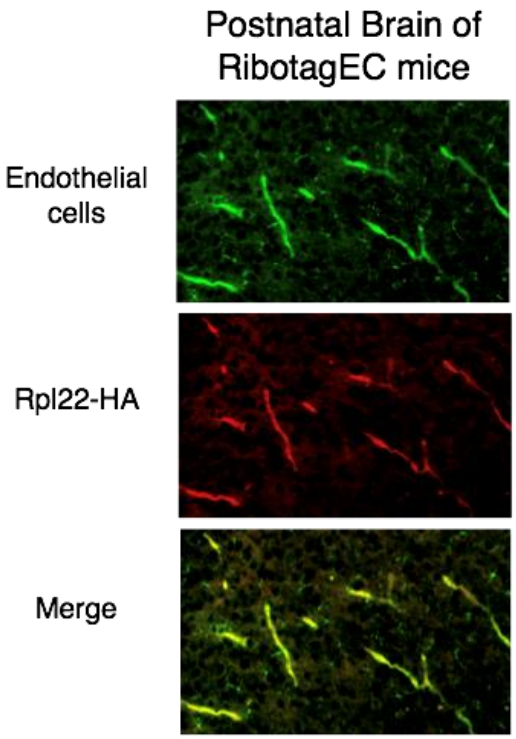

Figure 3-3. Rpl22-HA staining

Rpl22-HA expression (Anti-HA, red) was detected specifically and efficiently in the endothelial cells (IB4, green) of P5 brain of RiboTagEC mice

3.2.1.2 HA Antibody ab9110 generated higher yield of RNA compared with the previously established antibody

To optimize immunoprecipitation of Rpl22HA polysomes, we screened multiple anti-HA antibodies. Using tumor tissues collected from RiboTagEC mice, we found that the ChIP-

grade polyclonal antibody ab9110 (Abcam) yielded higher quantity of RNA with good quality (with RNA integrity number (RIN) > 9), compared to other antibodies including the antibody previously published in RiboTag studies (HA11, Covance) (Figure 3-4) (Gonzalez et al., 2014; Sanz et al., 2013; Sanz et al., 2009). A recent study indicated that these two antibodies were similarly effective in precipitating RpL22HA, but ab9110 co-purified increased amounts of 80S ribosomes than antibody HA11 and thus generated higher yield, consistent with our findings (Shigeoka et al., 2016).

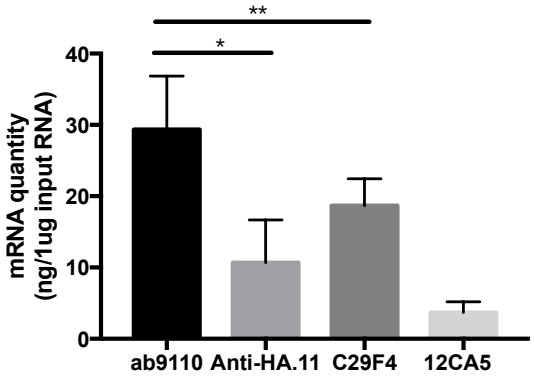

Figure 3-4. Comparison of IP efficiency using selected antibodies

Four different anti-HA antibodies including ab9110 (Abcam), Anti-HA.11(BioLegend), C29F4 (Cell Signaling), and home purified antibody 12CA5 were tested in the RiboTag IP process using xenografted tumor tissues (LLC tumors) collected from RiboTagEC mice. Anti-HA.11 was mostly widely used in previous studies. Ab9110 yielded significant higher amount of mRNA after IP compared with the other three antibodies. IP efficiency was measure as the quantity (ng) of mRNA after IP out of 1μg of input total RNA.

3.2.1.3 Negative control study indicated little contamination of the IP system

One challenge of the RiboTag technique is the non-specific binding of mRNAs to antibodies and/or antibody-binding proteins that are used to precipitate antibodies and their associated complexes. To examine the level of background RNA binding, brains from Cre-negative RiboTag mice were used as negative controls and were found to give extremely low yield (<1ng out of 1μg input total RNAs after IP) of mRNA after the RiboTag IP process, indicating very little contamination of the system when the HA-tagged Rpl22 is not expressed (Figure 3-5). We also tested other tissue types and found that some tissues, such as xenografted tumor, exhibited more non-specific RNA binding, but this background could be reduced by pre-clearance of the tissue lysates with Protein A magnetic beads.

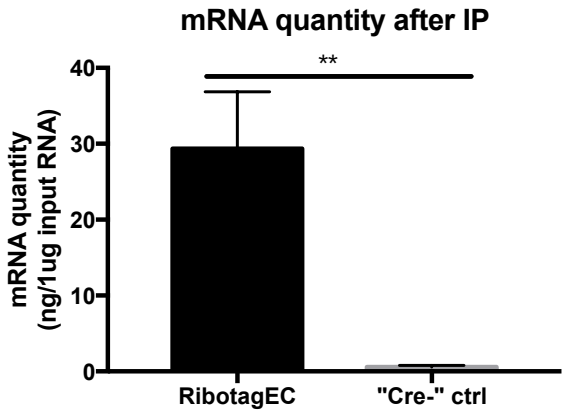

Figure 3-5. IP effeciency of RiboTagEC mice and Cre negative control mice

Cre negative mice from the same litter was used as negative control. Low amount of RNA (<1ng) was detected after IP from Cre negative mice, indicating little contamination of the system.

3.2.2 Pharmacological modulation of Notch- time course study

To capture the dynamic process and establish the earliest robust response, we performed a time-course screen by harvesting P8 brains and retinas from mice at 4, 6, and 8 hours after a single dose of 100mg/kg DAPT or vehicle (10% ethanol and 90% corn oil) injection. RNA was extracted from tissue homogenates and quantitated the expression levels of canonical Notch targets by RT-qPCR.

As expected, DAPT treatment significantly reduced the expression of canonical target genes in all conditions and timepoints compared to vehicle. The effects of DAPT treatment were measurable as early as 4 hours. However, treatment with DAPT for 6 hours showed the strongest effect on expression levels of select canonical targets (Figure 3-6). From these experiments, we determined that 6 hours treatment enabled an early yet robust response after DAPT injection.

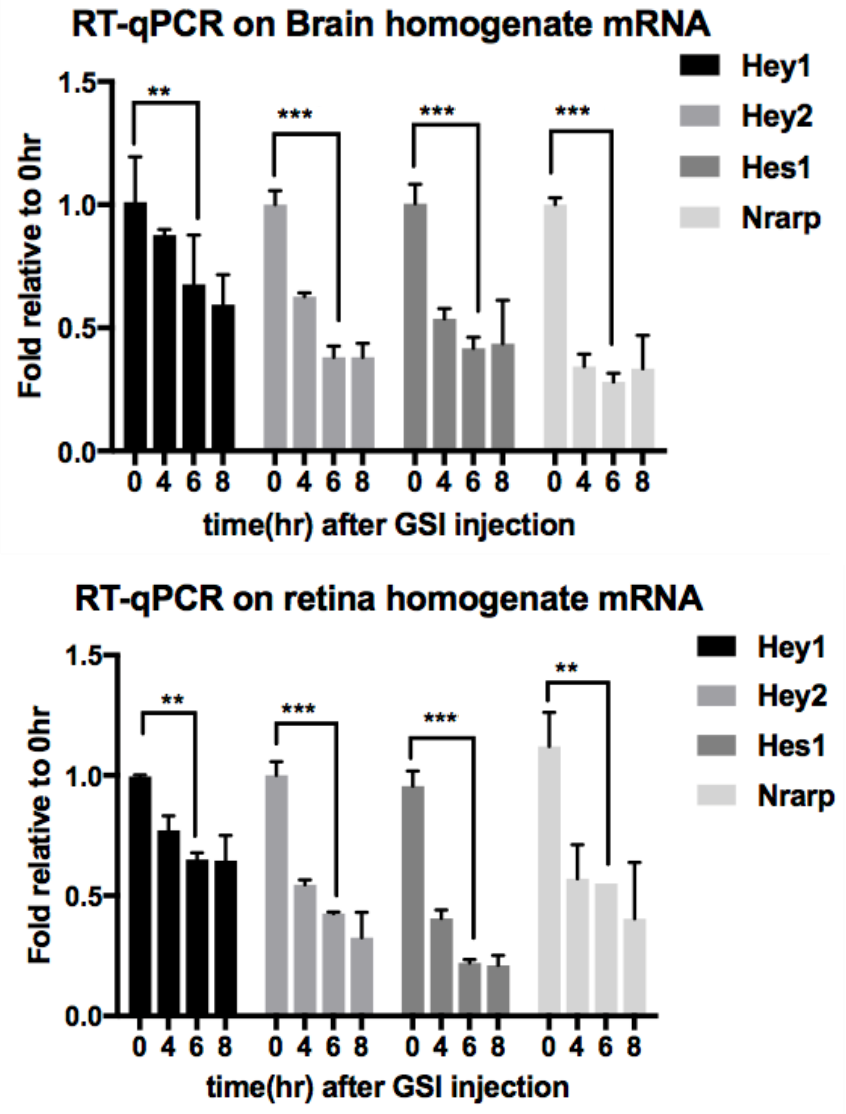

Figure 3-6. Time course study of DAPT treatment in postnatal mice

Brains and retinas were harvested from P8 mice at 0, 4,6,8 hours after 100mg/kg DAPT or vehicle (10% ethanol and 90% corn oil) treatment. RNA was extracted from homogenized tissues and was subjected to RT-qPCR to evaluate canonical Notch targets including *Hey1*, *Hey2*, *Hes1* and *Nrarp*. All four genes showed significant inhibition at 6 hours. No significant further inhibition was detected at 8 hours.

3.2.3 6-hour profiling of ECs from RiboTag mouse brain

To identify early response changes (altered after 6 hours of inhibition) in expression *in-vivo*, we selected 6 postnatal day 8 littermates mice for the study, where half were treated with DAPT and the other (control) half received the vehicle (*i.e.* 3 DAPT treated + 3 Vehicle treated/Control). 6 hours after DAPT administration, we collected different tissues (Brain, Retina, Lung, Liver) from these mice and isolated polysome-associated mRNA using the RiboTag IP process, as described in the workflow below (Figure 3-7). Here we focused on brains for RNA-seq analysis of endothelial, polysome associated mRNA.

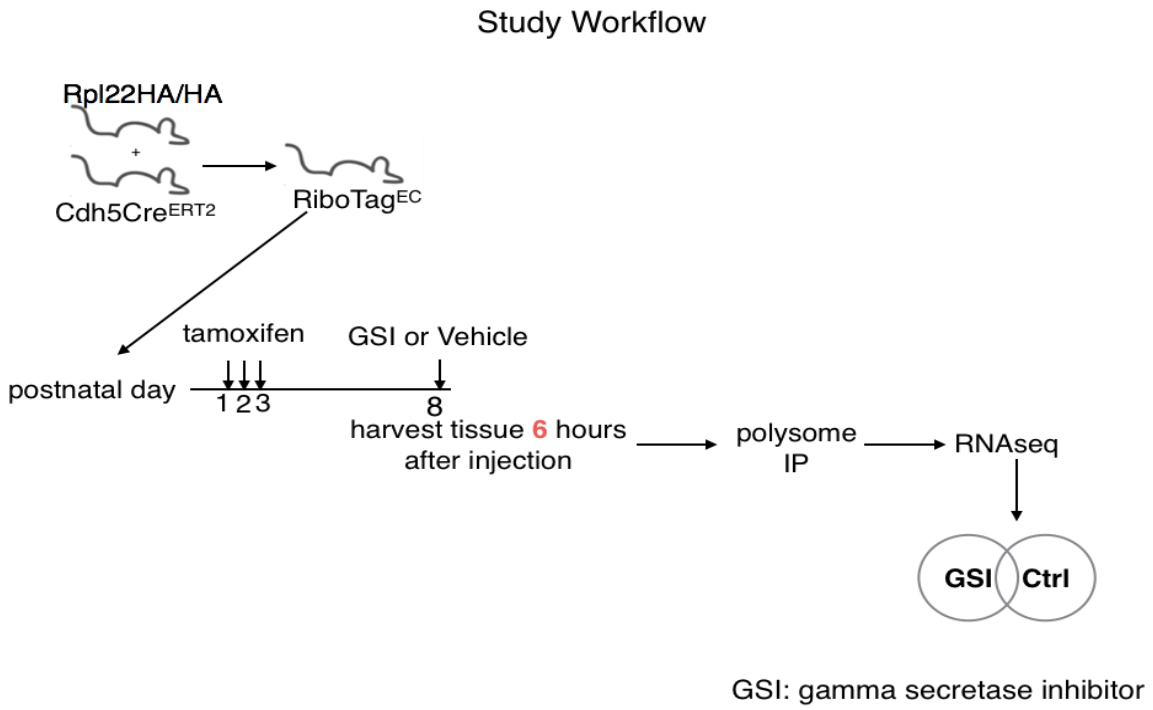

Figure 3-7. Experimental workflow of the 6 hour profiling studies using P8 RiboTagEC mice

Nursing females were gavage with (250mg/kg) tamoxifen from P1-P3 to induce Cre recombination in neonatal RiboTagEC mice. On P8, RiboTagEC pups were injected with either 100mg/kg DAPT (n=3) or vehicle (n=3). 6 hours later, mice were sacrificed and tissues including brain, retina, heart, liver, lung and kidney were collected and snap frozen in liquid nitrogen. Tissue can be stable in liquid nitrogen for months. Brains were used in this study for RiboTagIP and RNA-seq purposes. Both homogenate mRNA and the IP-derived RNA were sent for RNA-seq. A total of 12 samples were sequenced: DAPT-Input (n=3), DAPT-IP (n=3), Control-Input (n=3), and Control-IP (n=3).

The mRNA isolated from tissues was used to generate two distinct samples; 1) EC specific mRNA library obtained from RiboTag-IP fraction of the brain, and 2) a homogenate mRNA library isolated from the input fraction of the brain which represents mRNA from the whole tissue. Samples from four categories (GSI-IP, GSI-Input, Vehicle-IP, Vehicle-Input) were sequenced at a depth of ~30 million 100-base single-end reads on the TruSeq platform in the Sulzberger Columbia Genome Center. Reads from IP-ribosomes were analyzed first to remove rRNA reads with Bowtie2 and then mapped to the mouse transcriptome Mouse: (UCSC/mm10) using STAR and processed with Samtools. The counts obtained by FeatureCounts were analyzed by DESeq2 to identify differentially expressed genes.

3.2.3.1 Samples clustered into four group by PCA plot

Two-dimensional principal component analysis (PCA) was done to identify the variability along the samples. The samples segregated into four clusters: GSI treated homogenate mRNA, control homogenate mRNA, GSI treated RiboTag-IP mRNA, control RiboTag-IP mRNA. The biggest source of variability in the data (principal component 1/PC1) comes

from tissue types (homogenate VS endothelium), and another main variability source (principle component 2/PC2) is from drug treatment (vehicle VS control) (Figure 3-8).

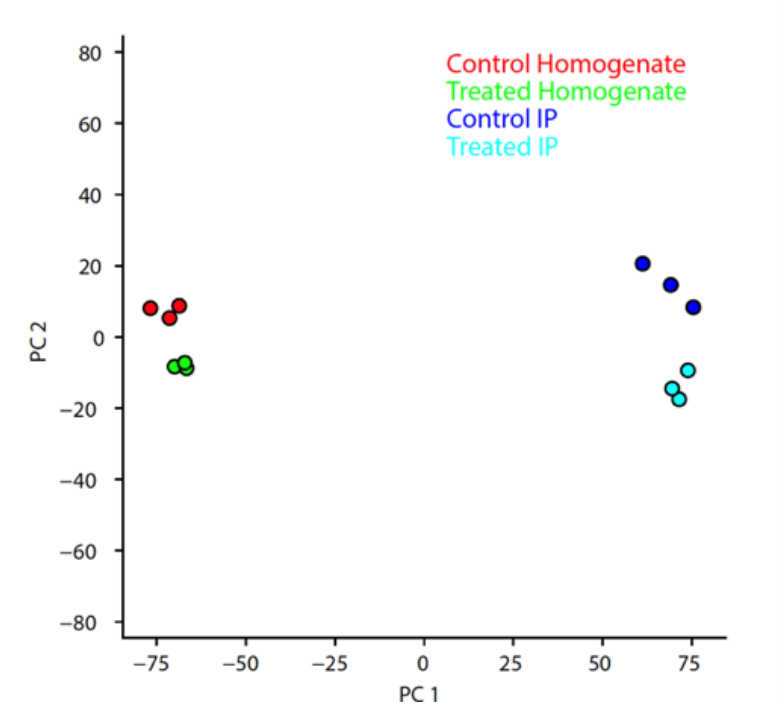

Figure 3-8. PCA plot of the 12 samples sequenced

Two-dimensional principal component analysis (PCA) plot showing segregation of the mice brain homogenate (red and green, left) and Endothelial fraction (dark blue and light blue, right) into two clusters. The analysis also segregated mice into two additional clusters after 6h treatment with DAPT, resulting in a total of four groups of clustered samples including control homogenate (red), control IP (dark blue), DAPT homogenate (green), and DAPT IP (light blue).

3.2.3.2 Significant enrichment of endothelial markers was detected in IP samples compared with control

To test the samples for successful immunoprecipitation of endothelial mRNA, we compared the expression levels of pre-selected endothelial-specific genes among the Input versus IP samples. As expected, the expression of endothelial specific markers was significantly and consistently enriched in the IP fractions in comparison to the Input, in all samples (Figure 3-9). This analysis confirmed endothelial-specificity achieved by the RiboTagEC system.

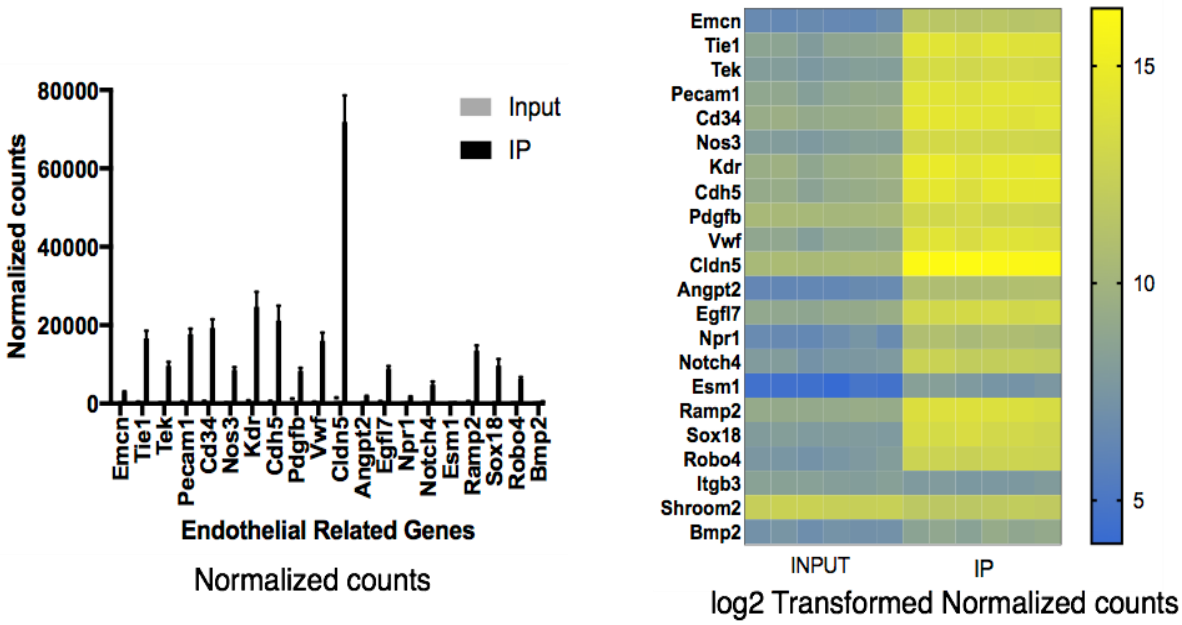

Figure 3-9. Enrichment of endothelial markers in RiboTag-IP samples

Differential expression analysis comparing homogenate (n=6) and IP isolated RNA (n=6) showed significant and consistent enrichment of pre-selected endothelial (including *Emcn, Pecam1, Cdh5, Cldn5,* and more) markers across all samples.

3.2.3.3 Gene set enrichment analysis confirmed successful inhibition of canonical Notch targets

To exam the Notch inhibition efficiency with GSI administration, we performed the Gene Set Enrichment Analysis (GSEA) of Notch signaling pathway and identified significant under-presentation of multiple established Notch targets in GSI-treated group in both homogenate and IP samples (

Figure 3-10). Known targets such as *Hey1*, *Hes5*, *Cxcr4*, *Dll4*, *Gja5* (connexin40), and *Nrarp* were significantly inhibited (with Padj<=0.05, Log2FoldChange>0.27) in both whole homogenate and brain endothelium. Interestingly, a small group of genes including *Hes1*, *Hes3*, *Efnb2*, *Flt4*, were detected as significantly down-regulated in the endothelium but not the brain homogenate. While other genes like *Hey2*, *Pdgfb* were detected in homogenate but not endothelium. This data suggested successful inhibition of Notch signaling 6 hours after GSI treatment. Moreover, it also revealed tissue-specific gene response to Notch that worth future analysis.

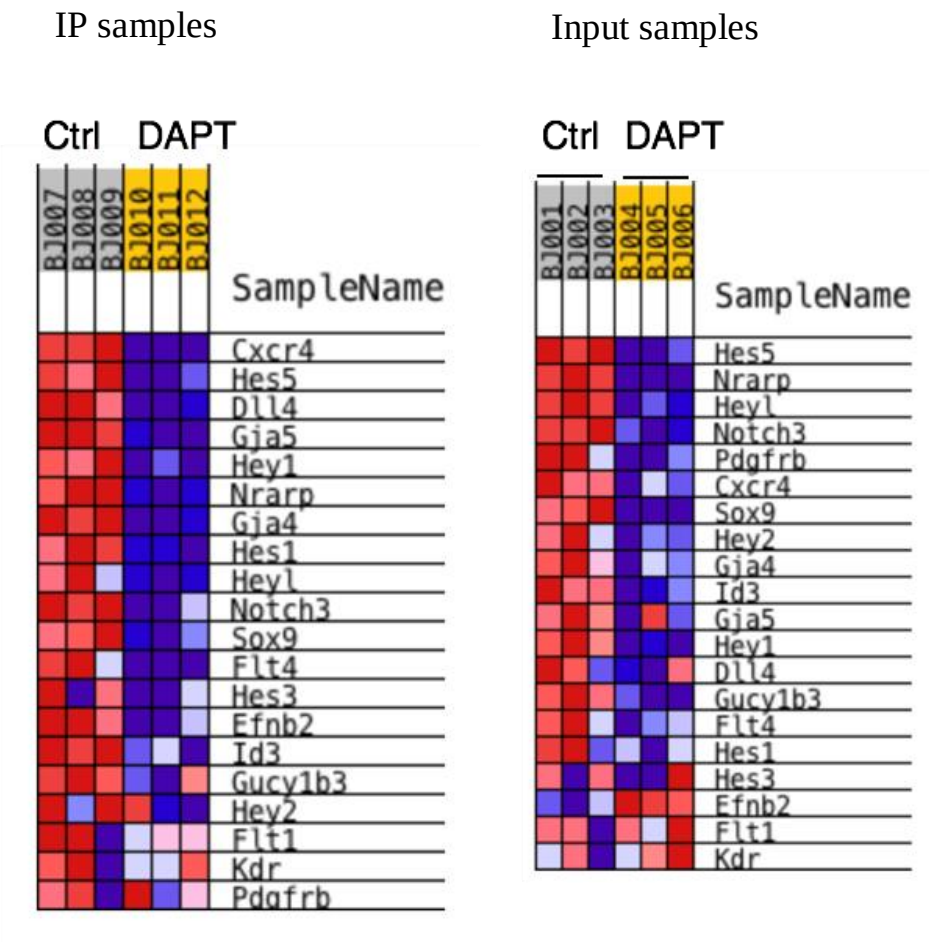

Figure 3-10. GSEA analysis of Notch signaling pathway

Gene Set Enrichment Analysis of Notch signaling pathway identified downregulation of majority of the established Notch targets such as *Hey1, Hes1, Cxcr4, Hes5* and *Efnb2* in the DAPT treated input (brain homogenate) and IP (brain EC) samples. This analysis confirmed the successful inhibition of Notch using DAPT, and more importantly, 6 hour after treatment was an appropriate timepoint to identify gene expression changes of primary Notch downstream targets.

3.2.3.4 Common and endothelial specific Notch targets were detected in GSI treated group

In order to identify Notch targets in brain endothelium, we interrogated the RNA-seq data for increased amounts (upregulated) or decreased amounts (downregulated) of mRNA in the GSI treated samples compared with control. Significantly changed mRNAs for specific genes were identified with an adjusted *P*-value of <=0.05. Potential candidate genes were chosen based on their significance and their log2foldchange values (log2FC with at least +/- 0.27, fold ~= +/- 1.2fold). In order to identify primary Notch downstream targets which should be down regulated by GSI, we only focused on the down regulated genes as potential candidates.

Analysis of the homogenate fraction identified 76 significantly downregulated genes of fold change at least 1.2 after GSI treatment. In the brain ECs (IP fraction), we identified 591 genes significantly repressed by GSI with fold change at least 1.2 at 6h. Among those 591 genes, 27 were common targets in both homogenate and the endothelium, while 564 genes were uniquely identified in endothelium which could be endothelial-specific Notch responsive genes (Figure 3-11 and Figure 3-12).

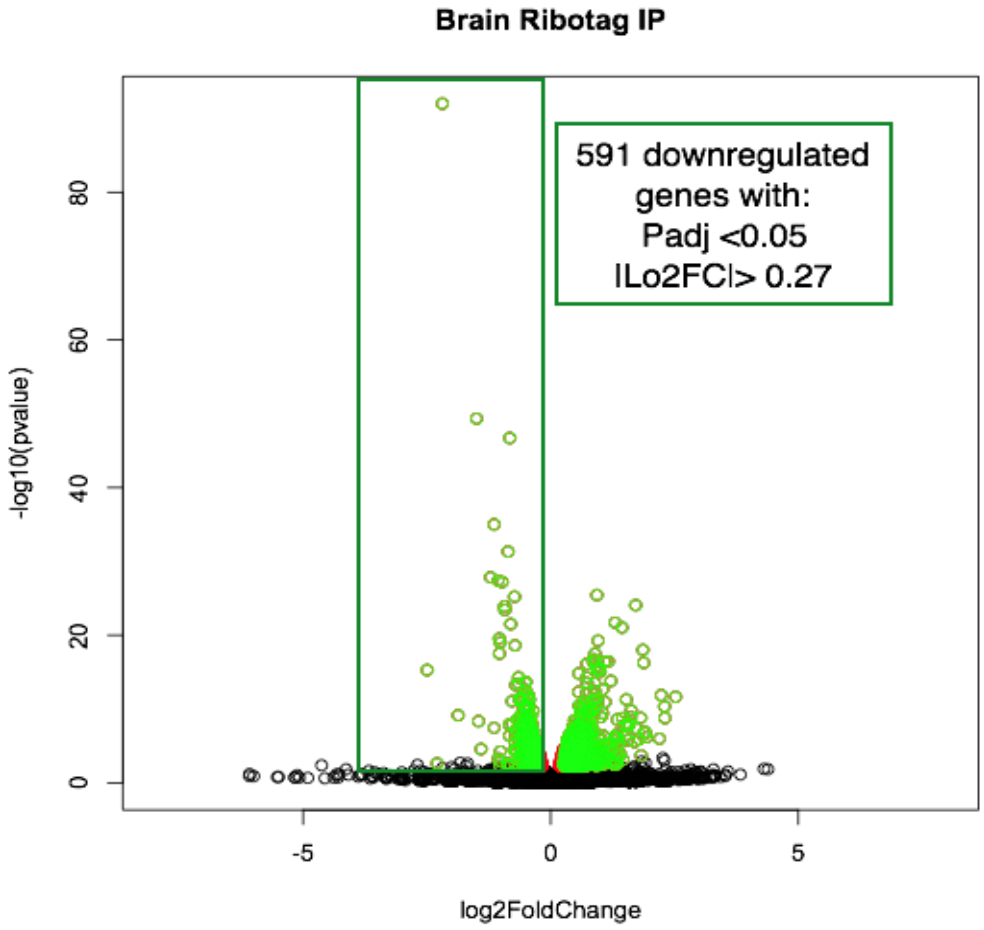

Figure 3-11. Volcano Plots: transcriptional changes of brain EC (IP fraction) after 6 hour of DAPT treatment compared with Vehicle

Volcano plots showing transcriptional changes after 6h of DAPT treatment on the IP fraction. The x-axis represents the Log fold change calculated in this analysis, and the y-axis shows the Log10 P values. Each gene is represented by a dot. Dots in red indicate genes that are statistically significant (Padj < 0.05). Additionally, the green dots represent genes that are up/downregulated 1.2fold. Black dots are genes that not significantly altered in expression level. Because Notch is transcriptional activator and GSI functions as Notch inhibitors, we only focused on significant down-regulated genes with a fold change at least 1.2 (green box).

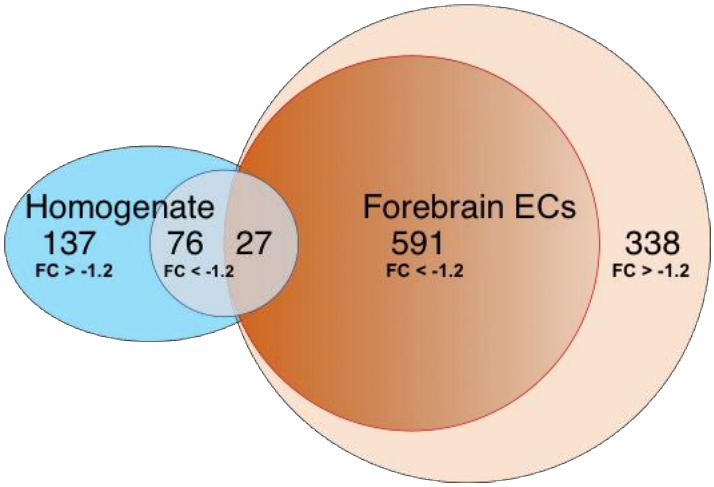

Figure 3-12. Comparison of significant downregulated genes in homogenate (brain) and IP (brain EC) fraction

Venn plots generated by comparing the homogenate and endothelial fraction from P8 mouse brain. In the homogenate fraction (shaded in Blue), 76 genes of 213 ($P_{adj} < 0.05$) were significantly repressed 1.2fold or higher, following DAPT treatment for 6h. Similarly, the endothelial fraction (shaded in Orange) identified 591 genes of 929 ($P_{adj} < 0.05$) to be repressed 1.2fold. Comparing the two fractions of genes (Fold Change of 1.2 or higher) identified 27 common genes between the two fractions.

Table 3-1 shows the top 30 downregulated genes identified in brain EC ranked by fold change. Among the top 20 EC-specific genes were canonical targets including *Cxcr4*, *Hes5, Dll4, Gja5*, and *Nrarp*, as well as multiple interesting novel candidates. For example, the netrin receptor *Unc5B* has been well established to play an anti-angiogenic role during embryonic vascular patterning, as well as in postnatal and pathological angiogenesis (Larrivee et al., 2007; Lu et al., 2004). However, it has never been linked with Notch signaling pathway in previous studies. Our data suggests a novel mechanism that Notch regulates the Unc5b pathway to carry out angiogenic functions.

Table 3-1. Top 30 genes ranked by fold change of GSI-treated brain EC

Symbol	Log2FC	Padj	common with Input?
Hes5	-2.49	2.30E-13	Y
Gpx6	-2.29	2.55E-02	N
Cxcr4	-2.19	1.43E-88	N
Kcnj8	-1.87	1.05E-07	Y
Unc5b	-1.50	3.29E-46	Y
Gm14207	-1.46	5.21E-07	N
Bricd5	-1.41	8.24E-04	N
Syt15	-1.22	3.40E-25	N
Scgb3a1	-1.14	3.38E-06	N
Dll4	-1.14	3.43E-32	N
Gja5	-1.06	8.36E-25	N
Foxs1	-1.06	8.46E-03	Y
Hey1	-1.04	2.41E-17	Y
Cmklr1	-1.04	1.96E-15	N
Rnase1	-1.03	4.33E-02	N
Tbx2	-1.02	1.49E-03	Y
Rhbdl2	-1.02	1.77E-02	N
Kcnj2	-1.02	7.25E-17	N
Efna1	-0.98	1.13E-24	N
Sat1	-0.93	1.47E-21	N
Nrarp	-0.93	4.19E-21	Y
Gipc3	-0.88	2.46E-02	N
Myh11	-0.88	3.42E-02	N
Mapk8ip2	-0.86	4.15E-02	N
Gja4	-0.86	1.34E-28	N
Cdkn2b	-0.84	1.36E-06	N
Zfp69	-0.83	2.59E-05	N
Mfsd2a	-0.83	9.36E-44	N
Ptp4a3	-0.81	2.94E-19	N

Table 3-1 shows the most inhibited genes in brain ECs 6 hours after DAPT treatment. Multiple canonical Notch target genes (red) were within the list, together with a great number of novel genes. Majority of the genes were not significantly inhibited in brain homogenate.

3.2.3.5 Gene Ontology analysis revealed G-protein coupled receptor pathway as potential Notch effectors.

We further interrogated the list of DEGs to identify pathways that were altered by GSI treatment in both the homogenate and EC population. We performed a Statistical Over-representation test using the Fisher's exact test (PANTHER GO). Analysis identified several significant pathways that are altered, as shown in Figure 3-13. As expected, Notch pathway was repressed by GSI treatment in both the homogenate (Fold enrichment = 12.56, FDR= 0.00421) and the brain EC population (Fold enrichment = 4.64, FDR = 0.0189).

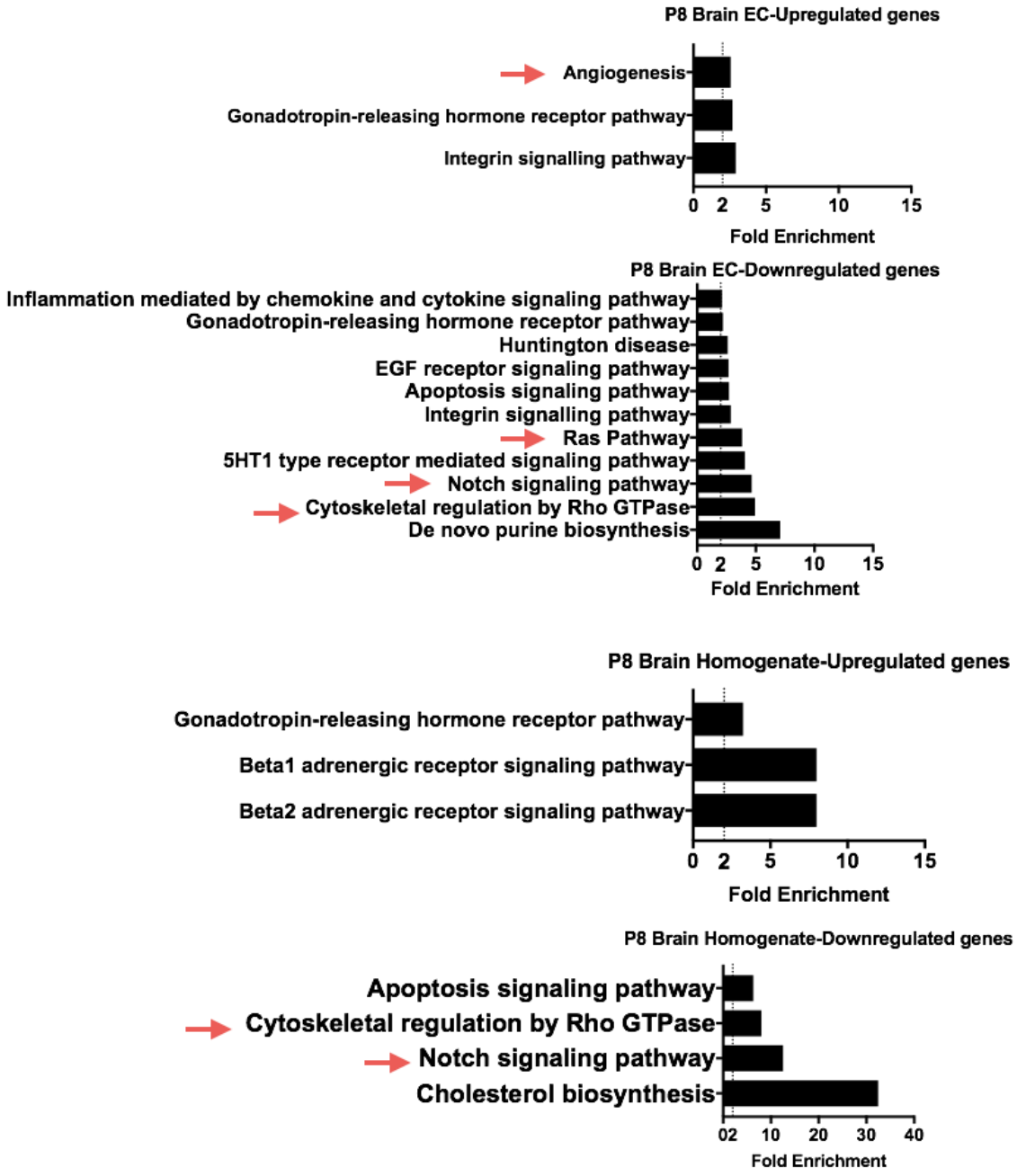

Figure 3-13. Gene Ontology Pathway Analysis

Figure showing the gene ontology pathways identified on genes repressed by GSI in the homogenate and endothelial fraction. The analysis was done using PANTHER DB using the over-representation test using the Fisher's exact test. The analysis identified enrichment of the Notch signaling pathway in both the homogenate and the endothelial fraction. Analysis on endothelial fraction additionally identified involvement of the Rho and Ras pathways, indicating involvement of the G protein related pathway.

Interestingly, the analysis indicated the Notch inhibition downregulates the Rho and Ras pathways, implicating the G-protein related pathway as effectors of Notch signaling, as highlighted in Figure 3-13. This finding is interesting because G-protein pathways plays fundamental role in regulating cell behavior but the role of this pathway in Notch signaling has rarely been reported. Figure 3-14 and Volcano plots showing transcriptional changes of selected G protein/GPCR related genes after 6h of DAPT treatment on the IP fraction. The x-axis represents the Log fold change calculated in this analysis, and the y-axis shows the Log10 P values. Each gene is represented by a dot. We only focused on significant down-regulated genes with a fold change at least 1.2 (green dot area).

Table 3-2 listed selected G-proteins related effectors that's been identified.

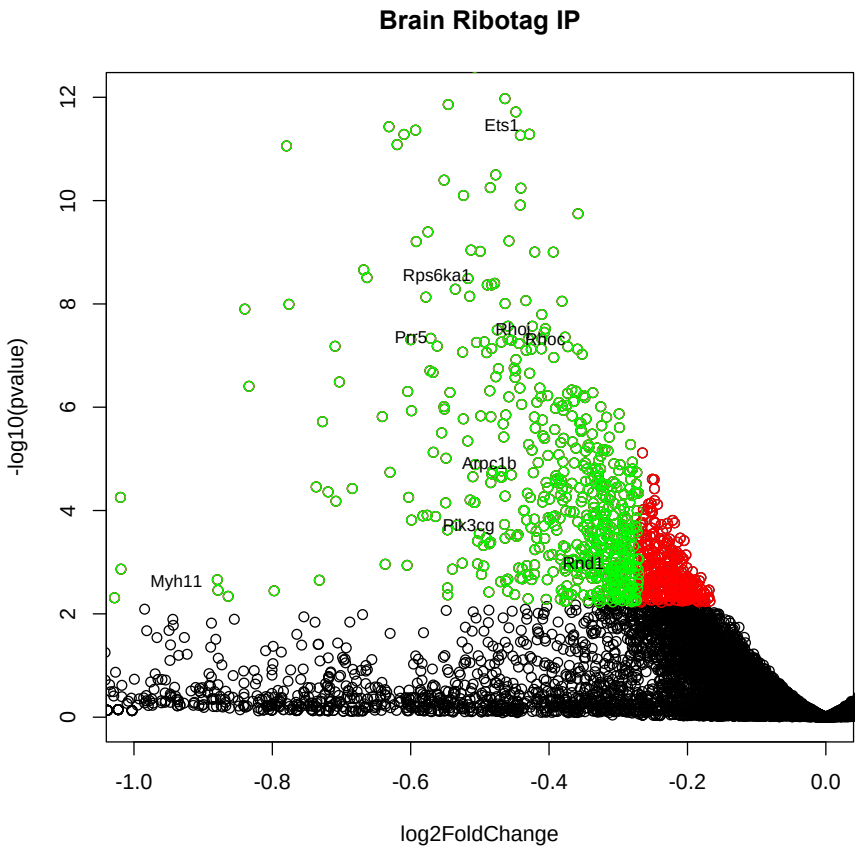

Figure 3-14. Volcano plot of selected G proteins identified as potential Notch targets in brain EC

Volcano plots showing transcriptional changes of selected G protein/GPCR related genes after 6h of DAPT treatment on the IP fraction. The x-axis represents the Log fold change calculated in this analysis, and the y-axis shows the Log10 P values. Each gene is represented by a dot. We only focused on significant down-regulated genes with a fold change at least 1.2 (green dot area).

Table 3-2. Listed of selected G proteins identified as potential Notch targets in brain EC

Gene	Log2FC	Padj
Myh11	-0.88	3.42E-02
Prr5	-0.56	5.62E-06
Rps6ka1	-0.48	5.19E-07

Pik3cg	-0.46	5.55E-03
Pfn1	-0.45	4.55E-06
Tubb6	-0.44	5.03E-05
Ets1	-0.43	1.24E-09
Vasp	-0.43	6.14E-06
Arpc1b	-0.42	6.34E-04
Rhoj	-0.41	4.31E-06
Actb	-0.39	4.67E-05
Tiam1	-0.38	4.10E-06
Rhoc	-0.36	6.14E-06
Ralb	-0.35	4.23E-03
Mapk12	-0.32	1.49E-02
Rnd1	-0.3	1.96E-02
Rps6ka2	-0.29	1.59E-02
Cfl1	-0.29	4.73E-03

Table 3-2 listed selected G protein/GPCR related genes significantly inhibited (Padj<0.05, LogFC<0.27) in P8 brain endothelium after 6h of DAPT treatment . Genes were listed by fold change.

3.3 Discussion

Notch signaling plays an important role in regulating angiogenesis by regulating complex transcriptional networks (Tung et al., 2012). However, the full repertoire of Notch target genes regulated in mammalian endothelium is largely unknown. In this study, we generated a mouse model to isolate EC specific mRNA from brain tissue homogenate from P8 mice. This allowed us to profile the transcriptional changes that occur within 6 hours of GSI based inhibition of Notch signaling. Our analysis showed that several known Notch targets and numerous novel genes were modulated at 6 hours (See section II.B.2). Of particular interest, “G protein pathway” was identified as significantly down-regulated in

the endothelial in response to GSI treatment, which may represent a novel mechanism of Notch regulation in endothelial cells (See section II.B.3,4).

While this screen allows us to understand the early response to GSI at the transcriptional and translational level, the study design is not without limitations:

1) While GSI has largely been used to modulate Notch signaling, it is important to consider that the results of the screen could also be caused by its effect on other gamma-secretase substrates such as VEGF Receptor signaling (Haapasalo & Kovacs, 2011). This is important and may influence the interpretation of this screening data.
2) Similarly, administering GSI subcutaneously targets a variety of cell types beyond endothelial cells. While, the RiboTag model used in our study, allows isolation of mRNA specifically from ECs, it does not control for signals that originate from the interaction between ECs and other cell types in the tissue of interest. This crosstalk could influence the gene expression patterns we observe.

One way to overcome these limitations, is to understand the early transcriptional changes that occur after specifically stimulating the Notch receptor in ECs. This can be done in an *in-vitro* setting by stimulating ECs with its ligands, but is currently difficult to accomplish ligand-dependent Notch signaling in a mammalian, whole animal setting. Therefore, we performed an unbiased screening by using primary endothelial cell types from two different tissues, human umbilical vein and retina, to confirm our findings from the *in-vivo* analysis.

Chapter 4 Tethered Notch Ligand-mediated and EGTA-mediated activation of endothelial Notch signaling define ligand specific Notch transcriptional response.

4.1 Strategy and Rationale

In the previous study, we assembled a dataset of endothelial genes that respond to Notch inhibition by GSI treatment *in vivo*. However, we anticipate that some of these candidate target genes are not bona fide endothelial Notch targets, but are instead modulated by non-Notch effects of GSI treatment or secondary effects caused by Notch signaling changes in adjacent cell types such as pericytes and smooth muscle cells. We therefore set out to validate endothelial Notch targets by specifically inducing Notch activity in isolated human primary endothelial cells using both Dll4 and Jag1 as Notch activating ligands. Further, the approach of ligand activation *in vitro* allows for description of ligand-specific (Jag1 versus Dll4) Notch transcriptional responses in endothelial cells. We hypothesize that an *in vitro* unbiased screen of genes upregulated by ligand-specific Notch induction will detect an overlapping set of genes as the *in vivo* screen and permit us to refine our *in vivo* dataset by focusing on candidates that are also directly induced by Notch ligand binding, in addition to being down-regualted by GSI *in vivo*.

We anticipate that some Notch targets are expressed at low levels under homeostatic *in vivo* conditions, and their further suppression by Notch inhibition will be difficult to detect. We therefore hypothesize that *in vitro* Notch induction will detect additional endothelial

Notch targets that may have only minimally been suppressed by Notch inhibition *in vivo*, but are strongly and rapidly induced by Notch signaling.

4.1.1 Ligand-specific activation of Notch

Both of the endothelial Notch ligands, DLL4 and JAG1, play important roles in regulating tip/stalk cell selection in angiogenesis (Benedito et al., 2009) but their activity has opposing effects in angiogenic regulation in endothelial cells. This difference has not been analyzed carefully at the mechanistic level, a goal of this Chapter. Identifying how each of these two ligands regulate Notch signaling will allow a better understanding how Notch regulates angiogenesis.

The ligand DLL4 has been extensively studied in physiological and pathological angiogenesis. Haploinsufficiency of Dll4 in mice caused embryonic lethality due to vascular defects (Duarte et al., 2004; Gale et al., 2004; Krebs et al., 2004). In the context of tumors, blockade of Dll4 signaling promoted excess but non-functional angiogenesis, thus inhibiting tumor growth (Noguera-Troise et al., 2006; Ridgway et al., 2006). Data from a microarray-based screening study in HUVECs with retroviral-mediated DLL4 overexpression (OE) identified DLL4 as a suppressor of VEGFR2 expression, and inducer of VEGFR1 and sVEGFR1 (Harrington et al., 2008). While these studies provided important insights into the network of DLL4-NOTCH regulation, the method of study did not allow identification of primary response genes following DLL4-NOTCH activation. In addition, these studies used overexpression of Notch ligands in the same cell as the receptor,

which can cause cis-inhibition of Notch, and counterintuitively, downregulation of Notch signaling (del Alamo, Rouault, & Schweisguth, 2011).

Unlike DLL4, the role of JAG1 in ECs remains controversial and elusive. It is suggested that JAG1, as an inactive or weakly-acting ligand, promotes angiogenesis by antagonizing DLL4-mediated activation of Notch signaling in fringe-modified endothelial cells (Benedito et al., 2009). However, data from our group and others suggest that JAG1 can activate EC-Notch signaling to promote angiogenesis(Chang et al., 2011; Kangsamaksin et al., 2015). Our lab demonstrated that blocking JAG1 activity in ECs using the JAG1 specific Notch1 decoy downregulated canonical Notch targets including *HEY1*, *HEYL*, and *HES1*(Kangsamaksin et al., 2015). But the mechanism of how JAG1 mediates Notch signaling still remains to be addressed. Thus, our studies implicate JAG1 as an active ligand in endothelium, however, the activity mediated by JAG1 may differ from that elicited by DLL4.

Therefore, we focused on identifying primary/early response genes that are differentially regulated following DLL4-NOTCH or JAG1-NOTCH activation using a more physiological stimulation approach: the tethered ligand assay. Under physiological conditions, the ligand and the receptor are on adjacent cells and thus embedded in different membranes. The interaction of the ligand and the receptor activates endocytotic mechanisms acting on the receptor and the ligand and creates a pulling force (Varnum-Finney et al., 2000). This pulling force exposes the negative regulatory region (NRR) of the Notch receptor to ADAM proteins, leading to S2 cleavage. In our model system, ligand

is immobilized onto coated dishes and cells are seeded on top, which supports tension against Notch and mimics the way that Notch ligand is presented on a cell surface(Li et al., 2007).

In order to validate our *in vivo* dataset and elucidate the possible separate mechanism(s) downstream of DLL4-NOTCH and JAG1-NOTCH, we performed an unbiased screening of endothelial Notch genes whose expression is stimulated by Notch ligands in human endothelial cells using the tethered-ligand assay combined with RNAseq, focusing on early transcriptional responses (within 6 hours) to Notch activation.

4.1.2 EGTA-dependent activation of Notch

In our attempt to detect genes that rapidly respond to Notch signaling, we have tried to limit the period between Notch inhibition/induction and RNA harvest as tightly as possible. While we optimized a chemical gamma-secretase inhibitor (DAPT) of Notch in the RiboTagEC study, DAPT still takes time to diffuse and function in the mouse. Similarly, in the tethered ligand activation assay, the cells seeded on to the ligand-coated plates can settle at variable rates and it is difficult to precisely control the time at which the seeded cells contact the immobilized ligand. Therefore, as a third approach, we employed an ion chelator-based Notch activation method that allows for very tight temporal control of Notch activation. By conducting this EGTA activation method with or without a GSI, we sought to identify endothelial genes rapidly regulated by Notch signal activation.

Notch proteins are composed of a ligand-binding extracellular domain (NEC), a single-pass transmembrane signaling domain (NTM) and the Notch intracellular domain (NICD). The NEC and NTM are bound by a non-covalent interaction stabilized by Ca^{2+} (Rand et al., 2000). Treatment of cells with the calcium chelators such as EDTA and EGTA leads to shedding of the Notch ectodomain and renders the residual transmembrane fragment open for ADAM and γ-secretase cleavage (S2 and S3 cleavage) resulting in immediate Notch activation(Gupta-Rossi et al., 2001; Krejci & Bray, 2007; Rand et al., 2000).

EGTA based Notch activation method offers the advantage of a precisely timed NOTCH activation method and counters the issues with the previous two methods (RiboTag and tethered ligand activation) in controlling the timepoint for detecting early response Notch targets. However, EGTA is not a specific activator of Notch and so this screen serves as a validation for candidates identified in the other two screens.

4.2 Strategy & Analysis: Profiling Notch-mediated gene expression using the Tethered-Ligand Assay (TLA)

4.2.1 Optimization of the tethered-ligand assay

In tethered-ligand assay (TLA), we immobilized the extracellular domains of human DLL4 fused to Fc (10171-H02H, Sino Biologicals Inc.), JAG1-Fc (11648-H02H, Sino Biologicals Inc.), or IgG-Fc control proteins (10702-HNAH, Sino Biologicals Inc.) with

extracellular matrix (ECM) on dishes. Then, we seeded ECs onto these coated plates for different periods of time after which we measured Notch activation by CSL-Luciferase reporter assay, focusing our analysis with the use of RT-qPCR of canonical target genes or via RNA-seq (Figure 4-1). In order to achieve the optimal activation effects, we started by testing different conditions including choices of matrix, dosage and timepoint.

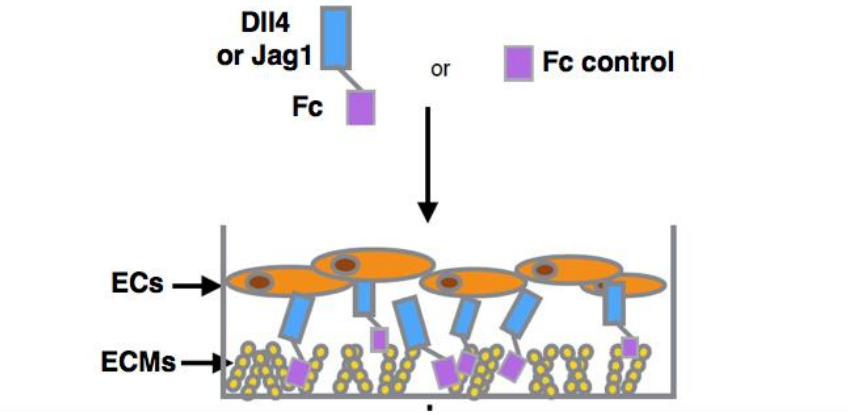

Figure 4-1. Schematic of Tethered Ligand Assay

4.2.1.1 No differences in Notch activation with different ECMs tested

We tested the effects of coating different cellular matrices on the level of Notch activation. We coated the ligands with fibronectin, gelatin or collagen and measured the level of Notch activation in HUVECs using CSL-Luciferase reporter assay. We identified no significant differences in the level of activation, as measured by Notch reporter luciferase signaling, caused by the different ECMs (Figure 4-2).

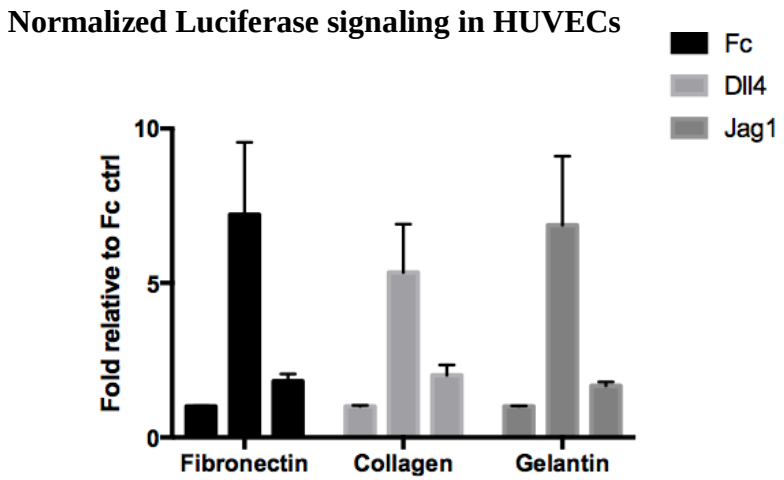

Figure 4-2. No significant difference in Notch activation detected using different ECMs

Luciferase was utilized to measure Notch activation by tethered ligand using different ECMs including fibronectin, collagen and gelatin. HUVECs transfected with pGL-11CSL-Luc and Renilla were seed on (10 μg/ml) Dll4-Fc mixed with different choice of ECMs for 24 hours. Notch signaling was measured by the dual-luciferase-assay (see Chapter II). No significant difference was detected utilizing different ECMs.

4.2.1.2 DLL4 more efficiently activated NOTCH in HUVEC than JAG1

We performed a ligand concentration estimation to determine the minimum dose with maximum levels of Notch activation. For both DLL4 and JAG1, we tested concentrations ranging from 1 μg/ml-100 μg/ml. For DLL4, 10 μg/ml was sufficient to activate Notch signaling in HUVECs (Figure 4-3). To test for the specificity of the DLL4 induction, we overexpressed pan-Notch inhibitor dominant negative Mastermind Like (dnMAML) in cells, which significantly reduced the induction signal caused by ligand-based stimulation (Figure 4-4). These results indicate that the signaling observed was due to interactions

between Dll4 and Notch that led to Rbp-Jk mediated transcriptional events, not any other incidentally activated pathways.

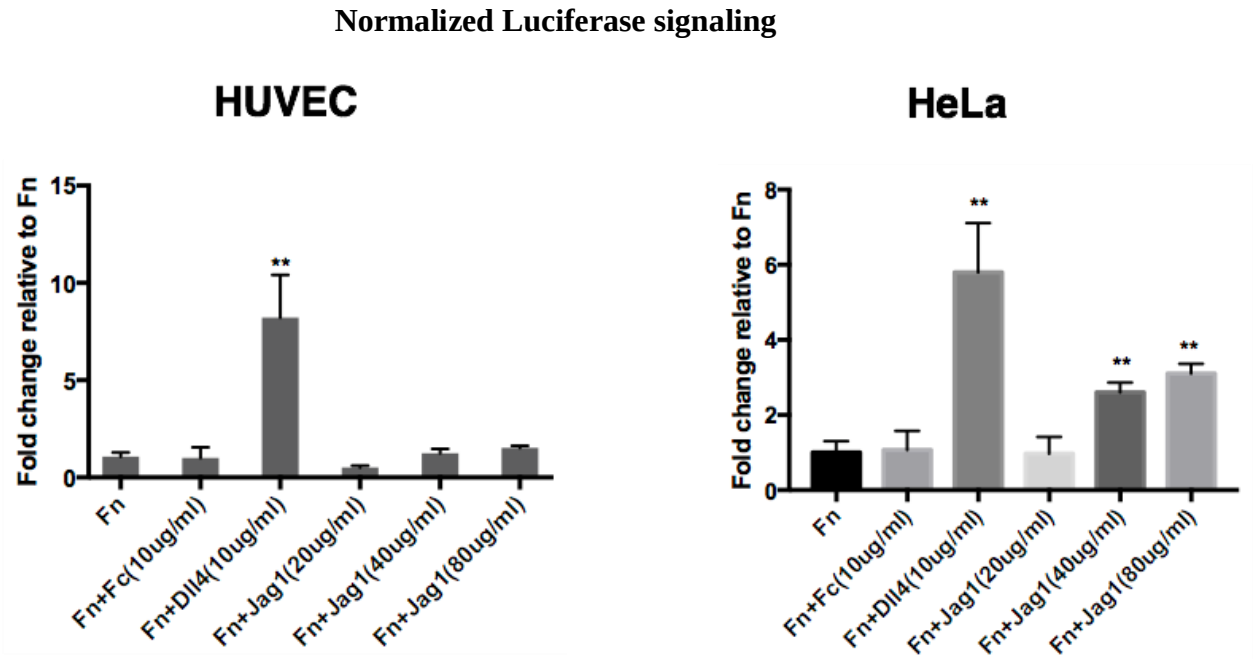

Figure 4-3. Low dose of Dll4 activated EC Notch, while Jag1 activated Notch in HeLa but not in HUVECs

Dose curve studies were performed on both ligands using Luciferase reporter assay. 10 μg/ml of Dll4 is sufficient in activating EC Notch. High dose(40-80 μg/ml) can activate Notch signaling in HeLa cells but not in HUVECs.

Normalized Luciferase signaling

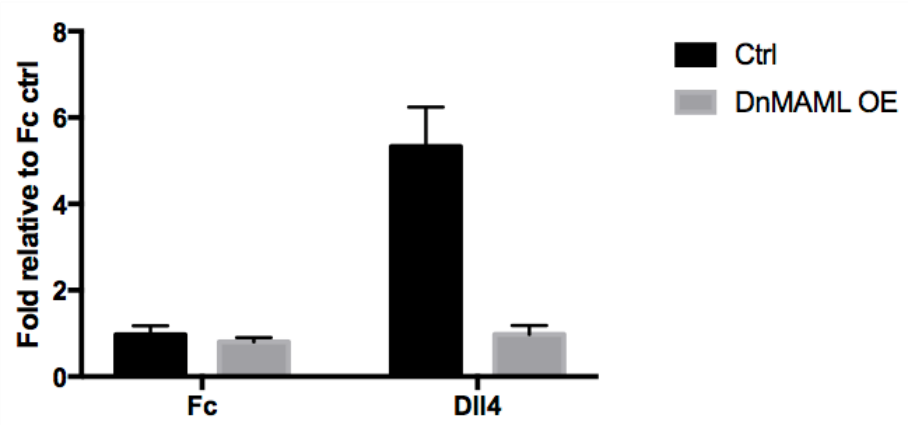

Figure 4-4. DnMAML OE inhibited tethered-Dll4 stimulated Notch signaling in HUVECs

Luciferase reporter assay was used to measure the Notch activation of lentiviral-mediated DnMAML Over Expression (OE) HUVEC stimulated by tethered-Dll4. DnMAML OE completely inhibited the Notch activation by Dll4.

When JAG1-Fc was used to induce Notch signaling, we observed lower responses relative to DLL4 in HUVECs, with no concentrations sufficient to achieve significant induction of luciferase activity that compared to that achieved by using DLL4-Fc (Figure 4-3). To determine if this was a HUVEC-specific response, we tested JAG1-Fc induction in HeLa cells. The magnitude of response was higher in HeLa, but a minimum of 40 μg/ml of JAG1 was necessary to significantly induce Notch signaling (Figure 4-3). We conclude that increasing the concentration of JAG1-Fc was not able to replicate the magnitude of the effect seen when DLL4-Fc was used to activate Notch in two different cell types. We were concerned that the low degree of JAG1-NOTCH response was due to inability to properly present JAG1 when using the tethered ligand system, so we repeated these assays using a co-culture system, where HUVEC cells expressing the Notch CSL-Luciferase reporter were co-cultured with HeLa cells expressing selected Notch ligands to stimulate Notch in

the context of normal cell-cell contact. In the co-culture system, JAG1-Fc continued to show lower induction of Notch signaling than that achieved by DLL4-Fc (Figure 4-5). This may be explained by poor responsiveness of endothelial cells to JAG1, or the possibility that endothelial JAG1 functions through a non-canonical, CSL-independent signal transduction, which cannot be efficiently detected by the CSL-luciferase reporter.

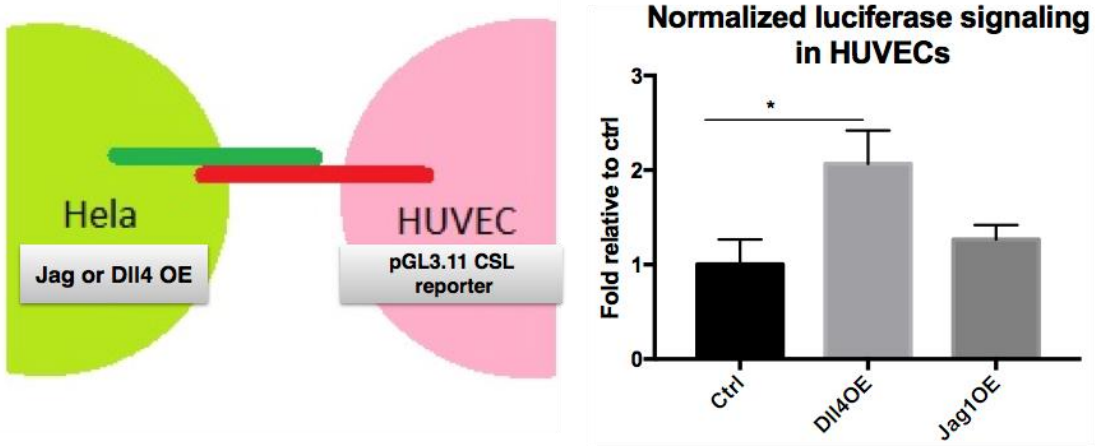

Figure 4-5. Dll4, but not Jag1 activated EC Notch using co-culture system

HeLa cells overexpressing Jag or Dll4 was co-cultured with HUVEC transfected with pGL3.11 CSL Notch reporter. Notch activity was measured using dual luciferase assay. Dll4, but not Jag1 activated Notch in HUVECs.

4.2.1.3 Robust Notch activation was detected 6 hours after seeding the cells

In order to identify early effectors/primary response genes after Notch activation, we performed a time course study by quantitating gene expression of selected canonical Notch target genes. We identified robust response 6 hours after seeding the cells (Figure 4-6). We estimate that this timepoint is a snapshot of the gene expression profile approximately 3-4 hours. after HUVECs fully contact the ligands, based upon visual assessments of the time it takes for HUVEC to fully settle onto plates and cell spreading to have occurred, which took approximately 2 to 3 hours.

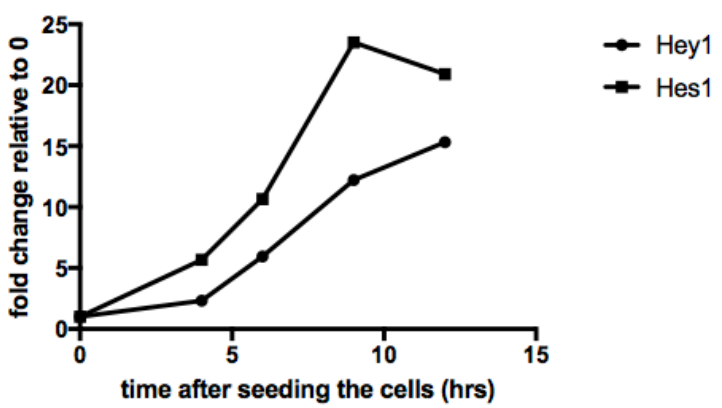

Figure 4-6. Time course studies of tethered-Dll4 stimulation

HUVECs were seed on tethered-Dll4, and RNA was collected at different timepoint. 4 hours after seeding cells, we were able to detected significant up-regulation of Hey1 and Hes1 but with a low fold change. 6 hours showed a robust response of both canonical targets.

In summary, our assessment led to optimization of the tethered-ligand assay where we coat the plates/well with 10 μg/ml of Fibronectin ECM along with 10μg/ml of DLL4-Fc/IgG-Fc or 40 μg/ml of JAG1-Fc. We also determined that the 6 hour timepoint may be optimal

for for gene expression profiling (comparable to the timepoint in the RiboTag study (See **Results1: II.A**).

4.2.2 Transcriptome profiling and Bioinformatic analysis of the tethered-ligand assay

To understand the mechanism by which Notch signals in endothelial cells, we profiled genes regulated by DLL4- or JAG1-Notch activation following 6 hours of ligand stimulation *in-vitro* using RNA-seq (Figure 4-7). We compared DLL4-Fc or JAG1-Fc stimulated ECs with IgG-Fc stimulated ECs in two different human primary endothelial cells whose sources were the human umbilical cord and the human retina (HUVEC and HRECs, respectively). Each experiment included 3 replicates for each condition. For the experiments with HUVECs, each experiment consisted of cells from a different isolate (biological replicates), while the experiments from HRECs were obtained from different frozen batches from a single commercially purchased vial Cell Systems (technical replicates). The sequencing conditions for HUVECs were ~30 million SE read depth with 100-base fragments on the TruSeq platform in the Sulzberger Columbia Genome Center. Conditions for the HRECs were ~30 million PE reads with 150base-paired fragments using the services of Novogene corporation.

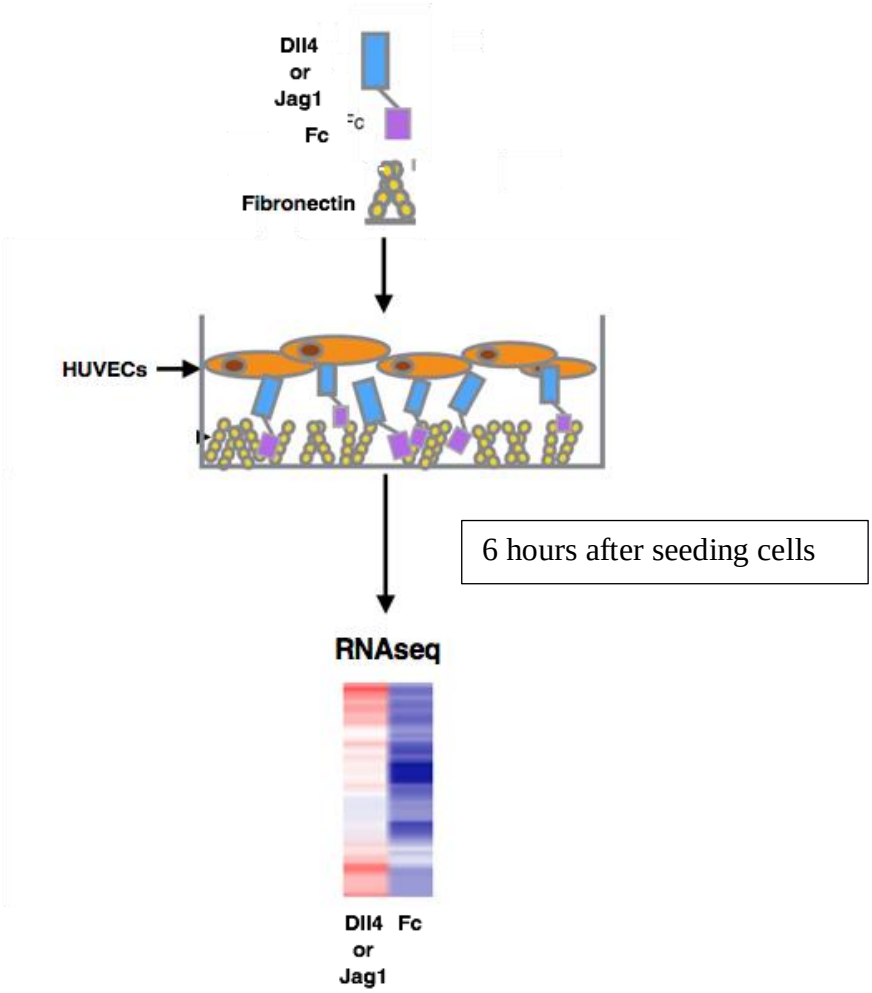

Figure 4-7. Schematic of TLA screening

10 μg/ml of Dll4-Fc, 40 μg/ml of Jag1-Fc and 10 μg/ml Fc control mixed with 10mg/ml Fibronectin were used to coat tissue culture dishes. HUVECs and HRECs were seeded onto the coated dishes at sub-confluency and incubate for 6 hours. RNA were then extracted and subjected to RNA-seq.

Raw reads from the HUVEC and HRECs were mapped to the Human database (ENSEMBL/GRCh38) using STAR (version 2.5.0a) and processed with Samtools (version 1.4.1). The counts obtained by FeatureCounts were analyzed by DESeq2 to identify differentially expressed genes.

4.2.3 Identifying endothelial gene transcripts significantly stimulated by Dll4-Fc

4.2.3.1 PCA of HUVEC samples showed significant batch effect, and HREC samples exhibits tight clustering

We assessed the quality of these samples by determining the clustering patterns using the PCA plots. The PCA analysis of the HUVECs showed a differential segregation of one sample in both conditions, indicating a batch effect. The PCA plot of the HREC showed tight clustering of the 3 replicates within each condition (Figure 4-8).

HUVECs

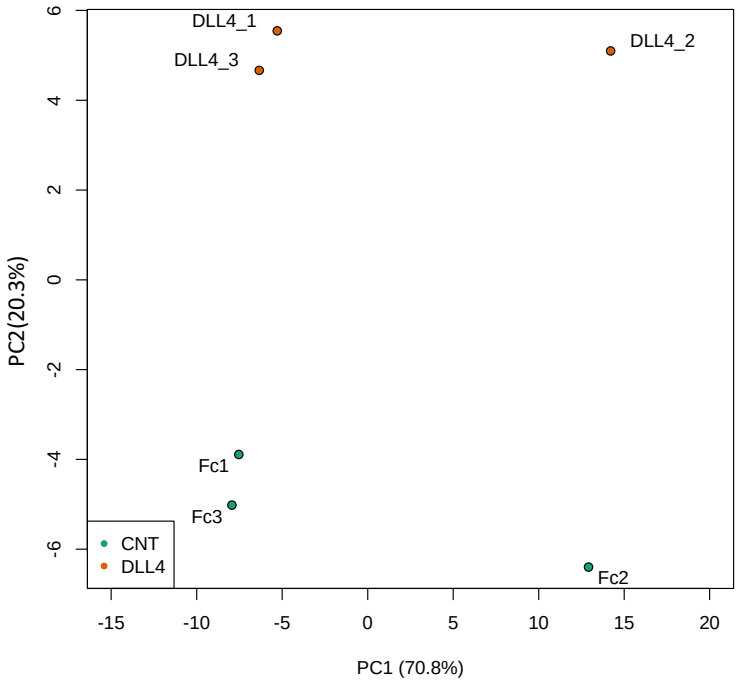

HRECs

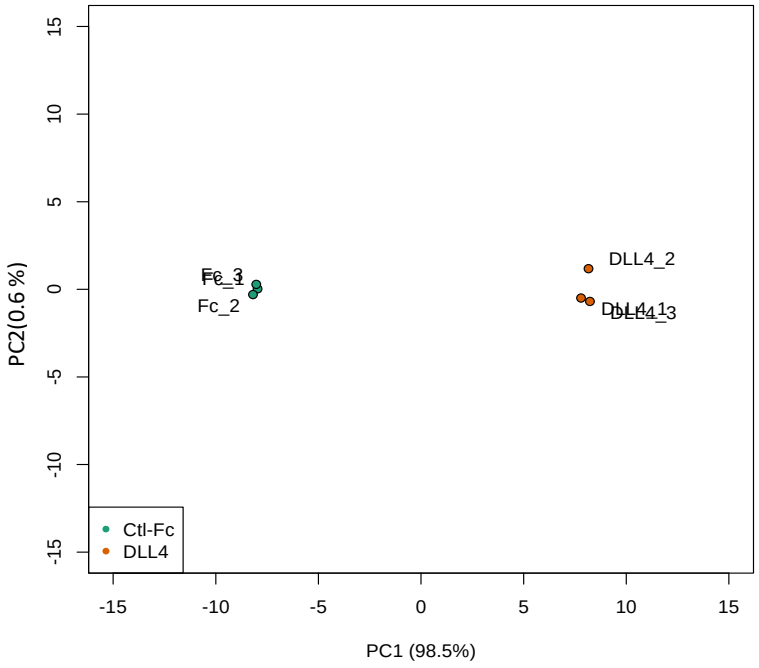

Figure 4-8. PCA plot of DLL4-TLA

Two-dimensional principal component analysis (PCA) plot showing segregation of the DLL4 stimulated samples and Fc samples into two clusters. HUVECs exhibited large variance between individual samples. HRECs showed tight clustering.

4.2.3.2 Gene Ontology analysis shows enrichment of genes in Angiogenesis and Notch pathways

Gene Ontology analysis (PANTHER Db) on the upregulated (P_{adj}=0.05) from both HUVECs and HRECs identified enrichment of several pathways. As expected, GO:Notch signaling pathway (Fold enrichment HUVECs/HRECs= 8.28/5.28, FDR= <0.05) and GO:Angiogenesis (Fold enrichment HUVECs/HRECs= 2.89/2.98, FDR= <0.05), were enriched in both cell types, as expected (Figure 4-9).

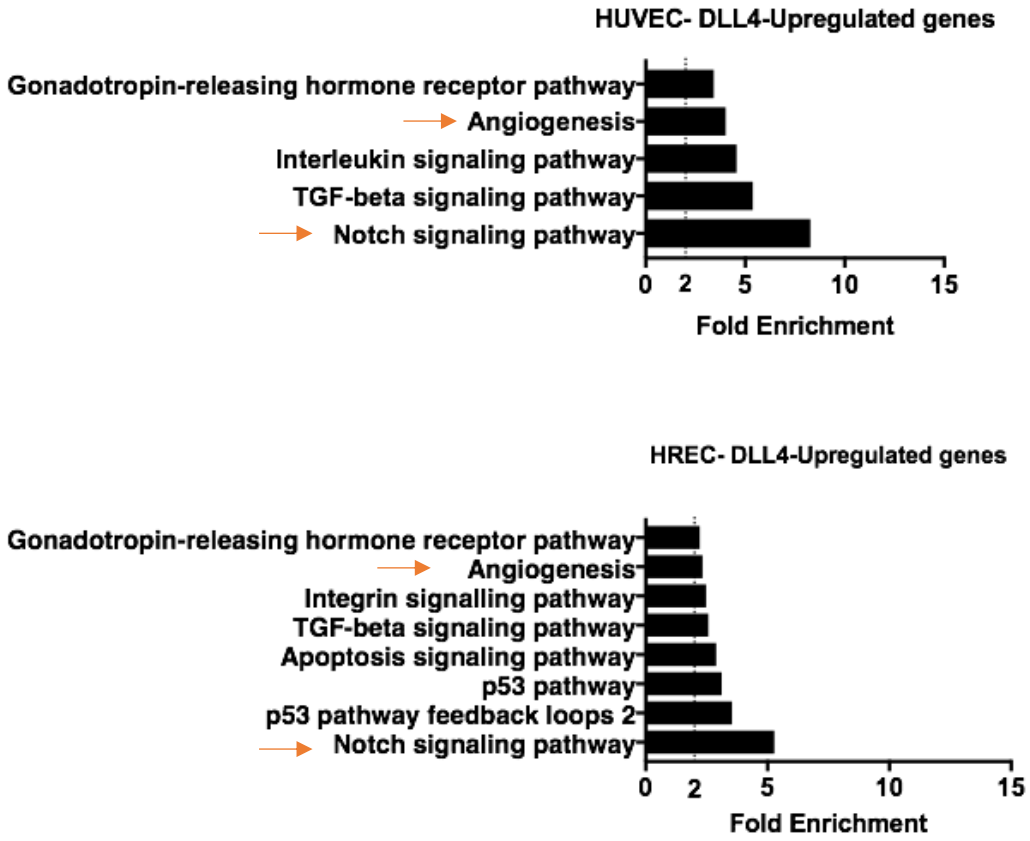

Figure 4-9. Gene Ontology Pathway Analysis

Gene Ontology pathway analysis showed significant enrichment of "Angiogenesis pathway" and "Notch signaling pathway" (indicated by the arrow) in Dll4-upregulated genes in both HUVECs and HRECs

4.2.3.3 Novel and canonical DLL4-Notch targets were identified after 6 hour. of DLL4-stimulation

Differential gene expression analysis of the HUVECs and HRECs identified both canonical and novel gene targets with significant expression changes in the DLL4-Notch induced ECs. Since the aim of our study was to identify direct/primary Notch effectors and

Notch signal activation leads to transition of repressed genes to transcriptional activated genes we focused on upregulated genes in this screen.

Of the 719 genes ($P_{adj} < 0.05$) in HUVECs that were significantly altered, 388 genes were upregulated with a fold change of at least 1.2-fold ($Log_2FC = 0.27$). In HRECs, a total of 3330 genes ($P_{adj} < 0.05$) were significantly altered, of which 956 were upregulated by a fold change of at least 1.2-fold.

A comparative analysis between the HUVECs and the HRECs showed overlapping genes (n=692) of which 340 up-regulated genes ($P_{adj} = 0.05$, $Log_2FC = 0.27$) had a foldchange of at least 1.2-fold. (Figure 4-10)

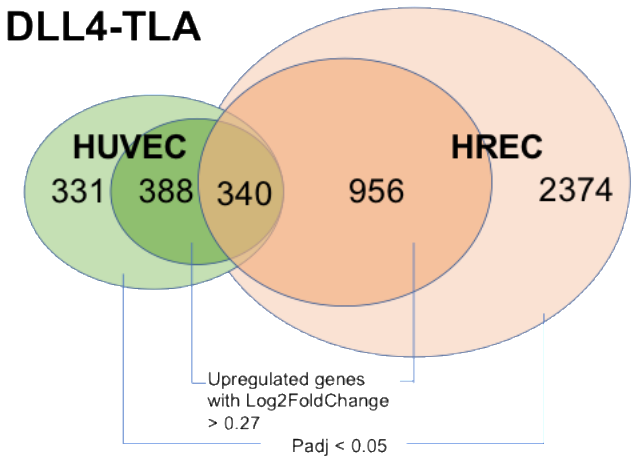

Figure 4-10. Comparison of significant Dll4 up-regulated genes in HUVECs and HRECs

Venn plots compared genes regulated by Dll4 between HUVEC and HREC. 719 genes were significantly regulated (Padj<0.05) in HUVEC, among which 388 genes were up-regulated (Padj<0.05, Log2FoldChange>=0.27). In HREC, 3330 genes were significantly regulated (Padj<0.05) , of which 956 genes were up-regulated(Padj<0.05, Log2FoldChange>=0.27). A

comparative analysis between the HUVECs and the HRECs showed 340 significantly up-regulated genes in common(Padj<0.05, Log2FoldChange>=0.27).

As expected, we observed upregulation of multiple canonical Notch targets such as HEY2, DLL4, NRARP, HES1, GJA5 and EFNB2 (Figure 4 10. Comparison of significant Dll4 up-regulated genes in HUVECs and HRECs). Among the novel genes identified, we uncovered a set of G-protein coupled receptor (GPCR) related genes rapidly induced by DLL4 in both cell types (See Table 4-2). These findings are in accordance with the findings from the RiboTag screen, which showed GSI mediated downregulation of GPCR genes. This finding is of interest because GPCRs play critical roles in cell migration, proliferation, changes in cell shape and polarity, and organization of cells into multicellular structures. A few genes like RASA1(Eerola et al., 2003) and FZD4(Ye et al., 2009) also influence disease states and are linked to human vascular diseases.

Among the GPCRs related genes, upregulation of the Rho-GTPase RND1 was significantly stronger and ranked in the top 20 list of differentially expressed genes by fold change (See Figure 4-10. Comparison of significant Dll4 up-regulated genes in HUVECs and HRECs, Table 4-2 and Figure 4-11), and will be discussed in more detail in Chapter 5.

Table 4-1. Top 20 hits induced by Dll4 in both HUVECs and HRECs, ranked by fold change in HUVECs

Symbol	Gene	log_2FC	P_{adj}
GJA5	Gap junction protein alpha5	5.86	1.1E-10
RND1	**Rho family GTPase**	4.56	2.4E-12
SLC46A3	Solute carrier family46 member3	2.93	3.5E-14
DLL4	Delta like canonical Notch ligand4	2.62	1.5E-14
SETBP1	SET binding protein1	2.60	6.3E-11
SLC45A4	Solute carrier family45 member4	2.56	9.2E-15
SNAI2	Snail family transcriptional repressor2	2.46	2.1E-07
EFNB2	Ephrin B2	2.39	5.2E-09
PRICKLE2	Prickle planar cell polarity protein2	2.31	3.9E-11
ABCA1	ATP binding cassette subfamily A1	2.27	4.4E-05
GUCY1B3	Guanylate cyclase1 soluble subunit beta3	2.20	2.4E-04
ROR1	Receptor tyrosine kinase- orphan receptor1	2.17	6.1E-10
HES1	Hes family transcription factor1	2.15	3.3E-12
DKK2	Dickkopf WNT signaling pathway inhibitor2	2.14	3.5E-03
IL33	Interleukin 33	2.11	3.0E-03
SAT1	Spermidine/spermine N1-acetyltransferase1	2.11	1.8E-13
EFNA1	Ephrin A1	1.87	4.8E-04
SORBS2	Sorbin and SH3 domain containing2	1.82	9.5E-05
SERPINB9	Serpin family B member9	1.76	1.8E-17
NRARP	NOTCH-regulated ankyrin repeat protein	1.75	2.9E-14
RAPGEF5	Rap guanine nucleotide exchange factor5	1.60	4.5E-16

P adj: adjusted P value

Blue: canonical targets
Red: top fold change novel gene
Box: G protein family gene

Table 4-2. GPCR/G proteins induced by Dll4 in both HUVECs and HRECs, ranked by fold change in HUVECs

Symbol	Gene	log_2FC	Padj
RND1	Rho family GTPase 1	4.56	2.4E-12
GUCY1B3	Guanylate cyclase 1 soluble subunit beta	2.20	2.4E-04
RAPGEF5	Rap guanine nucleotide exchange factor 5	1.60	4.5E-16
RGS4	Regulator of G-protein signaling 4	1.24	3.0E-02
ARHGEF17	Rho guanine nucleotide exchange factor 17	1.16	4.2E-06
F2RL1	F2R like trypsin receptor 1	1.01	4.3E-03
ARHGAP24	Rho GTPase activating protein 24	0.95	6.3E-06
F2R	Coagulation factor II thrombin receptor	0.78	1.0E-03
FZD4	Frizzled class receptor 4	0.70	1.0E-02

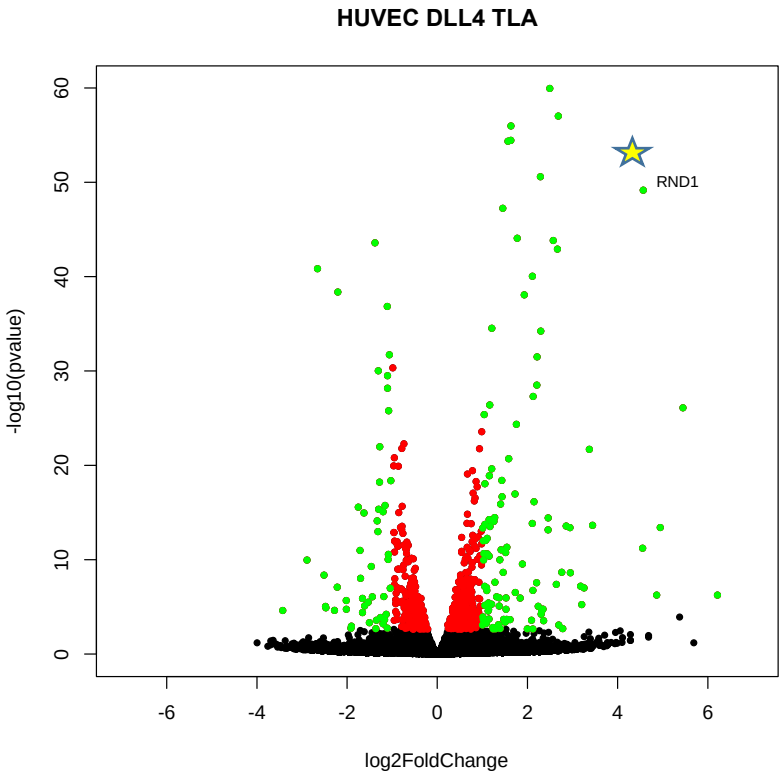
HUVEC DLL4 TLA
RND1
-log10(pvalue)
0
10
20
30
40
50
60
-6
-4
-2
0
2
4
6
log2FoldChange

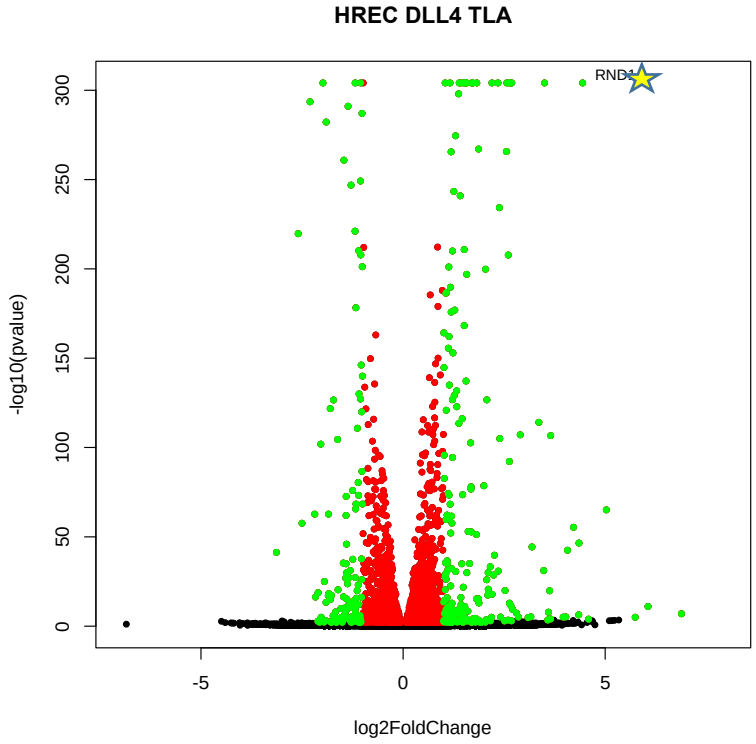
HREC DLL4 TLA
RND1
-log10(pvalue)
0
50
100
150
200
250
300
-5
0
5
log2FoldChange

Figure 4-11. Volcano plots of DLL4-TLA in HUVECs and HRECs

Volcano plots showing transcriptional changes of DLL4 stimulation compared with Fc Control. The x-axis represents the Log fold change calculated in this analysis, and the y-axis shows the Log10 P values. Each gene is represented by a dot. The dots in red indicate genes that are statistically significant (Padj < 0.05). Additionally, the green dots represent genes that are up/downregulated 1.2 folds. Small GTPase *RND1* was highlighted with star due to significant stronger induction fold and significance compared with other targets in both cell types.

4.2.3.4 Novel genes identified by RNA-seq analysis of DLL4 regulated genes show similar trends when validated using quantitative PCR.

We validated the expression patterns of a few GPCR related genes that may be novel targets with high interest by DLL4-stimulation of HUVEC and HRECs and identifying the expression levels after GSI treatment. We found GSI to repress the expression levels of these novel targets, indicating that the expression induction of these genes was Notch dependent (Figure 4-12).

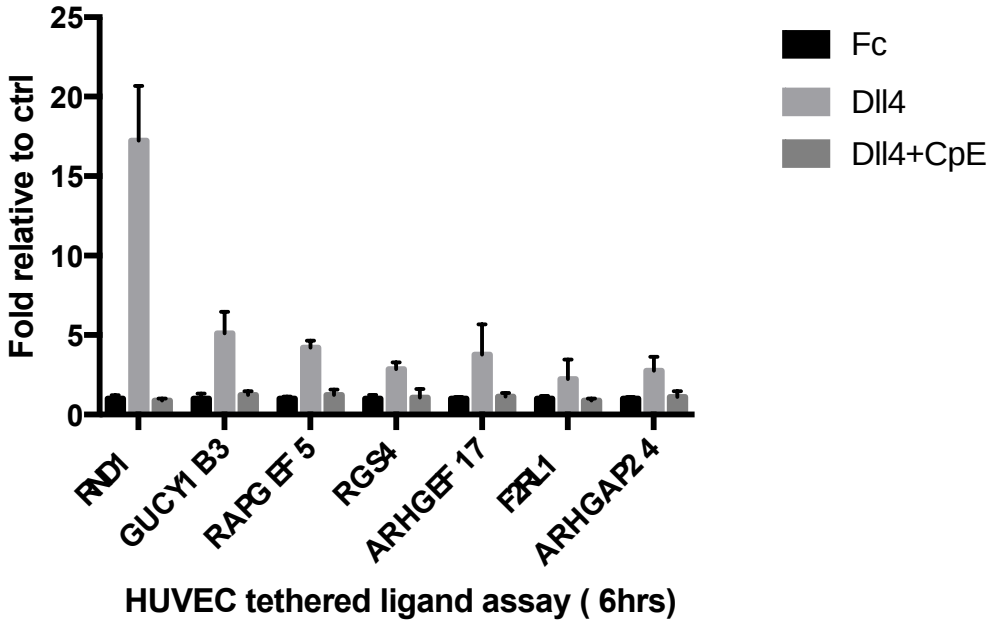

Figure 4-12. Validation of selected novel G-protein family Notch targets using RT-qPCR

RNA-seq analysis of the TLA results was confirmed using RT-qPCR. Selected Novel Notch targets-G-protein family genes were up-regulated with Dll4 stimulation, and CpE treatment significantly inhibited the induction to basal level. This experiment have only been performed twice.

4.2.3.5 Identification of genes identified both by the RiboTag brain profile and TLA screens

Of the common genes identified by the TLA (n=692, $P_{adj} < 0.05$, Log2FC>+/- 0.27), 18.2 % (n=126) overlapped with the RiboTag *in vivo* screen list (Brain IP). Of the 126 overlapping genes, 40 genes that were upregulated by DLL4 stimulation were downregulated in the brain of GSI treated RiboTag mice (Figure 4-13). Gene Ontology pathway analysis of these 40 common genes identified GO: Notch signaling to be enriched 29.47fold (FDR=0.0143).

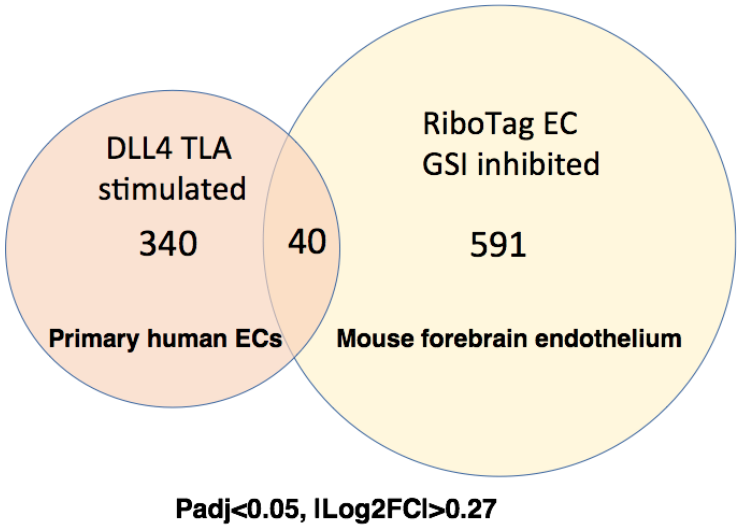

Figure 4-13. Identification of rapid (6 hour) Notch targets by Comparing Dll4-TLA and RiboTag screens

Venn plots comparing the 340 common upregulated genes (Padj<0.05 FC>1.2) induced by DLL4-TLA and the 591 DAPT repressed genes (Padj<0.05 |FC|>1.2) in the endothelial fraction of the P8 brain. 40 genes overlapped between the two analysis.

As expected, the 40 genes included canonical Notch genes- *GJA5*, *DLL4*, *HES1*, *HEY1*, *NRARP* and *EFNB2*, as well as a number of novel genes. Based on their novelty for Notch function in endothelium, we chose to focus further on GPCR related genes such as *RND1* (Table 4-3).

Table 4-3. 40 Common genes between Dll4-TLA and RiboTag EC screens

Gene	Log2FC		
	HUV	HREC	Ribotag-IP
GJA5	5.03	5.45	-1.06
RND1	4.44	4.57	-0.30
NPR3	4.35	4.55	-0.55
INHBB	4.07	3.44	-0.38
SLC45A4	3.50	2.66	-0.29
EFNB2	2.64	2.50	-0.35
DLL4	2.20	2.68	-1.14
UNC5B	1.81	1.41	-1.50
DKK2	1.68	2.11	-0.60
HEY1	1.61	1.58	-1.04
SORBS2	1.56	1.84	-0.55
NRARP	1.55	1.63	-0.93
SAT1	1.54	2.11	-0.93
MECOM	1.22	0.52	-0.55
KCNJ2	1.21	1.02	-1.02
EFNA1	1.14	1.93	-0.98
TSPAN15	1.09	0.72	-0.48
OAZ2	1.07	0.49	-0.51
SPSB1	1.06	1.16	-0.49
GJA4	0.98	1.89	-0.86
MAOA	0.89	1.01	-0.27
HES1	0.80	2.13	-0.61
SH2D3C	0.78	0.99	-0.41
CLMN	0.71	0.74	-0.43
LMO2	0.69	0.72	-0.50
FHL3	0.69	0.86	-0.52
HIC1	0.68	0.49	-0.31
CDKN2B	0.54	0.78	-0.84
RGS3	0.54	0.68	-0.73
PMEPA1	0.53	0.58	-0.65
FAM84B	0.52	0.68	-0.30
PEX5	0.48	0.42	-0.33
SLC29A1	0.45	0.33	-0.33
FLT4	0.45	0.53	-0.42
ENDOD1	0.44	0.44	-0.29

TGFB1	0.38	0.39	-0.54
RHOJ	0.38	0.34	-0.41
TNFRSF21	0.37	0.43	-0.30
STX6	0.33	0.34	-0.35
LIMS1	0.29	0.47	-0.39

In summary, the TLA with immobilized recombinant DLL4 induced Notch signaling in both ECs tested. Analysis of the expression profile successfully identified known canonical Notch targets (marked in red), as well as novel genes targets including a set of GPCR related proteins. Cross comparison with RiboTag EC in vivo screening dataset identified 40 overlapped genes. We conclude that these novel candidates rapidly respond to Notch signaling *in vitro* and Notch inhibition *in vivo*. One interesting gene identified by both the RiboTag and DLL4-TLA screen was RND1, a Rho GTPase (highlighted in Table 4-3).

4.2.4 Identifying endothelial transcriptional responses to JAG1/Notch signaling using tethered ligand assay

Similar to the DLL4 induction of Notch signaling, we performed an experiment with JAG1-Fc to understand the effect of JAG1 on Notch signaling. Comparison of the DLL4- and JAG1- induction levels in HUVECs and HRECs led to the observation that JAG1 was able to induce Notch signaling, albeit weaker in comparison to DLL4.

4.2.4.1 Principal component analysis showed tight clustering of samples for JAG-Fc TLA in endothelial cells

Principal component analysis of the normalized counts from JAG1 induction profile demonstrated a tight clustering of samples with the same conditions (Figure 4-14). The

data on HUVECs was generated with two samples (biological replicates) while the data with HRECs was generated with three samples (technical replicates).

HUVEC

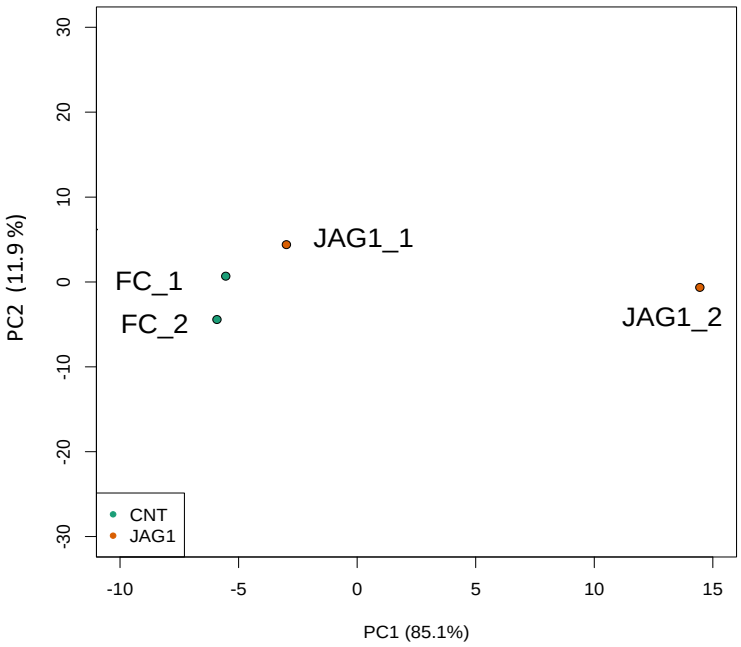

HREC

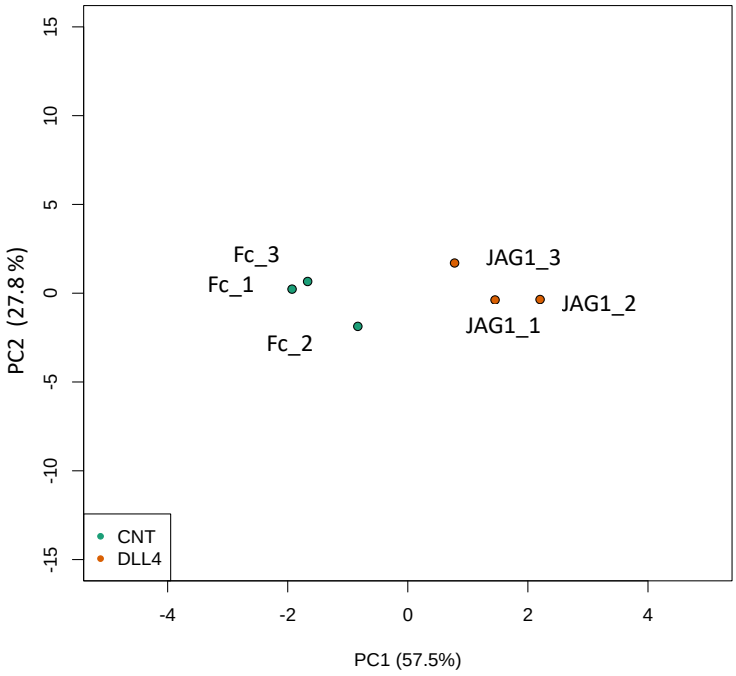

Figure 4-14. PCA OF JAG-TLA

Two-dimensional principal component analysis (PCA) plot showing segregation of the JAG1 stimulated samples and Fc samples into two clusters. HUVECs exhibited large variance between individual samples. HRECs showed tight clustering.

4.2.4.2 Gene Ontology analysis shows enrichment of genes in Angiogenesis in HREC after JAG stimulation

Similar to the DLL4, we analyzed the JAG1 upregulated genes (P_{adj} <0.05) for over-represented pathways (Gene Ontology analysis using PANTHER Db) in both HUVECs and HRECs. Surprisingly, no statistically significant pathways were identified in the HUVEC analysis. This could be due to the limited replicated (n=2) we included in this study. Analysis with the upregulated genes in HRECs identified a few pathways including GO: Angiogenesis (Fold enrichment = 7.32, FDR= 0.00105).

4.2.4.3 Differential gene expression profiling detected weak but significant induction of Notch targets by JAG1

Data from RNA sequencing of HUVEC and HRECs stimulated by JAG1 identified few genes to be differentially regulated. Analysis of the screen with HUVECs identified 730 significantly (P_{adj} <0.05) up/downregulated genes Log2FC of 0.27 (~1.2 Fold), among which 200 genes were upregulated. In HRECs, 120 genes were significantly up/down

regulated ~1.2 Fold (P_{adj} <0.05, Log2FC of 0.27). Comparing the profiles from the two screens (HUVECs and HRECs) identified 18 common genes (11 upregulated, 6 downregulated, 1 conflict) with a Log2FC of 0.27 (~1.2 fold) in both the screens.

All 11 upregulated genes, were common to the DLL4 profile (both HUVECs and HRECs) (Table 4-4). Among the 11 common genes were canonical Notch target *HES1* (labeled red) and several published Notch targets including *INHBA* (Chang et al., 2011), *PRICKLE2* (Katoh & Katoh, 2007) and *SORBS2* (Fouillade et al., 2013). Most importantly, several novel genes including *RND1* (highlighted in Table4-4, and Figure 4-15) was also detected as genes commonly induced by both DLL4 and JAG1.

Table 4-4. Up-regulated genes by Jag1 in both cell types

Gene	Log2FC			
	HUV-JAG1	HREC-JAG1	HUV-DLL4	HREC-DLL4
RND1	2.47	1.28	4.57	4.44
HES1	1.95	0.77	2.13	0.80
PRICKLE2	1.58	0.83	2.29	2.60
F2RL1	1.31	0.54	1.00	1.25
INHBA	1.30	0.72	1.44	1.30
SLC46A3	1.13	0.70	2.94	2.56
YPEL2	1.05	0.30	1.24	0.69
ZNF702P	1.04	0.27	#N/A	0.94
SORBS2	1.01	0.39	1.84	1.56
PLD1	0.95	0.30	1.11	1.14

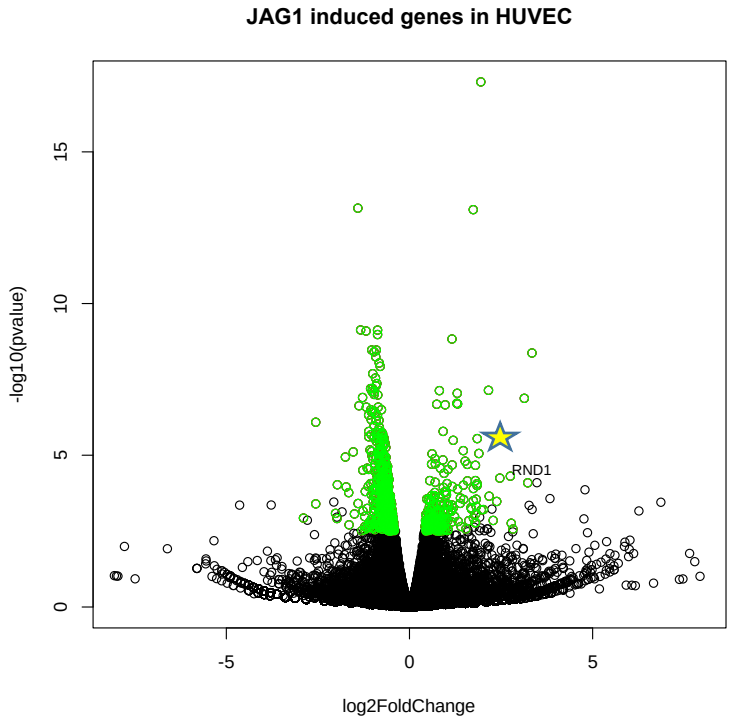

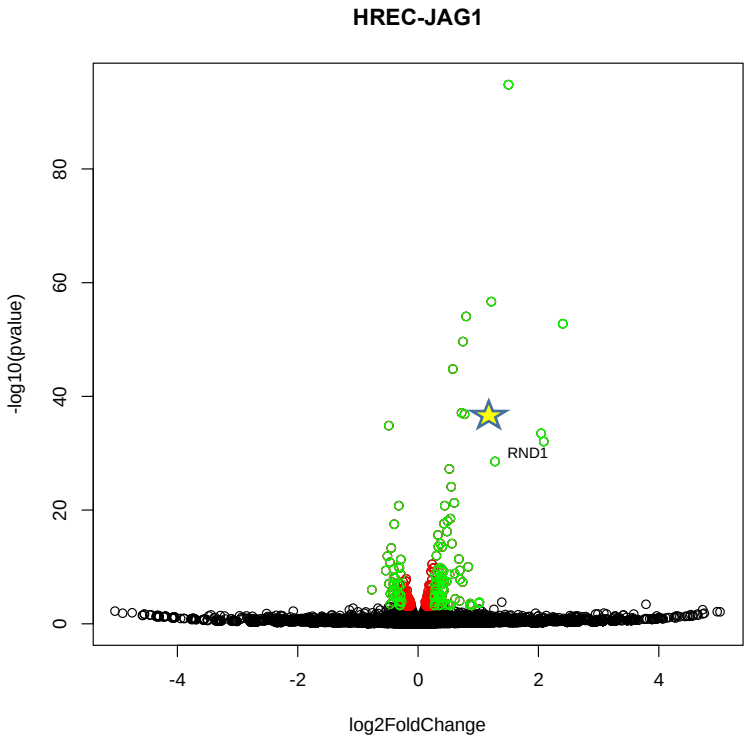

Figure 4-15. Volcano plots of Jag1 TLA

Volcano plots showing gene changes 6 hours after Jag1 stimulation. The x-axis represents the Log fold change calculated in this analysis, and the y-axis shows the Log10 P values. Each gene is represented by a dot. The dots in red indicate genes that are statistically significant (Padj < 0.05). Additionally, the green dots represent genes that are up/downregulated 1.2fold. RND1 was highlighted in both cell types, showing a relatively strong fold change.

In summary, our analysis on ECs stimulated by JAG1 identified a weak activation potency. We did not see significant down-regulation of canonical Notch targets, which may occur if JAG-Fc blocks the EC specific DLL4 activity which is exhibited in cultured EC. Furthermore, comparison of the DLL4 and JAG1 profiles (using Common genes between HUVEC and HREC) identified 88% genes (16 of 18 genes) to be common. Among the 11 common upregulated genes by JAG1 were both canonical targets and novel genes, including the GTPase *RND1*. Our data suggested that JAG1 functions as a weak activator of Notch signaling in endothelial cells.

4.3 Analysis: Profiling Endothelial Notch signaling using EGTA assay

As discussed earlier (See **Results2: I.B.**), using EDTA/EGTA to activate Notch signaling eliminates the need to trypsinize and plate cells and so allows us to perform a tighter time control of Notch activation and screen for rapid response genes earlier than 6 hour. Primary targets are expected to be much more rapidly induced by EDTA/EGTA and the secondary effectors would be transcribed slower than the primary targets. We hypothesized that by focusing on early timepoints of EGTA induction, we would be able to screens for direct/primary transcriptional targets. In combination of the dataset generated by the

RiboTagEC screens and the TLA screens, we would be able to identify direct/primary endothelial Notch effectors with both in vivo and in vitro relevance.

Our strategy included suppressing endogenous Notch signaling with 200nM Compound E (CpE), a GSI inhibitor treatment overnight and treating the recuperating cells (after 2x washes with PBS) with 10 μM EGTA for 15 minutes in PBS. The cells were then replenished with normal media and the RNA collected from these cells at various timepoints of interest (Figure 4-16). We included a condition where the EGTA stimulated ECs are co-treated with CpE to identify Notch-specific target; that is, we compared transcripts with and without a GSI. CpE treatment should be able to down-regulate the induction by EGTA if the target is canonical Notch dependent.

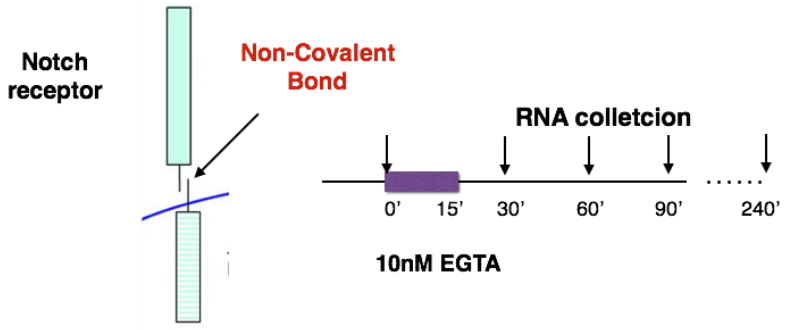

Figure 4-16. Schematic of EGTA assay

Notch proteins are heterodimers composed of extracellular domain and transmembrane signaling domains, which are held together by non-covalent bond. Calcium depletion dissociates the heterodimer and activate Notch in ligand independent way. In this assay, ECs were cultured with

200nM CpE overnight to inhibit endogenous Notch signaling, followed by 15 minutes treatment of 10nM EGTA. RNA was extracted at different timepoint after EGTA treatment (0-4 hours).

4.3.1 Analysis of time course study of EDTA/EGTA assay

In order to choose an early timepoint that allows us to capture primary and early response targets, we quantitated samples at different timepoints after EDTA/EGTA treatment for the levels of canonical Notch targets using a quantitative PCR (Figure 4-17).

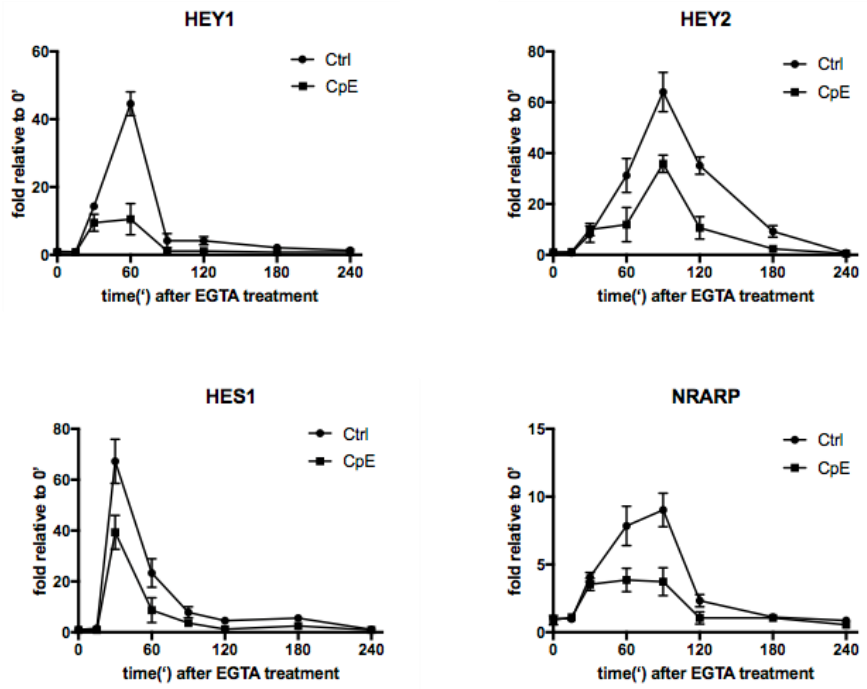

Figure 4-17 . Rapid induction of canonical Notch target in HUVECs after EGTA treatment

RNA was extracted every 30 minutes from 0 hour to 4 hours after EGTA treatment. RT-qPCR on canonical Notch targets *HEY1, HEY2, HES1 and NRARP* showed rapid induction of those genes, which peaks at 0.5-1.5 hours and return to basal expression in 2-3 hours.

Quantitative analysis of canonical targets showed that the induction starts as early as 15-30 minutes, peaks at 0.5-1.5 hour. and returns to basal at 2-3 hours. Expression levels of *HEY1*, *HEY2*, *HES1*, *NRARP* in EDTA stimulated HUVECs increased rapidly and returned to basal levels within 3 hours (data not shown). CpE treatment significantly down regulated the induction in all gene targets. We repeated the experiments using EGTA in both HUVECs and HREC and detected a similar pattern.

4.3.2 Rapid gene expression changes were identified at 1 and 1.5 hour. after EGTA stimulus

Based on the observation that EDTA and EGTA rapidly induced expression of the canonical Notch targets and the induction peaks at 1-2 hours, we performed an unbiased screen of HUVECs at 1h and 1.5h timepoints after EGTA induction. We sequenced RNA from these two timepoints with a read depth of ~20 million PE reads with 150base-paired fragments using the services of Novogene corporation. Raw reads from the HUVEC and HRECs were mapped to the Human database (ENSEMBL/GRCh38) using STAR (version 2.5.0a) and processed with Samtools (version 1.4.1). The counts obtained by FeatureCounts were analyzed by DESeq2 to identify differentially expressed genes.

The analysis identified 132 and 727 ($P_{adj} < 0.05$) differentially expressed genes to be significantly up/down-regulated within 1 hour and 1.5 hour (respectively) of EGTA induction. Because the aim of our study was to identify primary effectors of Notch

signaling, we limited our analysis to targets that were up-regulated. In the 1hour profile, 131 of 132 genes were upregulated (all with Log2FC > 0.27), while the 1.5 hour. profile showed 612 genes of 727 to be upregulated (600 genes with Log2FC > 0.27). In combination, 644 genes were upregulated in 1-1.5hour.

4.3.3 Common genes were identified between the RiboTagEC brain profile, TLA screens and 1.5hour. EGTA induced genes

Comparison of the 1-1.5 hour profile with the 40 common genes identified by RiboTagEC screening and tethered-DLL4 screening (See Results2: II.B.1.(e)), identified 17 of 40 genes (42.5%) from the 1 and 1.5 hour profile as overlapping (See Table 4-5 and Figure 4-18).Out of the 17 genes, we identified 6 canonical targets including *GJA5, DLL4, EFNB2, HES1, NRARP, HEY1*. The other genes are potential direct Notch targets, based upon regulation within 1.5 hours, with both in vivo and in vitro significance.

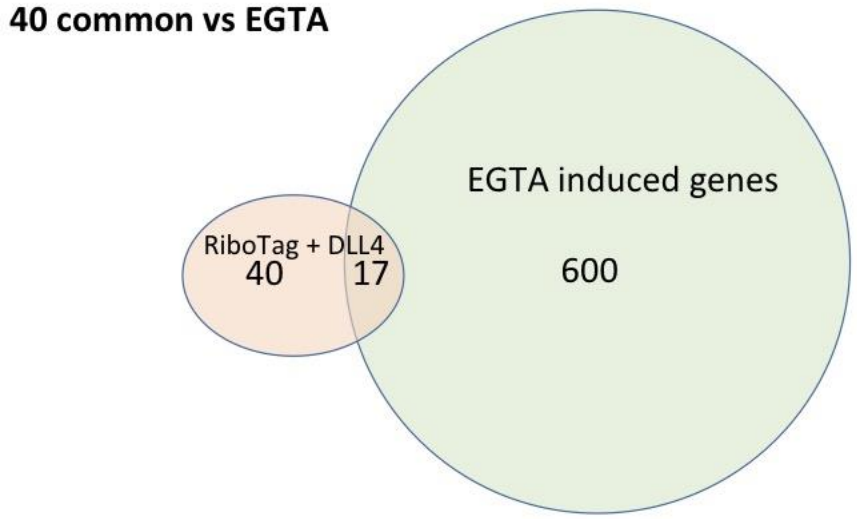

Figure 4-18. Identification of primary Notch targets by comparing EGTA, TLA and RiboTag datasets

Venn plots identifying direct early targets of Notch signaling. EGTA stimulation of HUVECs identified 600 genes to be significantly upregulated (Fold Change > 1.2, $P_{adj} < 0.05$). These 600 genes were compared to the 40 common genes identified comparing endothelial fraction from P8 mice brain and the primary endothelial cells stimulated by DLL4 for 6h. 17 genes overlapped between the two groups.

Table 4-5. 17 genes identified as potential Notch direct targets by RiboTag, TLA and EGTA screens

Gene	RiboTag IP	TLA-DLL4 Log2FC		EGTA Log2FC			Direct target on SpDAM IP list
		HREC	HUV	1hr	1.5hr	+ CpE	
HEY1	-1.04	1.61	1.58	5.36	6.17	-1.63	Y
RND1	-0.30	4.44	4.57	3.65	4.94	-2.16	Y
HES1	-0.61	0.80	2.13	5.76	4.53	N/A	Y
GJA5	-1.06	5.03	5.45	N/A	3.35	N/A	Y
DLL4	-1.14	2.20	2.68	2.88	3.35	-3.28	Y
NRARP	-0.93	1.55	1.63	2.59	3.28	-0.86	Y
UNC5B	-1.50	1.81	1.41	N/A	2.77	N/A	N
EFNB2	-0.35	2.64	2.50	N/A	1.87	-1.45	N
EFNA1	-0.98	1.14	1.93	N/A	1.55	N/A	Y
KCNJ2	-1.02	1.21	1.02	1.45	NA	N/A	Y
HIC1	-0.31	0.68	0.49	0.80	1.33	N/A	Y
SPSB1	-0.49	1.06	1.16	N/A	1.27	N/A	Y
SAT1	-0.93	1.54	2.11	N/A	1.01	N/A	Y
RGS3	-0.73	0.54	0.68	N/A	0.71	N/A	Y
PMEPA1	-0.65	0.53	0.58	N/A	0.64	N/A	Y
LMO2	-0.50	0.69	0.72	N/A	0.61	N/A	N
TGFB1	-0.54	0.38	0.39	N/A	0.32	N/A	N

Red: canonical targets

Table 4-5 listed genes (with Log2Foldchange presented) that were identified as potential Notch target by the RiboTagEC screens, TLA-Dll4 stimulation and EGTA screens. 17 genes were identified as overlapping targets (Padj<0.05, |Log2FC|>0.27) by all three screens. Canonical targets were highlighted in red.

4.3.4 Comparison with published SpDAM ID database with RiboTagEC/TLA/EGTA screens identifies endothelial genes that are known direct transcriptional Notch targets

To validate the 17 genes that we screened are direct Notch targets, we compared our data with the published spDAM ID database generated using mouse kidney cells to establish direct Notch targets.

The spDAM ID screen is based on the reconstitution of the split DAM enzyme that has been fused with two proteins from the Notch transcriptional activator complex, that binds to the CSL sequence found upstream of Notch target genes. This study allowed screening for targets of Notch dimers and Notch monomers (in combination with either RBPJ, MAML or P300). We compared the data from our screen (Padj = 0.05, Log2FC =0.27) to genes on the spDAM ID database. Our analysis showed 76% of our targets are detected in at least one spDAM combination in mK4 (metanephric) cells (Table 4-5).

4.3.5 EGTA induction combined with CpE treatment identified RND1 as Notch dependent responder

Of these 17 genes identified in common with our three major screens, the induction of 5 (33.3%) genes were significantly downregulated by CpE including canonical targets DLL4, EFNB2, NRARP, HEY1 (highlighted in Table 4-5) and one novel target RND1 (highlighted in Table 4-5). It was interesting to note that the induction of some established Notch genes like *HEY1* by EGTA were not significantly repressed by CpE at 1.5 hour. The possible explanation could be that EDTA/EGTA may also be stimulating other potent inducer of those Notch targets, which may mask the differences caused by CpE treatment. For instance, despite the fact that *HES1* are without doubt primary Notch targets, other signaling pathways (e.g. Hedgehog, FGF, Wnt, or serum-induced ultradian oscillators) have also been showed to control its expression(Woltje, Jabs, & Fischer, 2015; Yoshiura et al., 2007). CpE treatment provides important insight of targets that were solely or heavily Notch dependent in response to EGTA induction.

In summary, we performed an EGTA induction screen to allow identification of targets induced at 1-1.5 hour after EGTA-mediated Notch activation. Based on the initial quantitative screen that showed peak induction at 1 and 1.5 hour. Of various canonical Notch targets, we performed an RNA-seq screen of HUVECs collected at these time points. Analysis revealed known and novel targets to be upregulated within 1 hour and 1.5 hour. of EGTA stimulation. Comparison of the 1.5 hour. profile to the 48 common genes identified by the RiboTagEC screening and the DLL4-TLA, led to identification of 17

genes as early/potential direct Notch targets from both *in vivo* and *in vitro*. Among those 17 genes, the induction of 5 genes were significantly repressed with CpE treatment, including 4 canonical genes and 1 novel candidate-RND1.

4.4 Discussion

Notch signaling plays a critical role in angiogenesis through regulation of a wide network of target genes, however, very limited information has been obtained and reported regarding transcriptional event of Notch activation in endothelial cells, especially the primary targets. To identify rapidly-responding Notch downstream targets from both in vivo and in vitro, we have generated a comprehensive dataset using three distinct unbiased screenings, all focusing on early responsive genes of Notch. The majority of the genes we identified were also reported to be direct-transcriptional targets of Notch in mK4 cells.

Summary of our data:

1. RiboTagEC screens

In Chapter 3, we performed an in vivo screen of early Notch targets in mouse brain endothelium using RiboTag EC technique, focusing on gene downregulated 6 hours after GSI administration. 591 genes were identified as potential targets. Of particular interest, a set of GPCR related genes were detected as novel Notch targets.

2. Tethered Ligand Assay (TLA) screens

In Chapter 4-II, we activate endothelial Notch using a physiological relevant method-tethered ligand activation. We characterized genes that were rapidly (6 hours after plating cells) response to ligand-specific Notch induction in two human primary ECs. Among the 340 DLL4-Notch rapidly induced novel genes, were again a set of GPCR related genes.

3. EGTA screens

In Chapter 4-III, to perform an even tighter control of Notch activation, we screened for genes induced at 1-1.5 hours with EGTA-mediated Notch activation, and cross-compare with the first two datasets.

Figure 4-19 summarized the three layers of screening study. Comparison of dataset 1 (RiboTagEC screens) and 2 (DLL4-TLA screens) identified 40 overlapping genes including canonical Notch targets as well as novel potential targets. Those genes are rapid Notch responder with both *in vitro* and *in vivo* significance. Integrating data from EGTA-induction identified 17 genes out of the 40 genes as potential direct notch targets. Out of the 17 genes, Notch inhibitor CpE treatment significantly repressed the EGTA induction of 5 genes, including 4 canonical Notch target and 1 novel target *RND1*, a small GTPase. The CpE treatment identified genes that are largely or even solely dependent on Notch signaling during EGTA treatment.

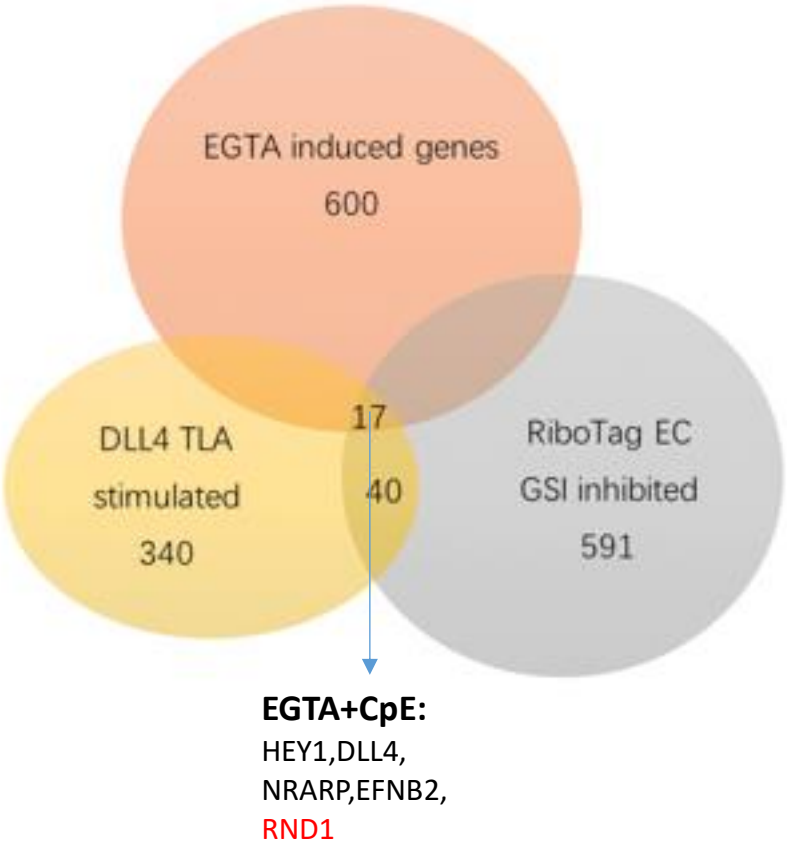

Figure 4-19. Summary of the three unbiased screens

RND1 is of our particular interest not only because it was identified as Notch target in all screens, but also of the following points:

1. Expression of *Rnd1* was significantly reduced in brain EC, but not brain homogenate after GSI treatment, indicating an endothelial specific regulation of Notch on *Rnd1*

2. *RND1* has a high magnitude of induction (ranked top 2 by fold change) by tethered DLL4 at 6 hours in both HUVEC and HREC. JAG1, as a weak activator, induced *RND1*

by more than 6-fold at 6 hour. (rank top 2 by fold change), thus both DLL4 and JAG1 can regulate *RND1*.

3. G proteins are critical in regulating cell behavior, but have rarely been linked to Notch signaling pathway in previous studies. RND1, as a Rho GTPase, may lead to discovery of intersects between G protein pathway and Notch signaling pathway in endothelial cells. All these data suggest a potential unexplored area of Notch regulation through GPCR signaling.

Chapter 5 Validation and functional study in angiogenesis of a novel Notch target; the GTPase RND1

5.1 Rationale

Data from the previously performed screens identified *RND1* to be a gene downregulated by GSI administration in mouse brain EC, upregulated by DLL4 (and JAG1) stimulation in the TLA, and EGTA-mediated activated in two primary human EC types. Thus, several methods were used to support with high confidence that *RND1* is a consistent and highly induced Notch target in endothelial cells. Several other genes met these criteria, namely *HEY1*, *DLL4*, *NRARP*, and *EFNB2*. Each of these genes are already known and characterized as Notch targets with a function in angiogenesis or vascular development. We have therefore focused on *RND1* as a candidate Notch target for detailed exploration of its mechanistic role in angiogenesis using functional and signaling analyses. We hypothesize that Rnd1 is a downstream effector of endothelial Notch signaling that acts to regulate angiogenesis.

The Rnd family includes Rnd1/Rho6, Rnd2/Rho7 and Rnd3/Rho8/RhoE in humans and is a distinct structural sub-group of the Rho family of GTP-binding proteins [88]. Most G proteins cycle between an active GTP-bound and a resting GDP-bound form and their activity is controlled by guanine nucleotide-exchange factors (GEFs) and GTPase-activating proteins (GAPs). However, Rnd proteins have a low affinity for GDP and thus remain in their constitutively active, GTP-bound state(Foster et al., 1996; Guasch,

Scambler, Jones, & Ridley, 1998; Nobes et al., 1998). This suggests that Rnd proteins are subject to regulatory mechanisms distinct from other G proteins, such as via transcriptional or protein stability mechanisms. Studies in neurons have provided important insights into the mechanisms that control the activity of the Rnd proteins, and revealed that their expression, localization and phosphorylation control their activity, rather than the GDP/GTP switch(Chardin, 2006).

5.1.1 Established function of Rnd1

Rnd1 has been well established to regulate cytoskeleton formation and function in various cell types including fibroblast and epithelial cells. In neurons, overexpression of Rnd1 promoted dendritic growth and branching in cultured hippocampal neurons(Ishikawa, Katoh, & Negishi, 2006). Furthermore, the Xenopus ortholog of Rnd1 has shown to be expressed in tissues undergoing extensive morphogenetic changes, such as marginal zone cells, somitogenic mesoderm, and neural crest cells, and overexpression of Xenopus Rnd1 induces the disruption of cell adhesion(Wunnenberg-Stapleton, Blitz, Hashimoto, & Cho, 1999). Recently, Rnd1 has also been shown to play a role in breast tumor progression: depletion of Rnd1 disrupted epithelial adhesion and polarity and induced epithelial-to-mesenchymal transition(Okada et al., 2015).

The three Rnd proteins have overlapping and distinct functions in a context-dependent way. For example, Rnd1 and Rnd3 have similar effects to inhibit formation of actin cytoskeleton in fibroblasts, whereas Rnd2 has little or no effect (Chardin, 2006). Rnd2 and Rnd3, but

not Rnd1, contribute to cortical neuron migration (Heng et al., 2008; Pacary et al., 2011). Consequently, the same protein might have different functions depending on the cellular context.

Unlike in fibroblasts or neurons, the role of Rnd1 in endothelial cells has been poorly understood. One study suggested that *Rnd1* knockdown in HUVECs enhanced VEGF-mediated cell migration towards SDF-1 and neovascular formation from aortic rings in response to VEGF (Suehiro et al., 2014). Another study indicated that Rnd1 induces stress fiber disassembly in HUVECs, while Rnd2 and Rnd3 enhanced stress fiber formation(Gottesbuhren et al., 2013). A thorough characterization of Rnd1 function in endothelial cells, especially in angiogenesis, will be of great value.

5.1.2 Signaling mechanism of Rnd1

Rnd proteins can interact with a variety of downstream targets to induce cellular responses (Riou, Villalonga, & Ridley, 2010). Rnd1 has been shown to indirectly inhibit Rho and Ras in a cell-context-dependent manner. Most studies indicate that the morphological effect of Rnd proteins are related to inhibition of RhoA-mediated contraction. Studies have shown that Rnd1 can interact and recruit p190 RhoGAP at the site where Rho should be inhibited (Wennerberg et al., 2003). Another study, however showed that Rnd1 silencing has no effect on Rho activation, but induces robust Ras activation in multiple cell types including MCF-10A, HMLE, HUVEC and HEK293 cells (Okada et al., 2015).

The involvement of Rnd proteins in axon guidance provides a very well described model to understand the mechanisms of how Rnd proteins controls Rho and Ras activity. In neurons, the signaling mechanism of Rnd1 depends on the presence of plexin-semaphorin signals. Plexin B1 is Sema-4D receptor and has been shown to simultaneously interact with both Ras and Rnd1. When plexinB1 is not activated with Sema-4D, the interaction between Rnd1 and p190 RhoGAP inhibits RhoA-induced contraction. However, when a plexin recognizes a semaphorin signal, the interaction of Rnd1 with the plexin stimulates its R-Ras GAP activity, leading to inhibition of Ras. The plexin also traps Rnd1 away from p190 RhoGAP, which is then released, allowing efficient RhoA activation (Chardin, 2006).

In endothelial cells, however, the signaling effect of Rnd1 remains elusive and controversial. Tomoyo Okada *et al*. suggested Rnd1 inhibits Ras activation in HUVECs, and has no effect on Rho activity (Okada et al., 2015), while another group showed that knockdown of *Rnd1* leads to RhoA hyperactivation in HUVECs(Suehiro et al., 2014). So here we investigated the signaling event(s) mediated by Rnd1, focusing on Rho and Ras signaling.

5.1.3 Intersection between Notch and Rnd proteins

Very few studies have linked Rnd proteins to Notch signaling. One study showed that the expression level and pattern of Rnd1 and Rnd3 were controlled by Notch signaling in Xenopus somite formation (Goda, Takagi, & Ueno, 2009). Another study suggested that Rnd3 is a direct transcriptional target gene of Notch signaling in squamous epithelium,

mediating nuclear translocation of the activated portion of Notch1 (N1IC) through interaction with importins (Zhu et al., 2014). Rnd3 has also been demonstrated to negatively regulated Notch signaling through direct interaction and degradation of NICD in ependymal cells of CNS (Lin et al., 2013). However, Rnd1 has never been shown as Notch effector in mammals.

Since Rnd1 is an important regulator of Rho and Ras, we considered whether Notch and Rho/Ras pathway have been shown to interact with each other in previous studies. Interestingly, in *C. elegans* vulval development, Ras and Notch pathways antagonize each other so that only one of the two pathways can be highly active (Shaye & Greenwald, 2002). Notch induces the transcription of undefined Ras inhibitors in the P5.p and P7.p cells of *C. elegans* and in undifferentiated eye cells of *Drosophila*(Sundaram, 2005). Despite Notch and Rho signaling pathway having been shown to influence common sets of cells and common processes such as dendritic development (Redmond & Ghosh, 2001), the evidence of direct interplay of the two pathway is still sparse.

Collectively, very limited insights were gained from previous studies about the role of Rnd1 in regulating endothelial cell behavior and angiogenesis. The intersection between Notch signaling and Rnd1, as well as Ras/Rho signaling pathway, still remains to be addressed, especially in mammalian systems. In this chapter, we explored the function and the signaling mechanism of Rnd1 in endothelial cells.

5.2 Results: Validation of *RND1* as endothelial Notch target

5.2.1 Within the RND family, only *RND1* responds to EC Notch activation

Three Rnd proteins exist in humans. We examined Rnd family expression to determine the expression level of Rnd proteins in endothelial cells. The mRNA basal expression level of *RND1*, *RND2* and *RND3* were compared in HUVECs and HRECs using the RNA-seq data of baseline (control) endothelial cells used as reference points within the lab. *RND3* is expressed at much higher levels than other Rnds in endothelial cells. The basal level of *RND1* mRNA is low in both types of ECs. RT-PCR analysis of all three genes produced bands of varying intensity that were consistent with the expression levels observed by RNA-seq (Figure 5-1).

Counts from RNAseq

	HUVEC	HMREC
GAPDH	69990	93544
B-actin	189693	456841
Notch1	7410	26301
Notch4	1160	1578
Dll4	577.6	4077
Jag1	2957	4358.8
Rnd1	26	324.6
Rnd2	18	65.9
Rnd3	3700	6131.4

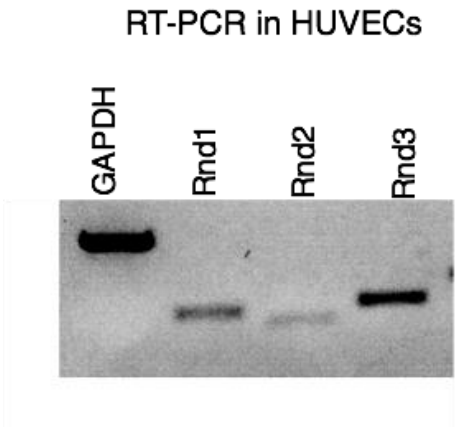

Figure 5-1. Expression of RND family genes in endothelial cells

Gene counts of *RND1*, *RND2*, and *RND3* from RNA-seq data indicated that *RND3* is the most highly expressed member of the family in ECs. Basal expression of *RND1* is very low in ECs. RT-PCR confirmed the RNA seq results.

To identify the response of all three Rnd proteins to Notch induction, sequencing data from RiboTagEC profile, TLA, and EGTA induction assays were examined. Interestingly, *RND1* is the only gene of the Rnd family that is induced by Notch activation in any of our screens. These sequencing results were confirmed by RT-qPCR analysis (Figure 5-2). Thus, this suggested *RND1* is the prime Notch target gene within the Rnd family, although *RND3* is more highly expressed in endothelial cells.

Currently available commercial antibodies do not differentiate well between the three Rnd proteins, so we examined mRNA level in our studies. In future studies, we may generate a custom Rnd1 antibody for protein analysis.

Normalized Counts from RNA seq (See Chapter III, IV)

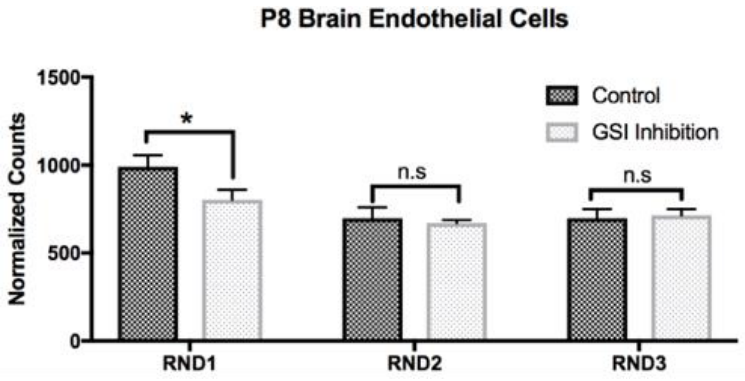

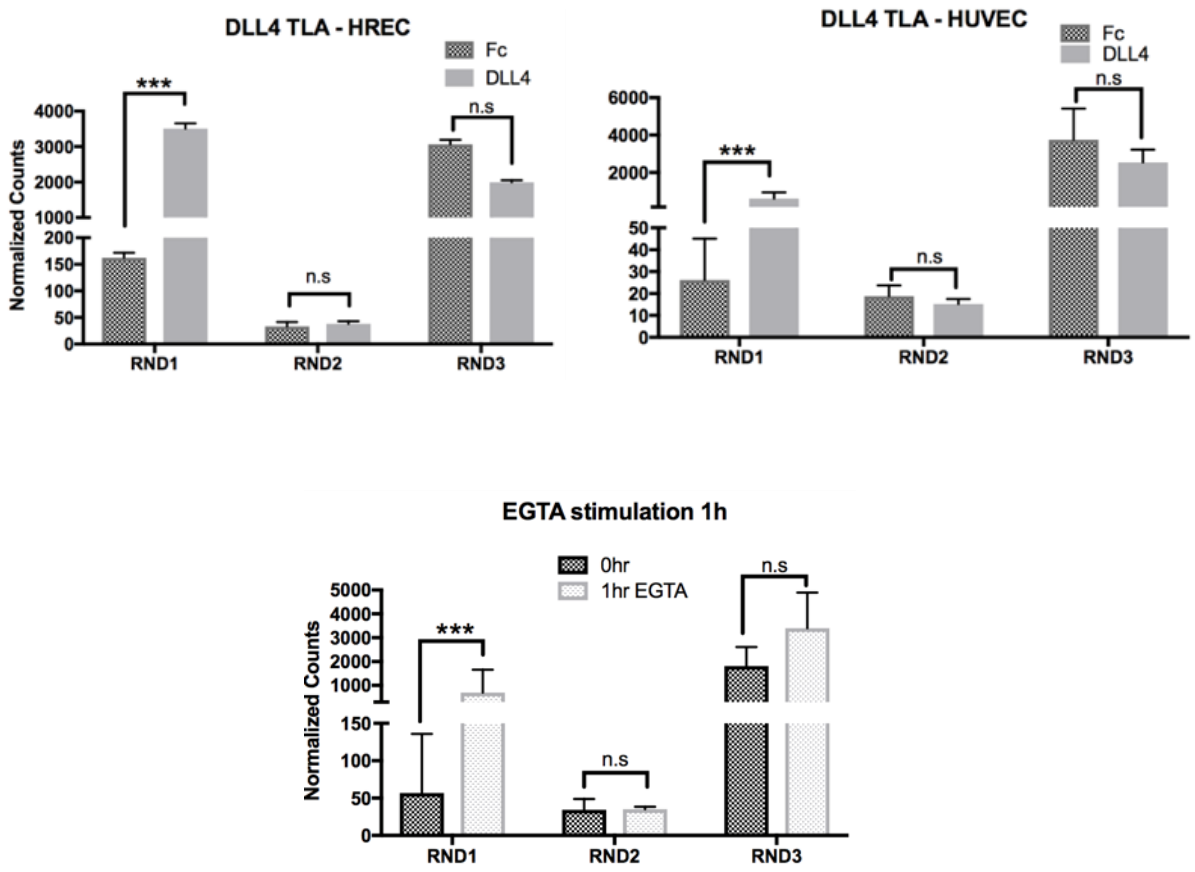

RT-qPCR validation using TLA

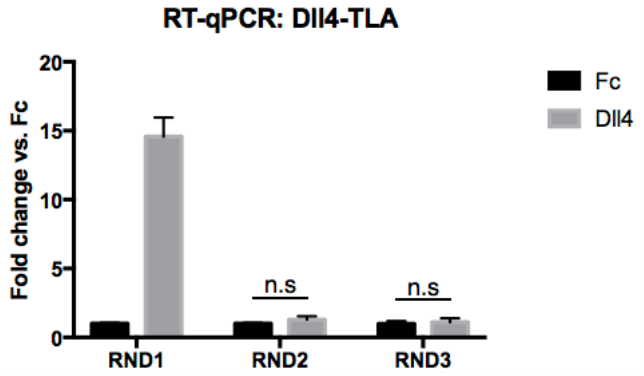

Figure 5-2. *RND1*, but not *RND2* and *RND3*, is Notch target

Figure shows a summary of the expression changes of RND family genes in response to Notch activation/inhibition. Normalized counts of *RND1*, *RND2* and *RND3* was generated from RNA-seq results of RiboTagEC profile, Dll4-TLA as well as EGTA 1-hour induction (Chapter III and

IV). *RND1* is the only gene responding to Notch signaling in all the systems. These results are confirmed by RT-qPCR on *RND1, RND2,* and *RND3* mRNA in cells stimulated with tethered-Dll4.

5.2.2 *RND1* was further validated as endothelial Notch target from *in vivo* and *in vitro* analysis

To confirm the RNA-seq results suggesting that *RND1* is Notch target, we validated the Notch responsiveness of Rnd1 expression by using RT-qPCR to examine expression in previously examined and novel endothelial contexts.

Rnd1 was downregulated rapidly by GSI in EC from multiple tissues in vivo

We performed RiboTag IP to isolate endothelial-specific mRNA from a variety of tissues including the whole brain, the cortex, and the heart of P6 RiboTagEC mice 6 hours after GSI administration and assessed Rnd1 levels in homogenate mRNA and IP mRNA using RT-qPCR. Rnd1 was significantly inhibited with GSI compared with vehicle-treated samples in all the vascular beds. The tissue homogenates did not show differential expression of Rnd1, indicating that Notch regulation of Rnd1 is EC-specific (Figure 5-3)

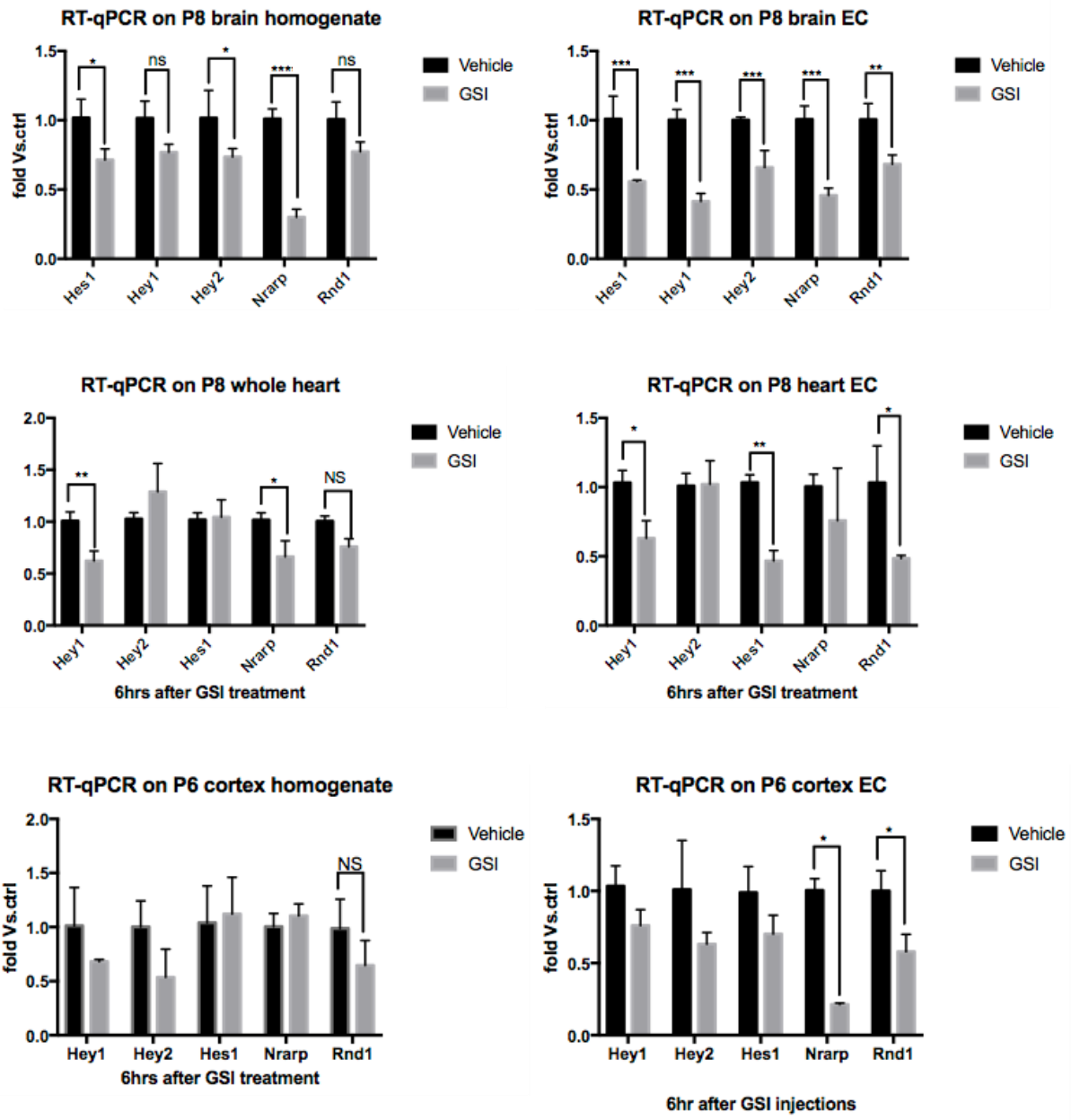

Figure 5-3. *Rnd1* was inhibted by 6 hour GSI treatment in multiple vascular beds

Multiple tissues (brain, heart, cortex) from postnatal RiboTagEC mice were collected 6 hours after GSI or vehicle treatment and were subjected to RiboTag IP process. RT-qPCR was performed to check *Rnd1* and canonical targets expression in both homogenate and IP fraction (EC). *Rnd1* was significantly inhibited in all EC samples tested, but not the tissue homogenate.

RND1 was induced rapidly by Notch ligand in a GSI-dependent manner in multiple primary endothelial cells in vitro

Consistent with the RNA sequencing results, tethered Dll4/ Jag1 significantly induced RND1 in all three primary EC we tested [(HREC, HUVEC, and human dermal microvascular endothelial cells (HDEC)]. RND1 induction was reduced to basal level with 500 nM CpE treatment, indicating that induction is dependent on gamma secretase activity (Figure 5-4).

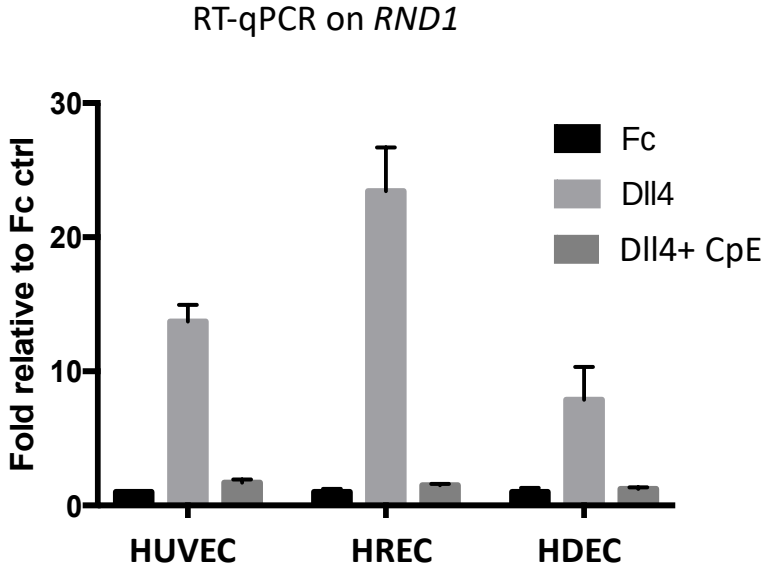

Figure 5-4. *RND1* induced by tethered-Dll4 in multiple ECs, and CpE completely blocked the induction.

RNA-seq analysis of the TLA results was confirmed using RT-qPCR in multiple primary endothelial cells (HUVEC, HREC and HDEC). *RND1* was up-regulated with Dll4 stimulation in 6 hours after seeding the cells, and CpE treatment significantly inhibited the induction to basal level.

RND1 was induced rapidly by EDTA and EGTA in a GSI-dependent manner in multiple primary endothelial cells in vitro

We performed the time course study of *RND1* expression after EGTA and EDTA induction in both HUVECs and HRECs. Induction of *RND1* started as early as 30minutes, peaked at 1.5 hours, and returned back to basal level in 4 hours, which is similar with the pattern of canonical Notch targets. Notch inhibitor CpE treatment completely blocked EGTA/ EDTA induction of *RND1*, while only partially blocked other canonical Notch targets, indicating that the induction of *RND1* is solely dependent on Notch signaling after EGTA treatment (Figure 5-5).

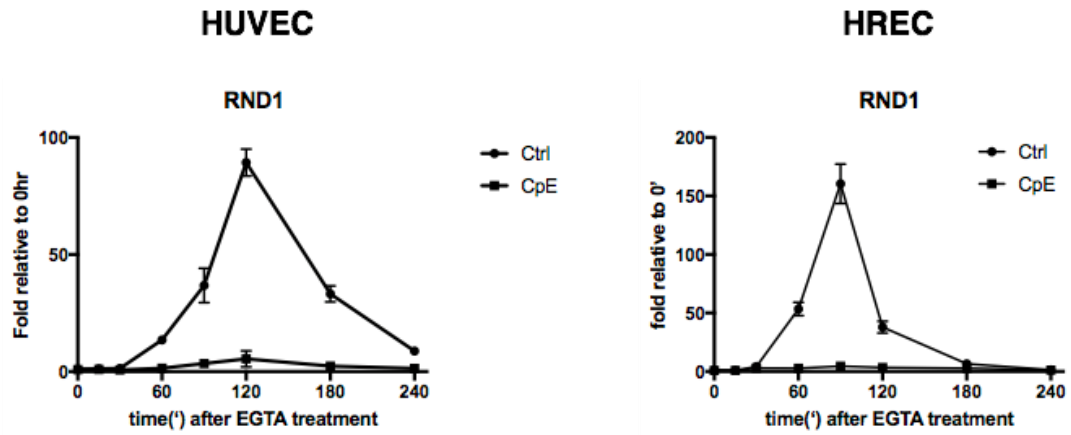

Figure 5-5. *RND1* rapidly induced with EGTA treatment

HUVECs and HRECs were treated with EGTA as previously described (Chapter 4), and the expression of *RND1* was measured at different timepoints (every 30minutes, from 0-4 hours) by RT-qPCR. Induction of *RND1* can be detected as early as 30minutes, peaks at 1.5-2 hours, and was back to basal level at 3-4 hours.

RND1 was induced by overexpression of NICDs in endothelial cells

As discussed in Chapter 1, the when the Notch intracellular domain (NICD) is cleaved from the membrane, it translocates to the nucleus to form an active transcriptional complex. Truncated versions of the Notch proteins act as constitutively active proteins and strongly induce target genes. Lentivirus-mediated NICD overexpression of Notch1 ICD (N1ICD) and Notch4 ICD (int3) strongly induced *RND1* expression level as predicted (Figure 5-6).

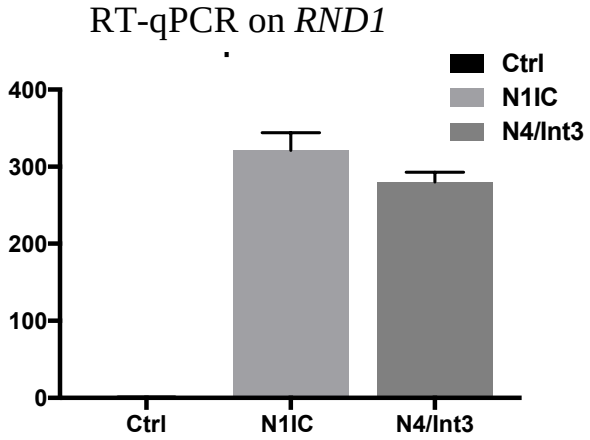

Figure 5-6. Overexpression of Notch strongly induced *RND1*

Lentiviral-mediated overexpression Notch1 intra cellular domain (N1CD) and Notch4/Int3 induced *RND1* by 300fold in HUVECs. N4/int-3 encodes 30 amino acids upstream of the transmembrane domain and the entire cytoplasmic domain of Notch4, and is naturally occurring active allele of Notch4(Shawber et al., 2007).

5.2.3 *In Silico* evaluation of open chromatin mapping in cultured cells reveals a putative endothelial-specific enhancer region of Rnd1 that is responsive to Notch activation

Data from the RiboTagEC screen identified *RND1* to be repressed by GSI specifically in the Brain ECs but not the brain homogenate, indicating cell type specific effects. Studies have shown that cell type specific gene expression profiles are regulated by promoters, enhancers and insulators. While promoters are important for the formation of the

transcription initiation complex and binding of RNA pol II, enhancers contain consensus sequences that recruit specific transcription factors that aid in the formation of the pre-initiation complex and are often required to regulate cell type specific gene transcription. Activity of enhancers are regulated by the chromatin organization and can be differentiated from promoters by the presence of histone marks (Calo & Wysocka, 2013; Heinz, Romanoski, Benner, & Glass, 2015). Therefore, we screened our target of interest, *RND1* locus for the presence of EC specific regulators using the ENCODE database (Rosenbloom et al., 2010) (https://genome.ucsc.edu/encode/). This data allows one to explore the chromatin organization and methylation patterns in the genome. The ENCODE data contains information from DNase I hypersensitive sites (DHS) sequencing screens, which indicate regions with open chromatin in a variety of cell types and tissues. DNase I hypersensitive sites (DHSs) are regions of chromatin that are sensitive to cleavage by the DNase I enzyme (Keene, Corces, Lowenhaupt, & Elgin, 1981) . In the nucleus, the vast majority of genomic DNA is wrapped around nucleosomes. Regions where local modifications to this chromatin structure displace these nucleosomes (such as for the activation of promoters) allow for easier digestion by DNase I. DNase I hyper-sensitive (HS) sites have been shown to be markers for many different types of genetic regulatory elements, including promoters, enhancers, silencers, insulators, and locus control regions (Felsenfeld & Groudine, 2003).

Our analysis showed a large DHS peak at the promoter region of Rnd1, but this peak appeared in all cell types examined, suggesting that was a region of open chromatin in most or all tissues. No significant EC specific DHS peaks were observed in the promoter

region. However, we identified a putative enhancer region located ~ 17 kb upstream from *RND1* that showed DHS peaks specifically in different ECs in the ENCODE database (HUVECs, HMVECs, HBMECs, HRGECs, etc.) and not in non-EC cell types (K562, HepG2, B cells, HeLA cells, etc.). Further interrogation of this region identified two Notch consensus sites with the sequence: (C/T)GTGGGAA (Figure 5-7).

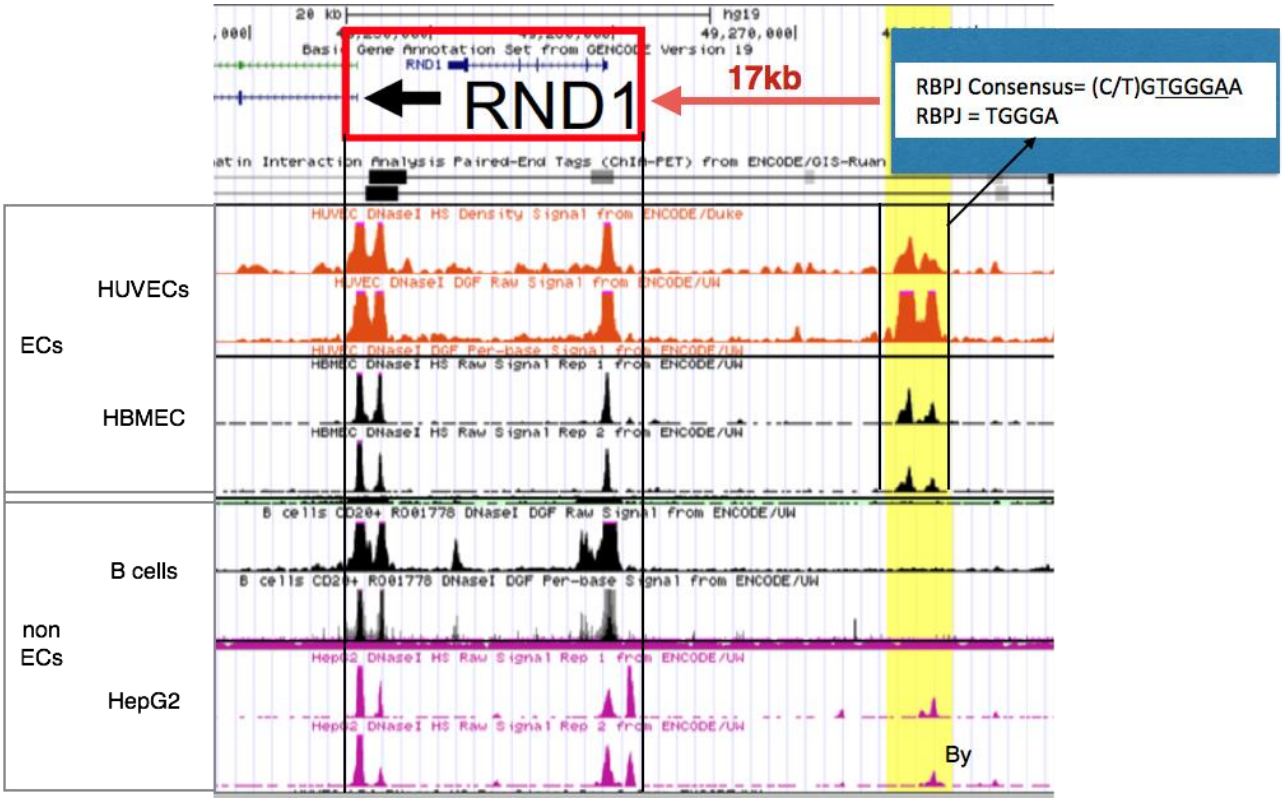

Figure 5-7. Open Chromatin Mapping of Rnd1 indicated putative EC-specific enhancer

Examination of ENCODE database for DHS peaks uncovers a putative enhancer (highlighted in yellow) 17kb upstream of *RND1* locus (circled in red box) in multiple ECs (Here listed HUVEC and HBMEC as examples). No DHS peaks was detected in non-EC cell types (Here listed B cells and HepG2 as examples). The enhancer region contains RBPJ consensus binding sites.

Enhancer regions are further classified as inactive, primed, or active, based on the histone marks present. Inactive enhancers have compact chromatin and prevent transcription factor binding. The primed and active enhancers both contain open chromatin regions and contain the histone marks H3K4me1 and H3K4me2, but are differentiated by the acetylation mark H3K27ac, which is only found in active enhancers(Calo & Wysocka, 2013; Creyghton et al., 2010; Heintzman et al., 2007) . Screening for these histone marks in the *RND1* enhancer locus, identified that the enhancer region defined above contained H3K4m1, m2, m3 and the H3K27ac, indicating that this EC specific enhancer was active. In non-EC cell types (HepG2, K562) the acetylation histone mark was absent.

These data indicate *RND1* possesses a putative enhancer, active specifically in ECs, with RBPJ-binding consensus sites 17 kb upstream of the *RND1* promoter, suggesting that this sequence binds the Notch transcriptional complex directly and is responsible for the endothelial-specific upregulation of *RND1* in response to Notch signaling.

5.3 Results: Function of Rnd1 in endothelial cells

Rnd1 has been well characterized as an important regulator of cytoskeleton rearrangement in multiple cell types. However, limited knowledge has been gained about its function in endothelial cells. As a potential novel effector of endothelial Notch, we hypothesize that Rnd1 functions to regulate endothelial behavior during angiogenesis. In order to investigate the function of Rnd1 in endothelial cells, a series of functional assay were

performed to assess the role of Rnd1 in viability, proliferation, migration, and sprouting angiogenesis in HUVECs.

5.3.1 siRNA successfully and specifically knocked down Rnd1 in HUVECs

To perform loss-of-function study of Rnd1 in endothelial cells, we started with lentivirus-mediated shRNAs, which has been widely shown as efficient and stable knockdown system in primary ECs for many genes. Unfortunately, all five Rnd1 shRNA constructs we tested, including published shRNA constructs, showed cellular toxicity and inconsistent knockdown efficiency in HUVECs.

Given the possibility that ECs poorly tolerate constitutive knockdown of Rnd1 with shRNA, we then sought to design an inducible shRNA system where we could acutely knockdown Rnd1 during experiments. We therefore attempted a Dox-inducible lentiviral shRNA system that allows transcription of shRNA upon the addition of doxycycline (Dox), which sequesters TetR and relieve repression at the TetO operon that drives shRNA expression (Frank, Schulz, & Miranti, 2017). We successfully detected TetR protein expression in HUVECs using this system, however, we were unable to detect any knockdown of Rnd1. Two possible reasons that could lead to this issue: 1) The efficiency of the system in primary cells could be poor, since most descriptions of this inducible system has been in immortalized cell lines. 2) Targeting sequences need to be further optimized to develop functional shRNA constructs.

We then utilized an siRNA approach to knockdown Rnd1 protein in HUVECs. Traditional Lipofectamine mediated transduction of siRNA resulted in low transfection efficiency in HUVECs. So here we used DharmaFECT4 transfection system, which resulted in >80% transfection efficiency in HUVECs. HUVEC treated with Rnd1 siRNA (Dharmacon J008929-05, sequence GGAUCUCCCUACUACGAUA, termed as siRND1) showed significant and specific knockdown of Rnd1 compared with control siRNA (Figure 5-8). Dose-response curve suggested that as low as 5nM siRND1 leads to significant knockdown (>60% reduction in expression), and with 25nM siRND1 the knockdown efficiency can reach >80% without observable cellular toxicity (Figure 5-9). siRNA is degraded over time in cells, so the knockdown effect is transient and lasted from 24-96 hours after transfection without passaging cells, or lasted for 24-72 hours if cells were passaged (Figure 5-10).

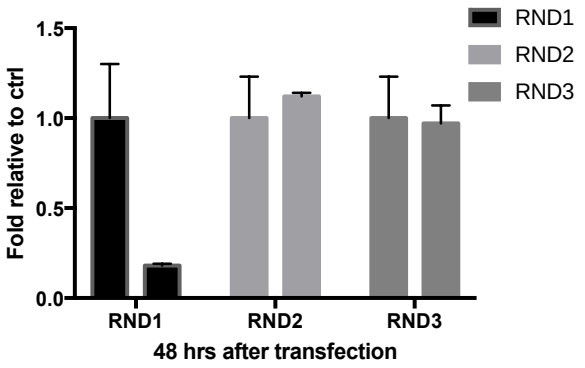

Figure 5-8. siRND1 specificly knocked down Rnd1 (RT-qPCR on mRNA)

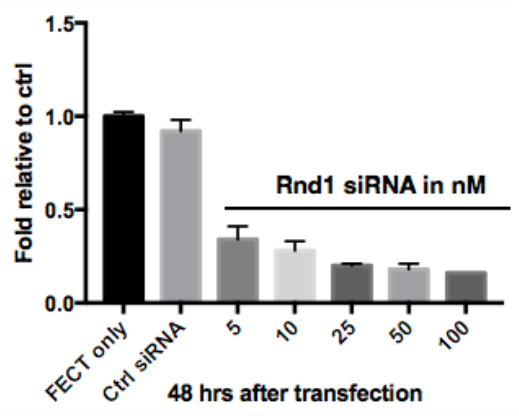

Figure 5-9. Dose curve of siRND1 (RT-qPCR on mRNA)

5nM of siRND1 significantly knockdown RND1 (~60% reduction in expression), and 25nM was determined as the minimal dose with the strongest knockdown effect (~80% reduction in expression)

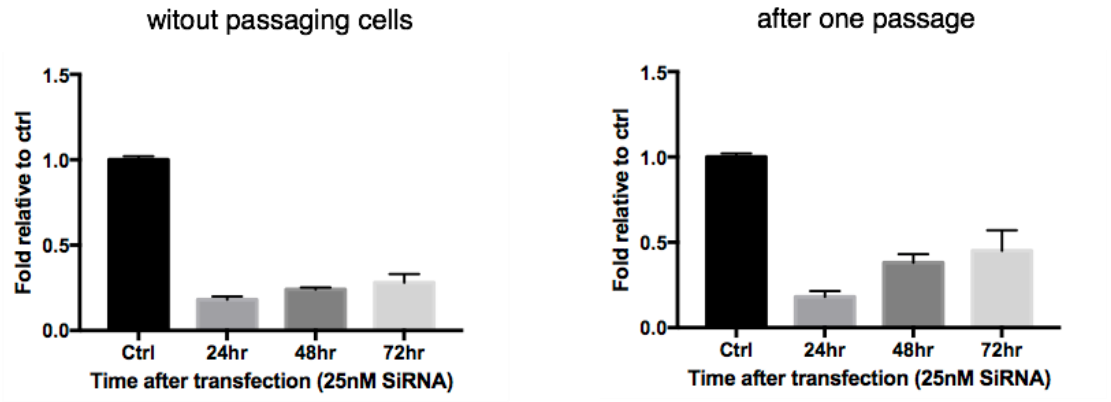

Figure 5-10. Time course of siRND1 KD effect (RT-qPCR on mRNA)

Knock effect of siRND1 lasted for at least 72 hours. after transfection, with or without passaging cells

To summarize, siRNA successfully and specifically, though transiently, knocked down Rnd1 expression in HUVECs. Given the dose curve and time course of siRND1 effects the following loss of function studies were performed within a time frame of 48-72 hours after transfection with 25nM siRND1.

5.3.2 Loss of Rnd1 showed no effects on EC viability and proliferation

Rnd1 has been established as regulator of Rho and Ras activity in multiple cell types, and G proteins such as Ras have been shown to affect cell proliferation and viability(Takai, Sasaki, & Matozaki, 2001). Thus, we explored the function of Rnd1 in endothelial cell viability and proliferation with an MTT assay, which measures the number of viable cells, and an EdU assay, which measures proliferation via incorporation of a labeled dNTP analogue into the DNA of dividing cells. HUVECs transfected with Rnd1 siRNA showed no significant difference in viability compared with control siRNA in both assays (Figure 5-11).

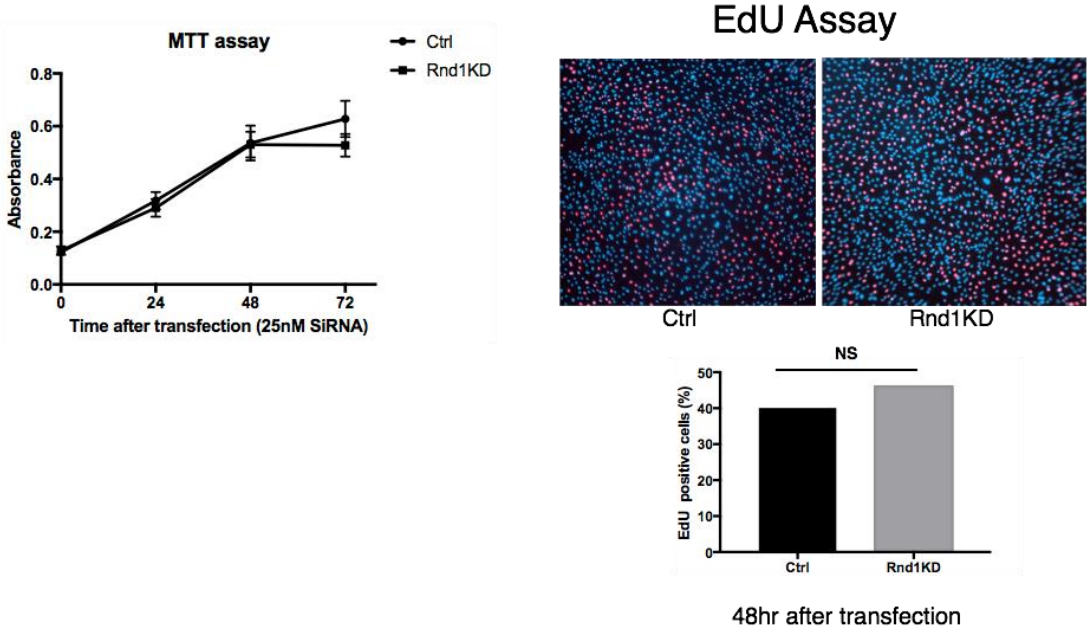

Figure 5-11. Rnd1KD shows no effects on HUVEC proliferation and viability

The effect of Rnd1 knock down (Rnd1KD) on HUVEC viability was measured using MTT assay as described in Chapter II. Proliferation was measured using EdU staining as described in Chapter

II. Data was presented as % of EdU positive cells/ total DAPI positive cells, as an average of three independent siRNA knockdown experiments. No significant difference was detected with Rnd1KD.

5.3.3 Loss of Rnd1 in basal and stimulated conditions shows no differences in EC migration using scratch assay

Rnd family proteins have been shown to contribute to cell migration such as cortical neuron migration [8,9]. We assessed the effect of Rnd1 knockdown in HUVEC migration. Scratch migration assays were performed by scratching the confluent layer of cells with a pipet tip, and the closure of scratched area by cells migrating into the open area was monitored over the course of 12 hours. No significant difference was observed between Rnd1KD cells and control cells in the migration rate (data not shown) .

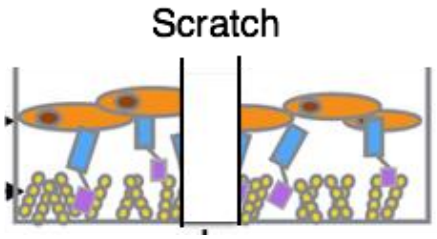

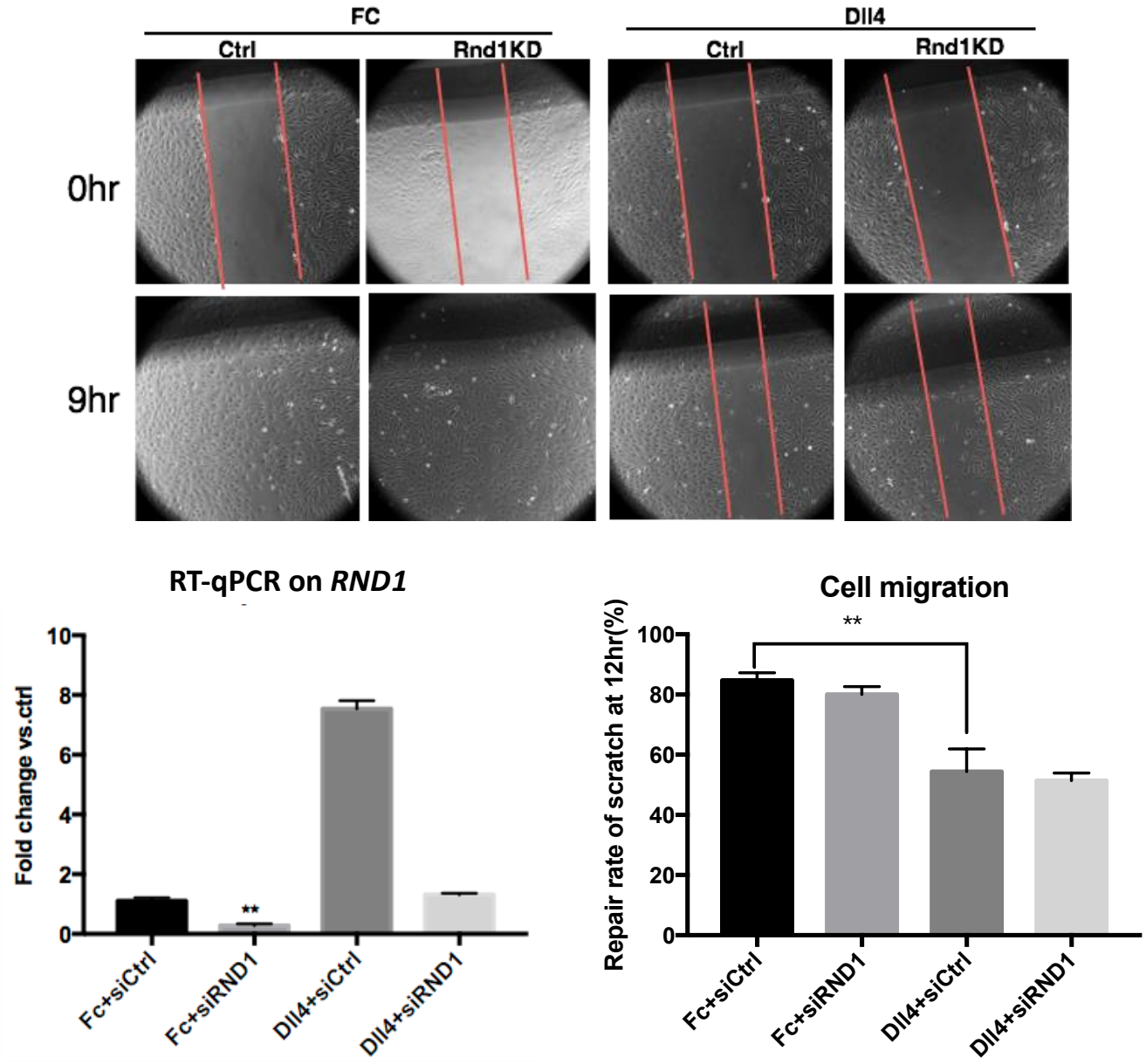

Figure 5-12. Rnd1KD shows no effects on HUVEC migration in scratch assay

Scratch assay was performed in combination of tethered ligand assay, allowing for investigating Rnd1 effects on HUVEC migration in both normal and stimulated conditions. Cells seeded on top of tethered-DLL4 or Fc control into confluency and a scratch was made. Image were taken every 3 hours until 12 hours. Contrast between the cellular area and the scratch was enhanced and the open wound area was measured by Image J as described in an established protocol

(Kees Straatman, 2008). DLL4 stimulated HUVECs migrated significantly slower compared with Fc control, but Rnd1KD failed to rescue the phenotype.

Given the low basal expression level of Rnd1 in HUVEC, we then asked the question whether the effects of loss of Rnd1 can be more easily detected when Rnd1 is stimulated. To stimulate Rnd1 expression, we combined the tethered ligand assay with scratch assay (Figure 5-12). The dish was coated with DLL4-Fc (or Fc as control) as described in Chapter IV. Cells were seeded to confluency on top of the Dll4 ligand (or Fc control) to stimulate RND1 expression. A scratch was made after the cells fully settled down and the remaining open area was monitored over time. RT-qPCR analysis confirmed the up-regulation of RND1 by immobilized DLL4, as well as the successful knockdown with siRND1 in both Fc or DLL4 stimulated cells. No significant difference was observed in the rate of migration between Rnd1KD cells and Control cells seeded on Fc control plate. As expected from previous literature, tethered-DLL4 stimulation significantly decreased HUVEC migration compared with Fc control. However, Rnd1KD cells still showed no effects in migration compared with control cells in the context of DLL4 activation (Figure 5-12).

To summarize, no significant difference was detected with Rnd1KD in EC migration using scratch assay. EC stimulated with tethered DLL4 exhibited significant slower migration compared with Fc control, but Rnd1KD failed to rescue this phenotype, indicating that Rnd1 may not mediate the Notch-induced suppression of EC migratory behavior.

5.3.4 Loss of Rnd1 augmented VEGF induced EC migration in basal and Dll4 overexpression condition

We hypothesized that endothelial cells migrating to a chemokine may require Rnd1 function, despite the lack of response of Rnd1KD cells in the scratch assay. Therefore, we carried out directional cell migration assay using Boyden chambers. To trigger chemokine responsiveness, siRNA-treated HUVECs were starved in 0.5% FBS overnight and then in complete, but serum free, media for an additional 3 hours. We assessed HUVEC migration towards different chemo-attractants including 50ng/ml hVEGF-A, 100ng/ml hSDF1, 1uM S1P and 2% serum. Knockdown of Rnd1 significantly augmented HUVEC migration towards hVEGF-A, but not the other attractants, suggesting that RND1 plays critical role in regulating VEGF-mediated migration (Figure 5-13).

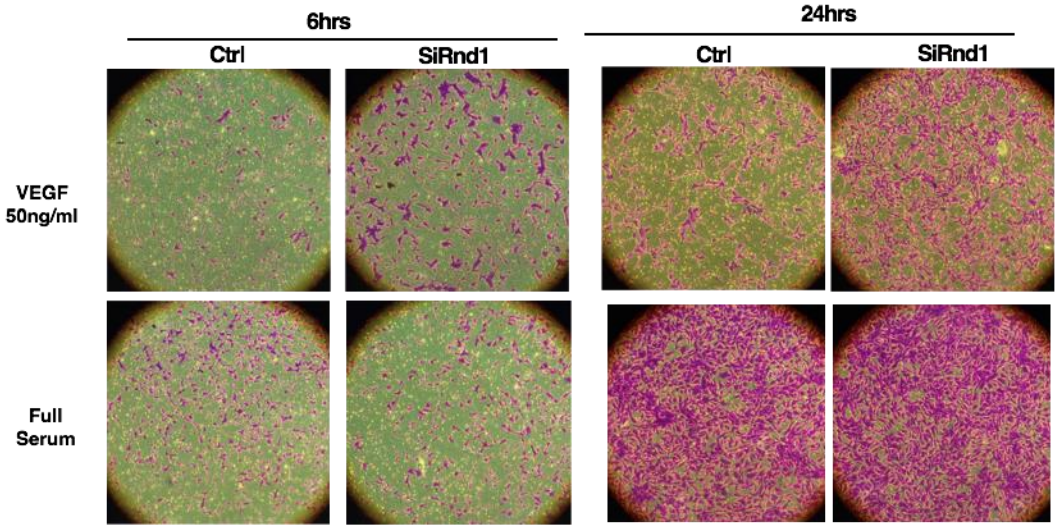

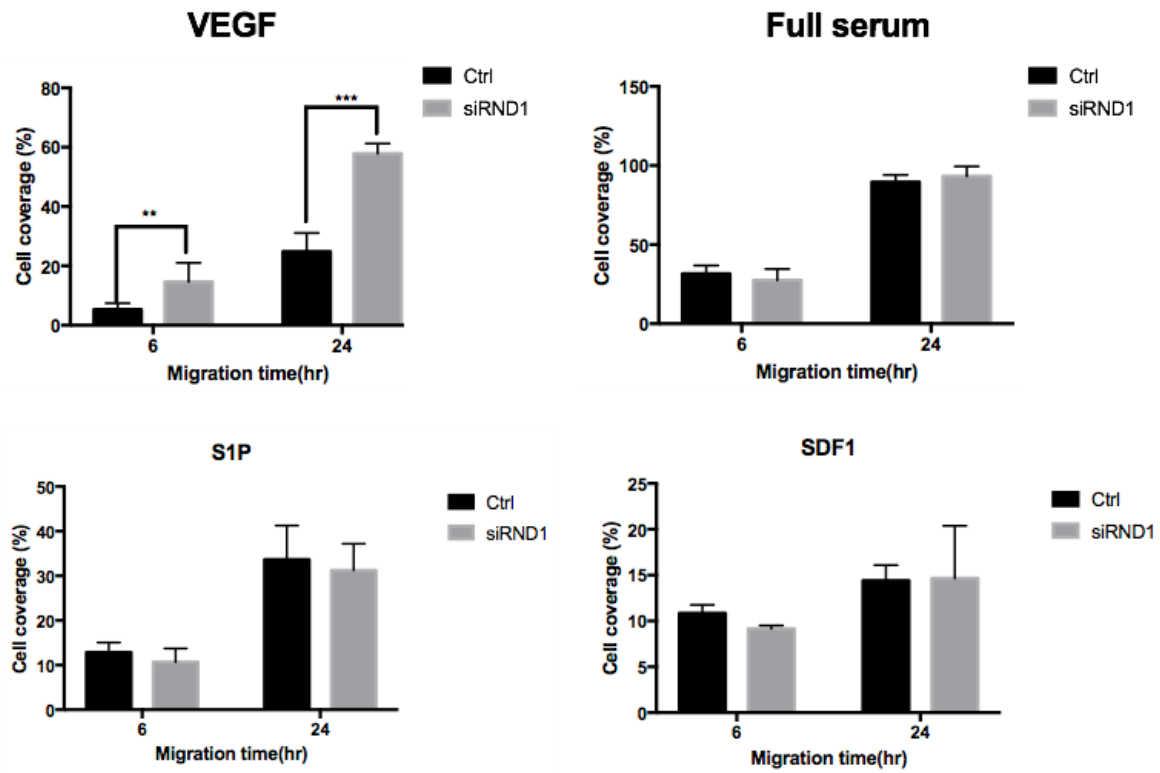

Figure 5-13. Rnd1KD accelerated HUVEC migration towards VEGF

HUVECs transfected with siRND1 or siCtrl were starved in 0.5% FBS overnight followed by a complete starvation with EBM-2 for 3 hours. Cells were then subjected to Boyden Chamber migration assay as described in Chapter II. Cell migration was measured by quantifying area covered by cells and dividing by total area of the image using ImageJ (3 different areas per well, 3 wells per sample), experiments was performed three times. Rnd1KD significantly accelerated HUVEC migration towards 50ng/ml hVEGF-A Interestingly, other chemoattractant (SDF-1, S1P and full serum) mediated-migration was not affected by Rnd1KD.

This finding is of particular importance because during angiogenesis, activation of Notch signaling leads to the loss of migration capabilities towards VEGF in stalk cells and sustained VEGF expression upregulates Notch signaling in EC (Funahashi et al., 2010). Rnd1 might function as a Notch downstream effector to mediate this phenotype in stalk

cell. To test our hypothesis, we activated Notch by overexpressing DLL4 in HUVEC, which significantly up regulated Rnd1 expression, and siRND1 successfully inhibited the Rnd1 induction to basal level. Our preliminary data shows that DLL4 overexpression led to a dramatic decrease in HUVEC migration activity towards VEGF. More importantly, siRND1 partially and significantly rescued this phenotype. This finding confirmed our hypothesis that Rnd1 functions downstream of Notch to inhibit endothelial cell migration towards VEGF. Migration towards VEGF is not fully restored in the absence of Rnd1, but this may be due to the presence of other Notch effectors, such as VEGFRs, that also serves as regulators of the migration activity (Figure 5-14).

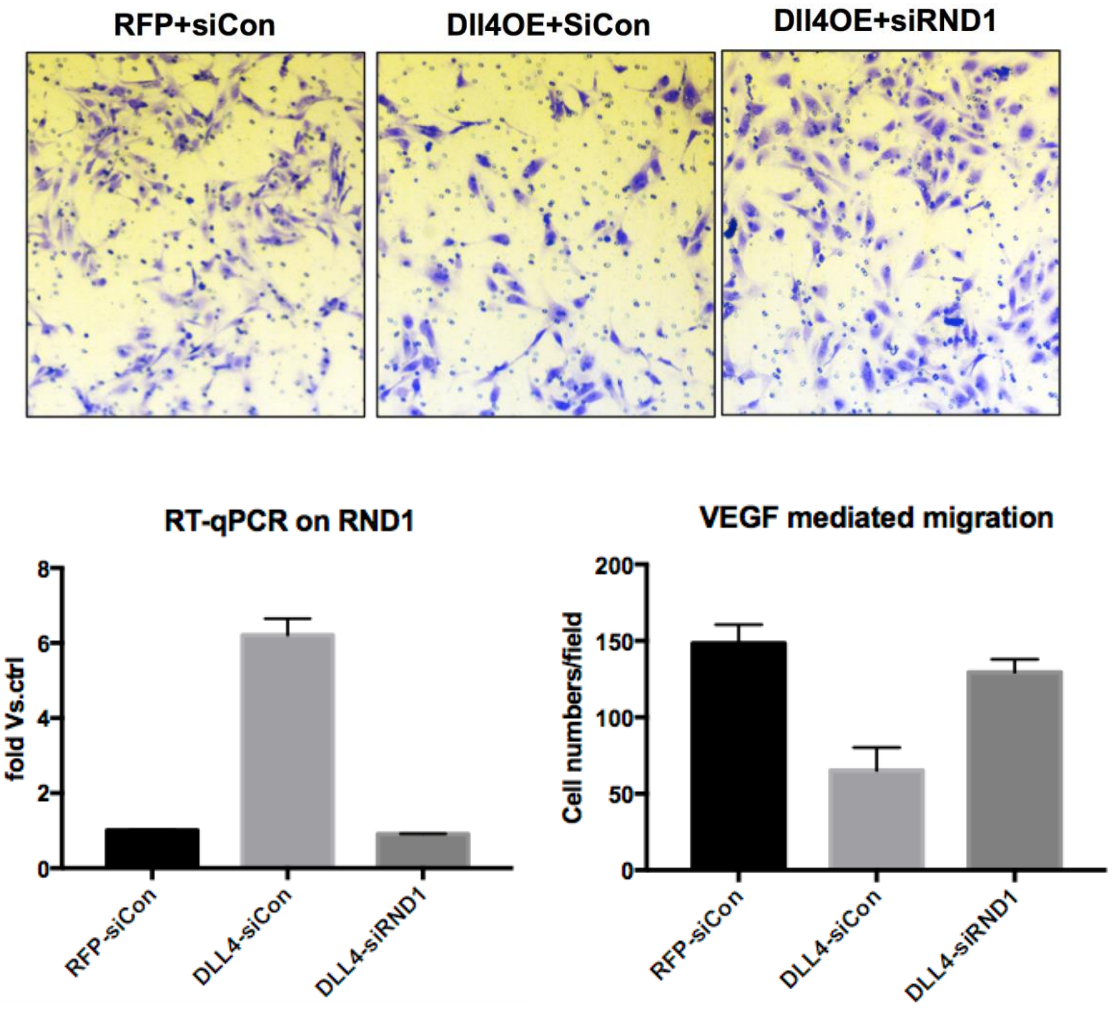

Figure 5-14. Dll4 OE decreased HUVEC migration towards VEGF, and Rnd1KD rescued the phenotype (preliminary)

Lentiviral mediated DLL4 over expression (OE) in HUVECs significantly decreased cell migration towards VEGF in the Boyden Chamber migration assay. Cell migration was measured by quantifying cell number per field using ImageJ, and this experiment has only been performed once. si-RND1 treatment on DLL4 OE HUVECs successfully rescued this phenotype. To note, this experiment has only been done once.

5.3.5 Loss of Rnd1 promoted sprouting and overexpression of RND1 restricted sprouting in Fibrin-bead angiogenesis (FIBA) assay

Notch plays critical role in regulating angiogenesis. Rnd1, as a novel EC Notch target, has been shown above to regulate VEGF-stimulated migration. Our next question is whether Rnd1 functions in regulating the multistep processed of angiogenesis. To characterize Rnd1 function in angiogenesis, we carried out an *in vitro* sprouting assay called Fibrin Bead Sprouting Assay (FIBA). FIBA is a 3D capillary sprouting assay that mimics the normal sprouting process *in vitro*. FIBAs consist of EC attached to latex beads, embedded in a fibrin clot, and overlaid with feeder cells that secrete critical growth factors to promote formation of vessel-like structures (Figure 5-15). Sprouting activity in FIBA can be well assessed 5-7 days after beads are embedded in fibrin, when endothelial sprouts form lumen-containing, branching networks (Nakatsu, Davis, & Hughes, 2007; Nakatsu & Hughes, 2008).

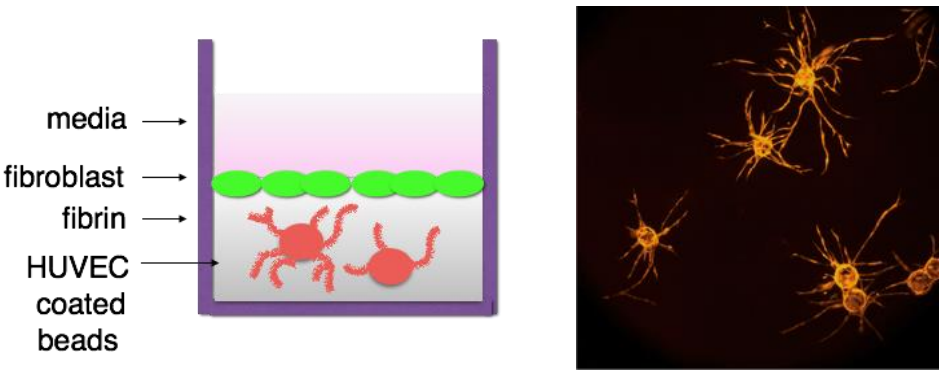

Figure 5-15. Schematic of Fibrin Beads Sprouting Assay

Endothelial cell-coated beads were embedded in a fibrin gel, overlaid with a fibroblast feeder layer, and cultured in endothelial cell culture media (Left). Sprouting with branches and tube- like structures can be observed in day5-day7 FIBAs (Right).

When Rnd1KD were used in FIBA assays, we observed a significant increase the number of sprouts on day 2 (Figure 5-16). However, this difference was lost over time, possibly due to the loss of siRNA knockdown efficacy, which we showed fades away after 3-4 days (Figure 5-16). The hyper sprouting phenotype caused by Rnd1 knockdown on day2 is consistent with the effects of Notch inhibition, which leads to enhanced endothelial sprouting, and further suggests that Rnd1 may also mediate Notch-induced sprouting inhibition.

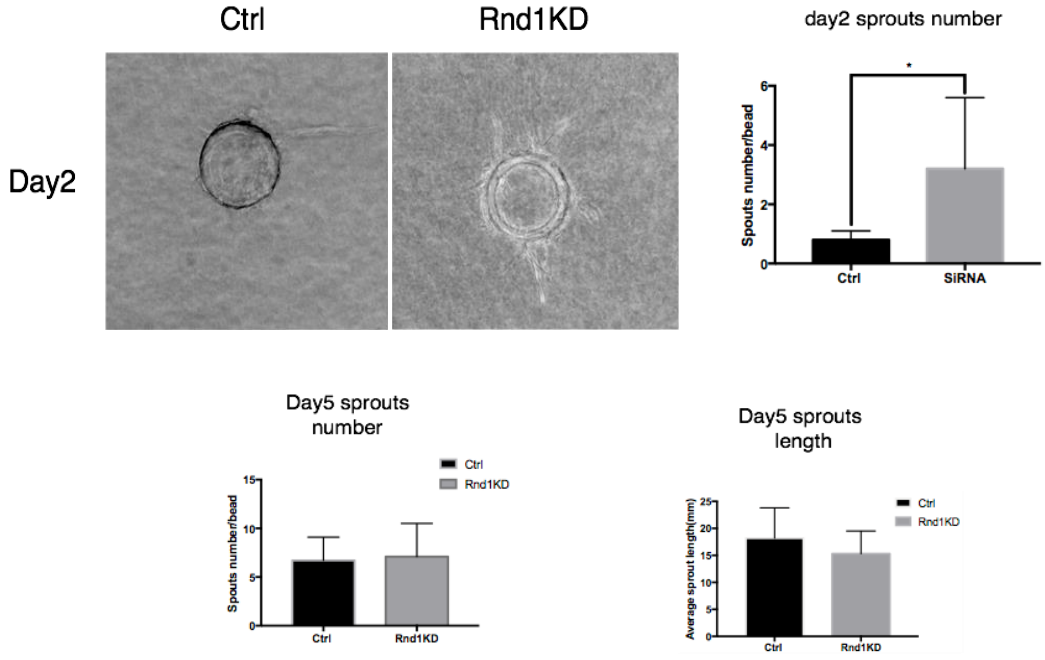

Figure 5-16. Rnd1KD enhanced sprouting angiogenesis in HUVECs

HUVECs transfected with siRND1 or siCtrl was embedded for FIBA assay 48 hours after transfected the cells. Rnd1KD HUVECs showed enhanced sprouting on day2 compared with control. To quantify the assay, sprouts number and length were measured using 5X image from each well, for a total of between 50-100 beads per group However, as KD effect of siRNA faded away, no significant differences were detected on day5.

We then investigated the effects of Rnd1 overexpression. HUVECs were co-infected with pCCL constructs expressing full length Rnd1 (or empty pCCL vector as control) and pCCL-RFP to better visualize the sprouting activity. As expected, HUVECs with lentiviral meditated stable overexpression of Rnd1 showed decreased sprouting number, sprout length and tip cell number on day 5-7 of FIBA assays, which is consistent with the effects of Notch activation that inhibit sprouting activity in endothelial cells (Figure 5-17).

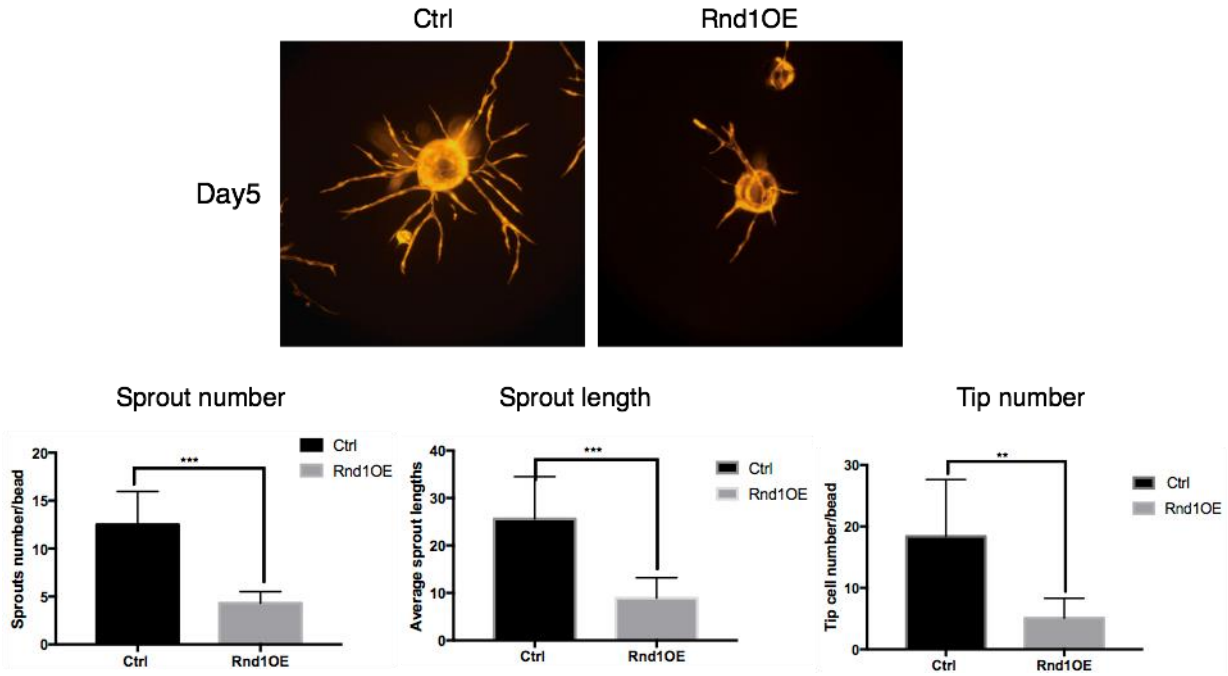

Figure 5-17. Rnd1 overexpression decreased sprouting angiogenesis in HUVECs

Lentiviral-mediated stable overexpression of Rnd1 significantly inhibited sprouting of HUVECs in the FIBA assay. To quantify the assay, sprouts number and length were measured using 5X image from each well, for a total of between 50-100 beads per group. Quantification of the assay showed decreased sprouts number, sprouts lengths as well as tip number in siRND1 HUVECs.

Taken together, these findings suggest multiple functions of Rnd1 in cultured endothelial cells, including regulation of cell migration towards VEGF and sprouting angiogenesis. More importantly, Rnd1KD significantly rescued the migration phenotype caused by Dll4 induction, indicating that Rnd1 is required downstream of Notch to mediate suppression of cell migration. During sprouting angiogenesis, Notch plays a critical role in restraining the migratory capability of stalk cells towards VEGF. Based on our data, we hypothesized that Rnd1 is rapidly and strongly induced by Dll4-Notch in stalk cells and contributes to the stalk cell phenotype through repressing migration and angiogenic sprouting in that cell.

5.4 Results - Signaling mechanism of Rnd1 in endothelial cells

We sought to examine the mechanism by which Rnd1 regulates endothelial behavior. It has been shown that Rnd1 can be an indirect regulator of either Rho or Ras in previous studies (see introduction). Here we performed G-LISA assays to detect the effect of Rnd1 knockdown on Rho and Ras activities. G-LISA is a colorimetric based assay that measures the GTP-loaded Rho/Ras protein in cell lysates(Alford, Wang, Feng, Longmore, & Elbert, 2010).

Knockdown of Rnd1 with siRNA showed no significant effects in basal Ras activation level in HUVECs (Data not shown) We then investigate the effects of Rnd1 on induced-level of Ras activity. EGF has been previously described to induce Ras activity in multiple cell types (Margolis & Skolnik, 1994; Rojas, Yao, & Lin, 1996). In HUVECs, EGF treatment caused a transient increase of Ras activation at 5 minutes. Inhibition of Rnd1 by siRNA significantly enhanced EGF-mediated Ras activation. We then explored the effects of Notch signaling on Ras activity. Overexpression of N1IC dramatically up-regulated *Rnd1* mRNA level by more than 300-fold as previously shown. Consistent with the Rnd1KD effect, N1IC overexpression completely abolished EGF-mediated Ras activation in HUVEC (Figure 5-18).

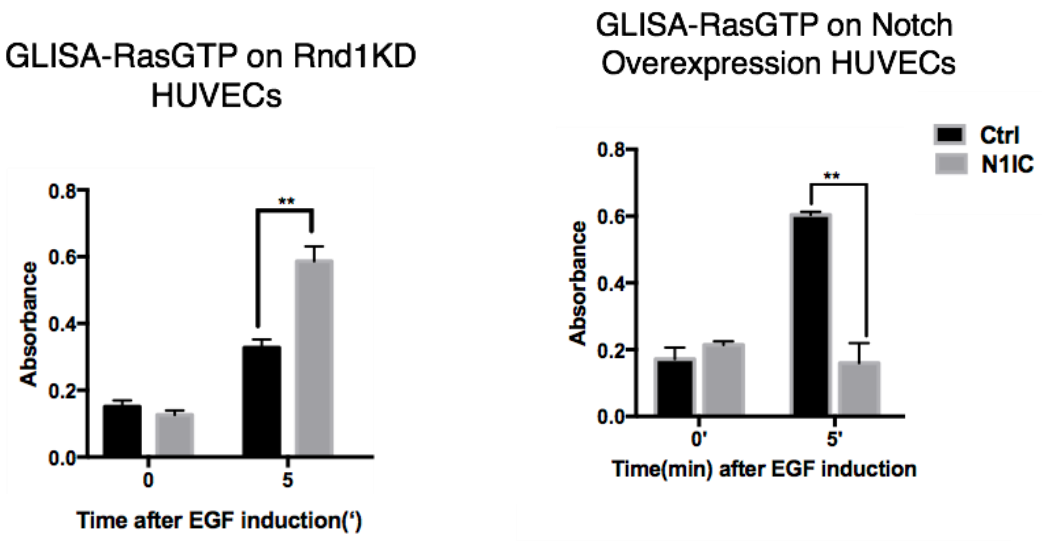

Figure 5-18. EGF-induced Ras activation was enhanced by Rnd1KD, and inhibited by Notch OE

EGF transiently induced Ras activation at 5minutes after treatment, detected with GLISA-RasGTP kit. Rnd1KD enhanced the EGF-mediated Ras activation. N1ICD overexpression strongly induced Rnd1 expression (see Figure 5-6), and completely blocked EGF-mediated Ras activation.

Most studies indicate that the morphological effect of Rnd proteins are related to inhibition of RhoA-mediated contraction. We then examine the possibility that RND1 regulates RhoA signaling in endothelial cells. Rnd1 knockdown, however, showed no effect on basal or thrombin-induced RhoA activation in HUVECs. Consistent with the Rnd1 knockdown, N1ICD overexpression did not affect Rho activation in HUVECs (Figure 5-19).

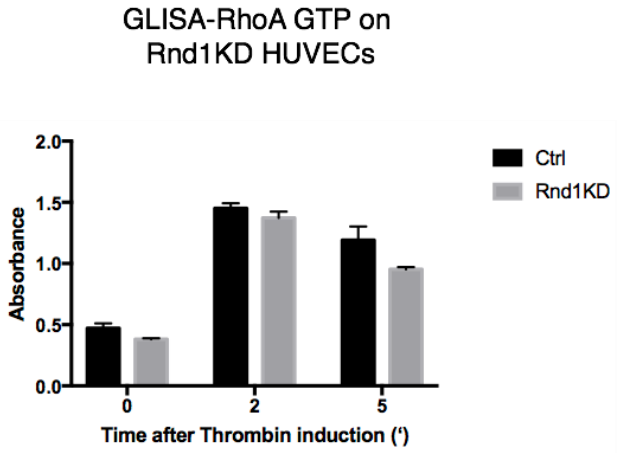

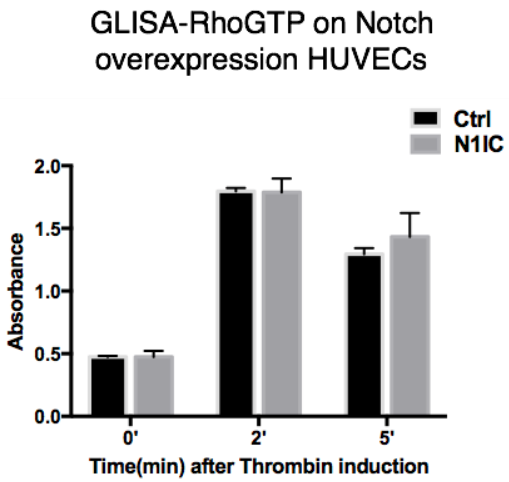

Figure 5-19. Rnd1KD and Notch OE has no effect on Thrombin-mediated RhoA activation

Thrombin transiently induced RhoA activation at 2minutes after treatment, detected with GLISA-RhoA GTP assay. Neither Rnd1KD nor NIC overexpression has any significant effects on Thrombin-mediated RhoA activation.

Collectively, our data suggests that Notch, and the downstream target Rnd1, regulate Ras but not RhoA activity in HUVECs.

5.5 Discussion/Working model

In this chapter, we interrogated the functional role of the Rho GTPase Rnd1, a novel endothelial Notch responsive gene identified in the screens described in Chapters 3 and 4. Rnd1 has been well established as a regulator of cytoskeleton activity in various cell types, while the role of Rnd1 in endothelial cells has been poorly understood. Here, we established that Rnd1 regulates VEGF-mediated migration and angiogenesis capability in

HUVECs. Loss of Rnd1 resulted in enhanced migratory and hyper sprouting of endothelial cells, which is consistent of the effects of Notch inhibition which lead to “tip cell” phenotype. Overexpression of Rnd1 blocked sprouting, which mimic the “stalk cell” phenotype. More importantly, Rnd1KD significantly rescued the migration phenotype caused by Dll4 overexpression, indicating that Rnd1 is required downstream of Notch signaling to mediate suppression of cell migration. These results strongly support Rnd1 as a downstream target of Notch signaling and support Rnd1 as a critical Notch effector in endothelial cells. Signaling mechanism studies revealed that Notch, as well as the downstream target Rnd1, regulate Ras activity but not Rho activity in endothelial cells.

It has been well established that Dll4 in tip cells activates Notch signaling in adjacent endothelial cells, which suppress tip cell fate in neighboring cells through regulation of VEGF receptor expression. VEGF receptors are secondary targets of Notch signaling, and are subjected to regulation of Hey2. Here, we propose a working model which reveals a novel mechanism of Notch regulation in angiogenesis through newly defined primary target and effector Rnd1 (Figure 5-20). Our date suggests that Rnd1 remains at a low expression level in quiescent endothelial cells. During angiogenesis, Dll4 in tip cells activates Notch signaling in adjacent endothelial cells, which rapidly and strongly up regulate Rnd1. High expression levels of Rnd1 inhibits Ras activity (and other potential signaling pathways), which contributes to stalk cell phenotype by inhibiting the migration activity towards VEGF and sprouting activity.

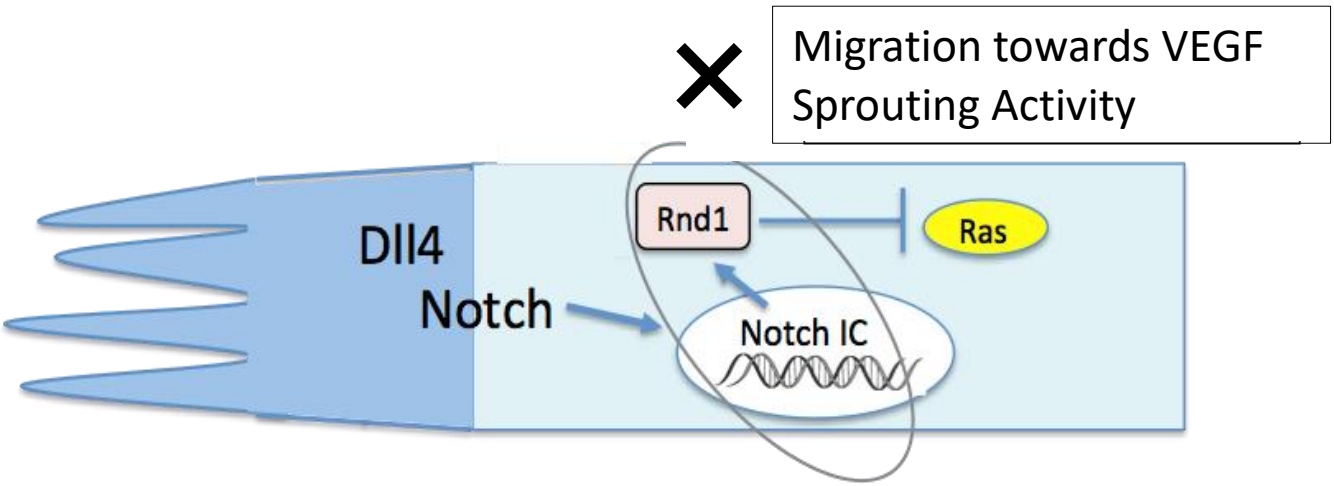

Figure 5-20. Working Model

Chapter 6 Discussion and Future Directions

This thesis work employs a variety of *in vitro* and *in vivo* unbiased screening approach to identify novel early Notch transcriptional targets in endothelial cells. We established an *in vivo* screening method that captures rapid response Notch targets in endothelial cells 6 hours after GSI injection using the RiboTag technique. *In vitro*, we identified a set of genes in primary endothelial cells that are activated 6 hours after Dll4/Jag1 stimulation and the genes that are stimulated within 1-1.5 hours by EGTA treatment and which are sensitive to GSI treatment. Combining these screens, we established a comprehensive data set that characterized the rapid Notch transcriptional events from both *in vivo* and *in vitro* contexts. A large number of novel Notch candidates were identified in the comprehensive dataset. We picked one of the most highly induced candidates, Rho GTPase *RND1*, for further study. *RND1* was successfully validated as a Notch target using a variety of assays. We discovered that Rnd1, was a bone fide Notch effector when analyzed using cultured endothelial cells, regulating endothelial cell migration towards VEGF and angiogenesis capabilities through the Ras signaling pathway. These studies make a significant contribution to our understanding of Notch-mediated angiogenic signaling through downstream effectors and established comprehensive methodology as well as datasets for future interrogation of novel Notch targets. However, many questions remain to be addressed and we will discuss here experiments to follow up on our current studies and further elucidate the roles of Notch effectors.

6.1 Determining the mechanism by which Notch regulates *RND1*

It is important to understand how the endothelial-specific expression of genes is controlled at the transcriptional level. The basal expression level of *RND1* was very low in endothelial cells, however the expression was upregulated in a rapid and dramatic manner upon Notch activation. Our *in-silico* analysis suggested a putative endothelial specific enhancer region of *RND1* that may be responsive to Notch activation. Our hypothesis is that this enhancer is a key player for increasing endothelial specific RND1 expression upon Notch activation. This hypothesis can be explored by characterizing the binding activity of NICD to the enhancer region using Chromatin IP, and the function of enhancer fragments from the *Rnd1* gene using Luciferase reporter assays and/or deletion analysis to study the effects of the enhancer regions on gene expression in response to Notch signaling in endothelial cells and other cell types.

We have considered possibility of creating a mouse model with a knockout of the endothelial-specific enhancer of Rnd1. However, while this enhancer can be clearly defined in human cells, the syntenic region in mouse is not well defined and the ENCODE DHS sequencing database does not contain sufficient coverage in mouse cells to identify this enhancer region in the mouse genome.

6.2 Deciphering signaling mechanism of Rnd1 in endothelial cells

Our data suggested that Notch, and its effector Rnd1, functions through Ras signaling in endothelial cells. It has been well established in other cell types that Rnd1 functions through Ras effectors to indirectly regulate Ras activity. Plexin-B1, a Sema-4D receptor, can interact simultaneously with Rnd1 and R-Ras•GTP, and this interaction stimulates the GAP activity of plexin-B1 on R-Ras(Yamamoto et al., 2018). We hypothesize that Rnd1 in association with plexins regulate Rap and Ras GAP in endothelial cells. To test this hypothesis, co-immunoprecipitation (co-IP) will be performed to exam direct binding partners of Rnd1. Rap and Ras activities will be examined in conditions of Rnd1 loss or gain function. Previous studies have shown that Rnd1 functions primarily through Rho activation in some cell types, so it is currently unknown why Rnd1 functions through Ras, but not Rho, in endothelial cells. We hypothesize that the presence of plexins play critical roles in regulating this process. We can test the hypothesis by knocking down plexin proteins in Rnd1 overexpressing endothelial cells to observe the effects on Rho and Ras activation.

6.3 Determining Rnd1 function in angiogenesis using mouse model

Our *in vitro* data demonstrates that Rnd1 regulates sprouting angiogenesis. It will be of great interest to characterize Rnd1 function in physical and pathological angiogenesis using mouse models. So far, no Rnd1 transgenic mouse models have been published. Our lab is in the process of generating Rnd1 conditional knockout mice ($Rnd1^{flox}$) using Crisper-Cas9 technology. $Rnd1^{ECKO}$ (*$Rnd1^{flox/flox}$* in combination with an endothelial specific inducible Cre allele, *Cdh5CreERT2)* mice can be used to interrogate Rnd1

function in different models of angiogenesis, such as postnatal retina angiogenesis and oxygen induced retinopathy. To determine if Rnd1 is required to mediate Notch function in angiogenesis, we can compare retinal angiogenesis in *N1ICD^{EC}; Rnd1^{ECKO}* with *N1IC^{EC}* mice and examine whether loss of Rnd1 is sufficient to rescue some or all of the effects of Notch overexpression *in vivo*. Furthermore, Rnd1^{ECKO} mice can be bred to RiboTag mice to characterize downstream changes caused by loss of Rnd1 *in vivo* using RNA-seq. These experiments will be of great value to examine the angiogenic roles of Rnd1 as a Notch effector and establish whether endothelial Rnd1 also has Notch-independent roles in the context of the living organism.

6.4 Exploring other targets of interest

Our *in vitro* and *in vivo* screens identified a large number of candidate endothelial Notch targets and effectors which remain unexplored. We identified a subset of G-Protein/GPCRs (including but not exclusive to Rnd1) as potential Notch targets. GPCRs are regarded as potent regulators of blood vessel formation, in both developmental and pathological angiogenesis. For example, one of the novel targets GPR126, has been shown to regulate developmental and pathological angiogenesis through modulation of VEGFR2 receptor signaling(Cui et al., 2014). However, a better understanding of the functionality and molecular mechanisms of the majority G-Protein/GPCR candidates in angiogenesis still needs to be characterized. Moreover, the observation that Notch regulates proteins that function in GPCR signaling is novel and unexplored area of endothelial Notch function.

Another group of interesting targets are those that have been well established as key regulator of vascular function, but have not previously been linked to Notch signaling, such as *UNC5B* and *MSFD2A*. As discussed in Chapter III, the netrin receptor UNC5B has been well established to play an anti-angiogenic role during embryonic vascular patterning, as well as in postnatal and pathological angiogenesis (Larrivee et al., 2007; Lu et al., 2004). Our data suggest *UNC5B* as a very rapid responder to Notch activation both *in vivo* and *in vitro* and is among the 17 genes identified by all three screens as Notch targets. Another target of high interest is *MSFD2A*, which is critical for the formation and function of the blood brain barrier (Ben-Zvi et al., 2014). Our data indicate that *MSFD2A* is a rapid responding gene of Notch in brain endothelium, and this may reveal an unaddressed area of Notch regulation on blood brain barrier.

6.5 Jag1 in endothelial cells: activator or inhibitor of Notch?

The regulation of Notch signaling in endothelial cells is attributed to Notch ligand, Jag1 and Dll4. High expression of Dll4 in tip cells is thought to activate Notch in stalk cells, and functions to suppress sprouting angiogenesis in stalk cell. The role of Jag1, unlike Dll4, is controversial and elusive. It is suggested that Jag1, as an inactive ligand, promotes angiogenesis by antagonizing Dll4-mediated activation of Notch signaling in fringe-modified endothelial cells (Benedito et al., 2009). However, data from our group and others suggest that Jag1 can activate EC-Notch signaling to promote angiogenesis (Chang et al., 2011; Kangsamaksin et al., 2015). Our lab demonstrated that blocking Jag1 activity in ECs

using the JAG-specific NOTCH1 decoy downregulated canonical Notch targets including *HEY1*, *HEYL*, and *HES1*(Kangsamaksin et al., 2015). The mechanism of how Jag1 regulates endothelial Notch signaling has been a great interest. We formed three hypotheses of the role of endothelial Jag1:

a. Jag1 functions as inactive ligand to antagonize Dll4-Notch signaling. If the hypothesis is real, we would detect down-regulation of canonical Notch targets upon presence of Jag1.

b. Jag1 functions as a weak ligand to stimulate low level of Notch activation. If the hypothesis is real, we would detect overlapping genes but with weaker fold induction by Jag1/Notch compared to Dll4/Notch.

c. Jag1/Notch signaling promotes unique downstream targets. If the hypothesis is real, we would detect distinct target genes of Jag1/Notch compared with Dll4/Notch.

Our RNA-seq analysis on ECs stimulated by tethered-Jag1 identified a weak activation potency. We did not see significant down-regulation of canonical Notch targets, which may occur if Jag1-Fc blocks the endogenous Dll4-Notch activity which is exhibited in cultured EC. Furthermore, comparison of the Dll4 and Jag1 profiles (using Common genes between HUVEC and HREC) identified 100% up regulated genes (11 of 11 genes) to be common. The induction fold change of stimulated genes by Jag1 is relatively lower compared with Dll4. Collectively, our data confirmed hypothesis *b* and suggested that Jag1 functions as a weak activator of Notch signaling in endothelial cells.

6.6 Application of RiboTagEC model to profile other vascular beds

The RiboTagEC model is a powerful tool to characterize endothelial transcriptional responses where cellular environment is maintained. We use the global Notch inhibitor GSI to detect Notch-dependent transcripts. In the future, we may detect ligand-specific Notch signaling targets using ligand-specific "Notch decoys" previously developed in our lab. By establishing a comprehensive catalog of endothelial global Notch, Dll-Notch, and Jag-Notch targets *in vivo,* we will have a better understanding of the regulation mechanism of ligand-specific Notch signaling. In this study, we focused on neonatal brains. However, the RiboTagEC model can be easily used to profile other vascular beds to characterize transcriptional events in developmental retina angiogenesis, oxygen induced retinopathy, cardiovascular disease, tumor angiogenesis and other model systems. As shown for the example of Rnd1, this powerful approach enables the identification of novel regulators and molecular processes mediating angiogenic growth, which will provide valuable insights to regulatory mechanisms of those process and novel targets to address pathological conditions. In next Chapter (Chapter 7 appendix), we utilized the RiboTagEC technique to profile Notch signaling in tumor endothelial using a xenograft tumor model.

Chapter 7 Appendices

Profiling Notch signaling in tumor vessels using RiboTag model

7.1 Introduction

7.1.1 Tumor angiogenesis and anti-angiogenic therapy

Angiogenesis is a critical step in tumor growth, malignancy and metastasis. Most solid tumors are avascular in the initial stage until the size reaches 1-2 mm in diameter. As the tumor continue to expand, "angiogenic switch" is triggered by tumor-derived angiogenic factors and inflammatory cytokines, recruiting surrounding host vessels to form new blood vessel capillaries, which supply growth factors for tumor expansion and metastasis(Weis & Cheresh, 2011). In contrast to the host vessel, these tumor-induced vessels are abnormal, fragile, and hyperpermeable.

Anti-angiogenic therapy has become an established therapeutic approach through reducing solid tumor growth. VEGF signaling is one of the most established signaling pathways in tumor angiogenesis. The first FDA approved anti-angiogenic drug, bevacizumab (Avastin), is a VEGF-A inhibitor used in several types of cancers and has proved somewhat successful(Bergers & Hanahan, 2008). However, anti-angiogenic agents targeting the VEGF pathway do not exhibit durable tumor responses, and they eventually induce drug resistance or even favor tumor metastasis in some cases(Bergers & Hanahan, 2008; Ebos, Lee, & Kerbel, 2009; Paez-Ribes et al., 2009).

7.1.2 Notch signaling in tumor angiogenesis

Notch signaling has been shown to play an important role in tumor angiogenesis. Notch proteins and ligands are widely expressed in endothelial and perivascular cells, but they are also shown to be up-regulated in several types of tumor cells. Dll4 was found to be up-regulated in tumor blood vessels and several types of tumors(Mailhos et al., 2001; Patel et al., 2005) and its blockade decrease tumor growth by inducing hyper sprouted-but-nonfunctional vasculature(Hoey et al., 2009; Ridgway et al., 2006). Therefore, Notch signaling, like VEGF, has become a focus for developing anti-angiogenic therapy by pharmaceutical companies. Pan-Notch inhibitor GSI, and Dll4 inhibitors have been developed for cancer therapy and are now in clinical trials; however, varying susceptibility among different tumors and safety concerns for long-term treatments have rendered those therapies less promising as reliable solutions (Jain, 2005; Shojaei et al., 2007; Yan et al., 2010). Notch signaling is involved in many cellular functions. Hence, altering Notch signaling may lead to severe side effect. In addition, the hyper-sprouting phenotype resulted from pan Notch (GSI) or Dll4 blockader is also worrisome.

Significant amount of studies over last two decades has revealed the complexity of signaling mechanism in tumor angiogenesis. Even though increased knowledge was gained on Notch signaling pathway in tumor angiogenesis, a comprehensive and complete understanding is still missing. In order to reveal the transcriptional landscape of Notch

signaling in tumor vessels, we used the RiboTagEC mice model and performed an unbiased profiling of Notch signaling in tumor vessel.

7.2 Results- Characterizing tumor angiogenesis in DNMAML^{EC} mice

Notch inhibition can be achieved either by conditional knockout of Notch or ligands, or expression of inhibitory construct. The former method can be efficient but with the possibility of compensation effect by other receptors and ligands. It is also more difficult to recombine both alleles in every cells. So here we ablate Notch signaling with expression of inhibitory protein-dominant negative Mastermind-like (DNMAML). In normal cells, activation of Notch signaling causes translocation of the Notch intracellular domain (NICD) to the nucleus, where it complexes with the CSL complex. Mastermind-like (MAML) binds to the CSL/NICD complex and facilitates the binding of an additional coactivation complex (CoA), which causes transcriptional activation of Notch/CSL targets (Nam, Weng, Aster, & Blacklow, 2003). The inhibitory dominant negative MAML (DNMAML) construct binds to CSL/NICD, but cannot recruit CoA. In the absence of CoA recruitment, CSL maintains its role as a transcriptional repressor, and canonical Notch signaling is inhibited. DNMAML has been well validated in cell-based assays and in mouse models as a specific Notch inhibitor that replicates phenotypes produced by Notch or RBPJ deficiency (McElhinny, Li, & Wu, 2008).

7.2.1 Working strategy

To inhibit Notch signaling specifically in endothelial cells, we crossed Cre-inducible DNMAML mice with Cdh5CreERT2 mice to get DNMAML^{EC} (Cdh5CreERT2/+; DNMAML-GFP flox/+) mice. Recombination was induced with tamoxifen 5 weeks after mice were born. For this experiment, we employed the Lewis Lung Carcinoma (LLC) tumor model, an established highly vascularized tumor model. At week 6, LLC tumor cells were subcutaneously implanted into mice. LLC tumor growth were monitored on a weekly basis and harvested after 2 weeks or when tumors reached the size of 2 centimeters in diameter.

7.2.2 DNMAML^{EC} mice showed no difference in tumor progression

DNMAML^{EC} mice exhibited similar primary tumor growth kinetics to control mice, as well as comparable primary tumor masses at endpoint day 14 (Figure 7-1).

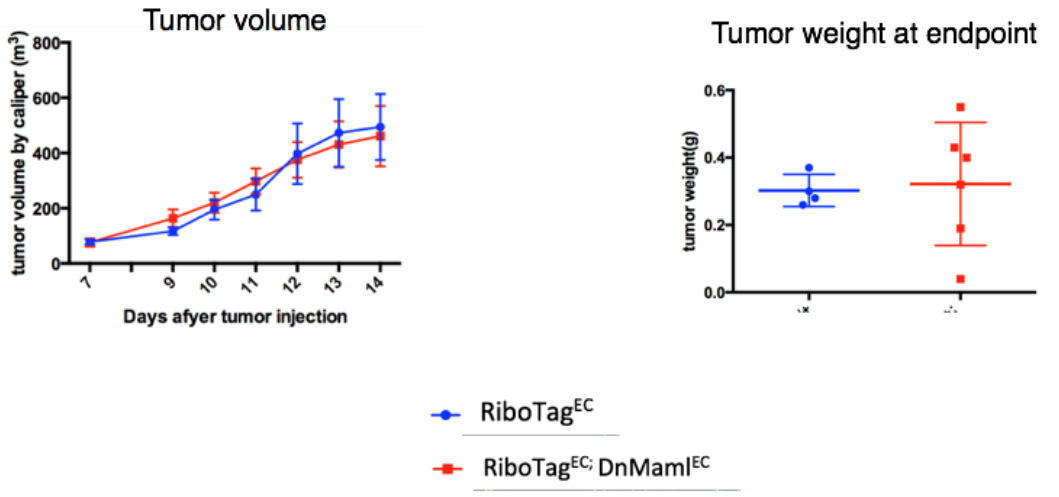

Figure 7-1. DNMAML^{EC} mice showed no significant difference in tumor progression

Recombination was induced with tamoxifen 5 weeks after mice were born. LLC tumor was implanted subcutaneously on week 6. Tumor volume was monitored by caliper measurement every day, and tumor weight was assessed at day 14 once they were dissected out of the mouse. No significant differences were observed between DNMAML^{EC} mice (n=3) and control mice (n=3).

7.2.3 DNMAML^{EC} mice showed significant enhanced endothelial cell density

Despite this, we did note that DNMAML^{EC} mice showed a significant increase in endothelial cell density when we analyze endpoint tumor vasculature by Endomucin staining (Figure 7-2). This is consistent with the hyper-sprouting phenotype resulted from blockade of Dll4-Notch from previous studies (Hoey et al., 2009; Ridgway et al., 2006)

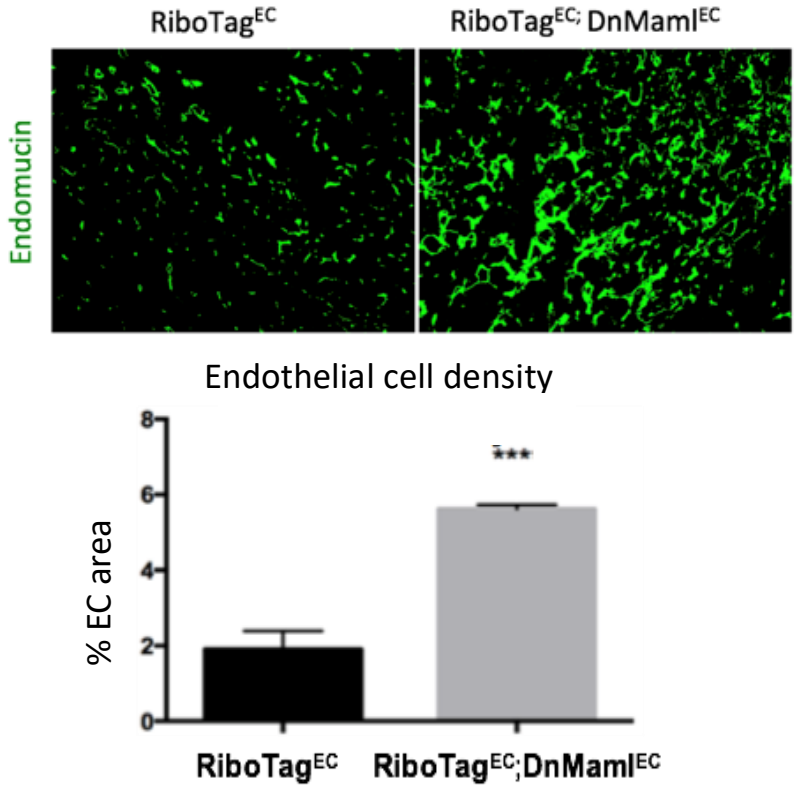

Figure 7-2. DNMAML^{EC} mice showed enhanced endothelial density in tumor

Tumors were fresh frozen in OCT. 7 μm sections were post fixed and stained for endothelial markers (Endomucin). Quantification was done using Fiji-ImageJ. Endothelial cell coverage was calculated by quantifying area covered by Endomucin positive signals and dividing by total area of the specimen. DNMAML^{EC} mice (n=3) showed significant enhanced tumor density compared with control(n=3).

To summarize, in this study, DNMAML^{EC} significantly increased tumor vessel density while showed no effect on tumor growth. The potential explanations could simply be that inhibition of Notch signaling solely in vessel may be efficient in changing vessel density, but have limited effect in changing tumor progression. Other explanation could be that LLC tumor grows aggressively and rapidly, which lead to potential complication that subtle differences in tumor dynamics may be lost due to the overwhelmingly aggressive

nature of the tumor cells themselves. It also allows limited time for the development of detectable metastasis. It is possible that changes of tumor growth by inhibition of Notch function in vessels will be detected using different types of tumor models.

7.3 Results- Profiling Notch signaling in tumor vessels using RiboTagEC model

Tumors have been recognized as aberrant organs composed of a complex mixture of highly interactive cells including cancer cells, stroma (fibroblasts, adipocytes, and myofibroblasts), inflammatory (innate and adaptive immune cells), and vascular cells (endothelial and mural cells)(Ziyad & Iruela-Arispe, 2011). Uncovering critical vascular specific genes in the complex tumor environment is challenging. Translational profiling using RiboTag represents a particularly useful technique to study specific cell types from complex tissues. Here we used the RiboTagEC mouse model in combination with the DNMAML^{EC} mice to profile Notch signaling in tumor vessels.

7.3.1 Working strategy

DNMAML^{EC}, RiboTag^{EC} (*Cdh5CreER$^{T2/+}$;DNMAML-GFP$^{flox/+}$;Rpl22$^{HA/+}$*) mice were used in the study, RiboTag^{EC}(*Cdh5CreER$^{T2/+}$;Rpl22$^{HA/+}$*) were used as control mice. Following tamoxifen-induced recombination at week 5, HA-tagged Rpl22 and DNMAML were specifically expressed in endothelial cells. At week 6, LLC tumor cells were subcutaneously implanted into mice. Tumors at endpoint (14 days) were harvested and snap frozen in liquid nitrogen. RiboTag IP were then performed as previously described,

and mRNA extracted from both whole tumor homogenate and IP ribosome were subjected to RNA-seq at a depth of ~30 million 100-base single-end reads. We included 3 DNMAML^{EC}, RiboTag^{EC} mice, and 3 RiboTag^{EC} mice as control in this study (Figure 7-3).

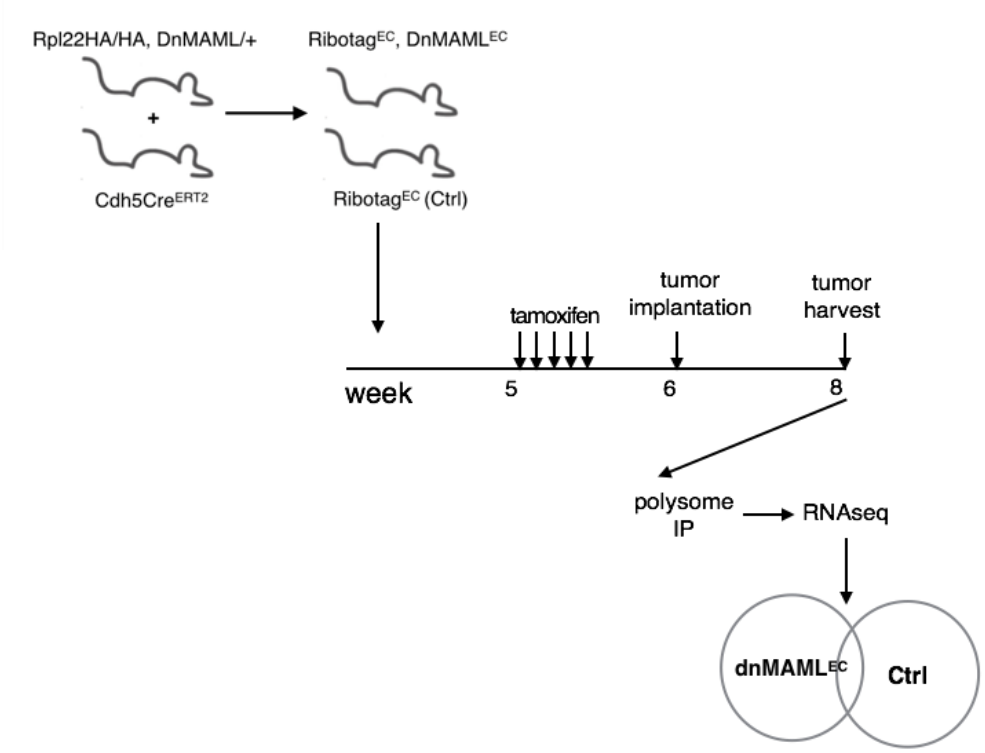

Figure 7-3. Working Strategy

7.3.2 RiboTag staining and endothelial marker enrichment confirmed tissue specificity of the IP system

Immunostaining of end-point primary tumor section detects specific and robust expression of Rpl22HA in endothelial cells (Figure 7-4). To confirm successful immunoprecipitation of endothelial-specific mRNA, we compared Input versus IP samples for expression of

multiple established endothelial markers. As expected, RNA for endothelial specific markers were significantly and consistently enriched in the RiboTag-IP fractions compared with the Input fraction in all samples, which validated endothelial specificity of the IP system (Figure 7-5).

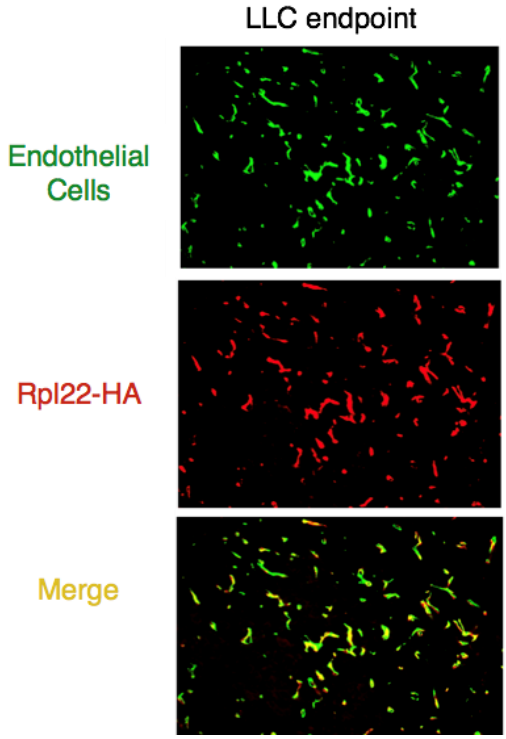

Figure 7-4. Rpl22-HA expression was detected specifically in ECs

Rpl22-HA expression (Anti-HA, red) was detected specifically and efficiently in the endothelial cells (IB4, green) of P5 brain of RiboTagEC mice

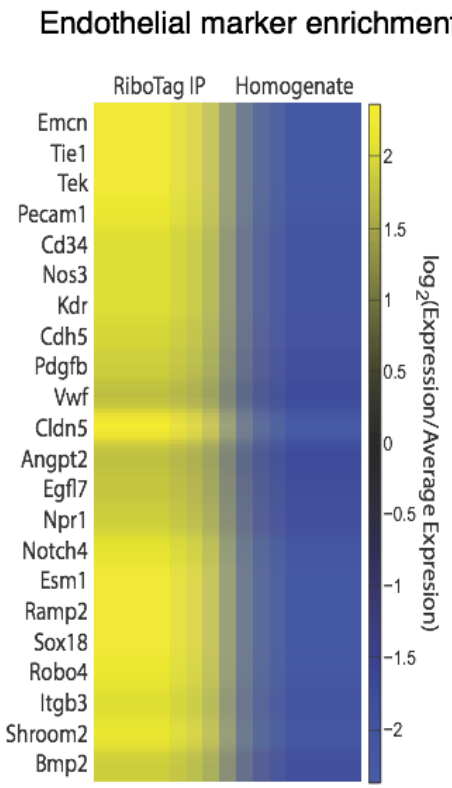

Figure 7-5. RiboTag IP samples exhibited enrichment of EC markers

Differential expression analysis comparing homogenate (n=6) and IP isolated RNA (n=6) showed significant and consistent enrichment of pre-selected endothelial (including *Emcn, Pecam1, Cdh5, Cldn5,* and more) markers across all samples.

7.3.3 PCA analysis revealed substantial variation between individual samples

Two-dimensional principal component analysis (PCA) analysis reveals clustering of homogenate samples versus IP-samples. However, the variation between individual sample are so substantial and this may mask the subtle differences caused by DNMAML expression (Figure 7-6). The big variation is not out of expectation, given the heterogeneity of tumors. A larger sample size is needed for a better interpretation of the results.

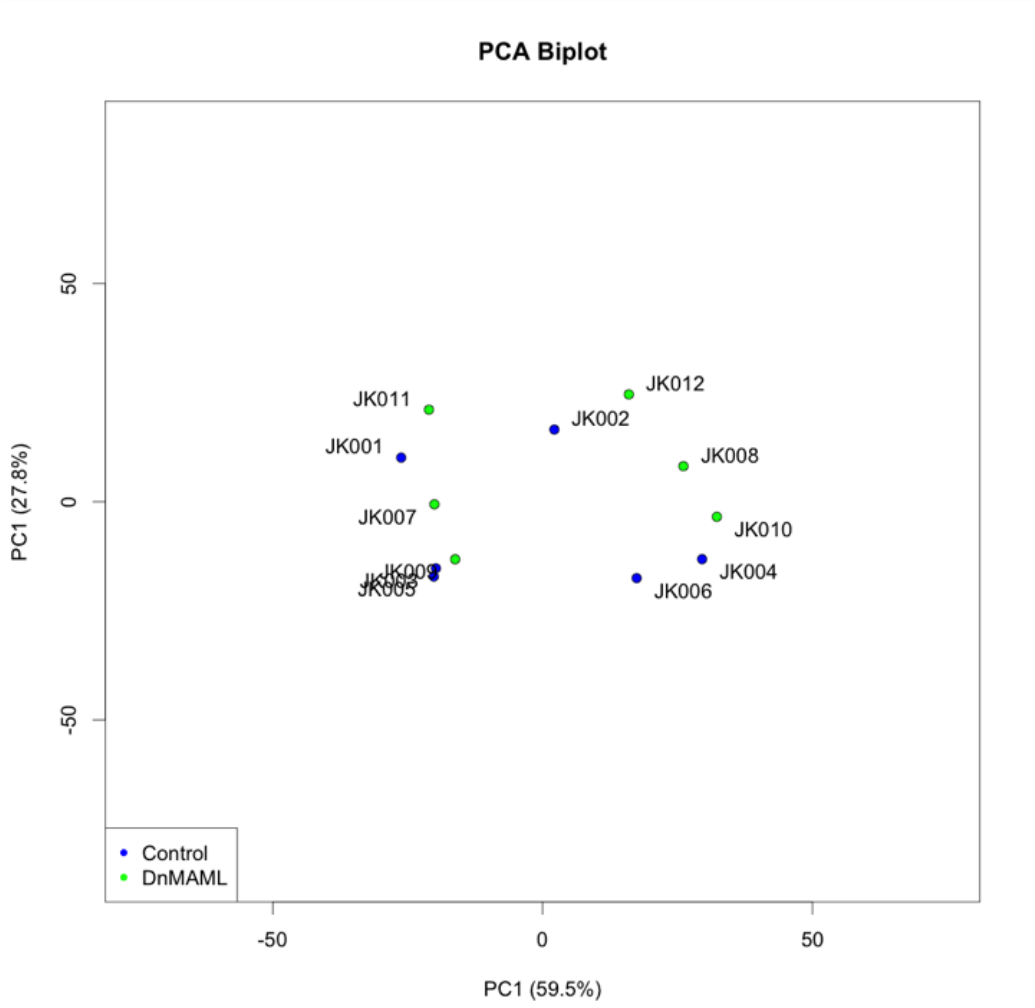

Figure 7-6. PCA plots showed segregation of homogenate and IP, and revealed substantial variability between individual samples

Two-way principle analysis (PCA) showed segregation of 2 groups: Homogenate (left) and IP (right). The DNMAML effects, however, did not further differentiate the samples (blue as control, green as DNMAML). Large variability between individual samples was revealed.

7.3.4 Differential analysis detected genes altered by DNMAML in tumor vessels, but without success identifying canonical Notch targets

Expression profiles of DNMAML mice were compared with the control group. Genes with Padj≤0.05 and fold change of log2≥0.6 fold were considered as candidate genes. No significant differences were detected in gene profiles comparing tumor homogenate from DNMAML and control mice. However, we were able to identify 31 significantly up-regulated genes and 87 significantly down-regulated genes in DNMAML mice RiboTag-IP sample compared with control (Figure 7-7). This is in consistent with the detection of altered tumor vessel density without differences in tumor growth. However, out of our expectation, canonical Notch signaling targets were not present in significantly regulated genes. We will discuss the potential reasons in "Discussion".

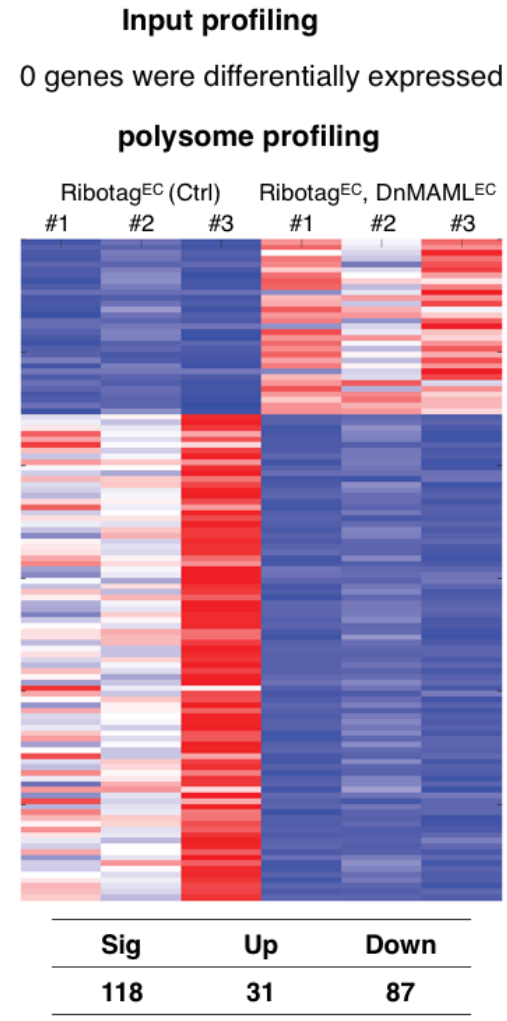

Figure 7-7. Significant gene changes caused by DNMAML^{EC} were detected in IP samples

Differential analysis comparing genes being altered in DNMAML^{EC} mice versus control mice detected no significant change in homogenate samples. Total of 118 genes including 31 upregulated gene and 87 downregulated gene were identified as significant (Padj<0.05) with a Log2FC at least 0.6. However, within those significant genes, we didn't detect any canonical Notch targets.

7.4 Discussion

Tumors are complex tissues that involve multiple cell types, and the transcriptional/translational machinery is highly dynamic. Tumor angiogenesis has been an important target for the treatment of many solid tumors and, in particular, their metastasis. Gaining a comprehensive understanding of cellular behavior and the molecular mechanism controlling the biological processes of tumor vessel can be of great value. Previous transcriptional profiling studies focus on endothelial cells isolated from malignant tissues, which are often complicated by expression altering tissue dissociation and cell sorting steps. The problem can be avoided with the RiboTagEC model. RiboTagEC model is a strong tool to identify altered patterns of RNA translation in specific cell types within a heterogenous background without the need of cell sorting.

We successfully used the RiboTag technique to profile endothelial cells from LLC late-stage tumors. We observed enhanced tumor density in DnMAML^{EC} mice, and detected significant gene expression alteration within tumor vessel using RiboTag IP and RNA-seq. However, we were unable to identify any endothelial canonical Notch targets that

significantly altered by transgenic inhibition of Notch in this study. This may be explained by the following reasons:

1. Genetic gain and loss of function mice model is a powerful tool to characterize phenotype, however these techniques lack the ability to resolve primary transcriptional events. It is challenging to detect Notch target genes when Notch signaling is integrated with the output from downstream signaling cascades, feedback loops, and compensation from parallel pathways. Instead, pharmacological inhibition could be utilized such as GSI, or ligand-specific "Notch decoys" previously developed in our lab to perform a stringently control of signaling kinetic.

2. Abnormality features of tumor vessels at end stage may lead to gene expression changes that are irrelevant to Notch signaling. It has been known that vascular density decreases as tumors grow, leading to zones of ischemia and ultimately necrosis(Nagy, Chang, Dvorak, & Dvorak, 2009). It is not surprising when the environmental cues like ischemia and necrosis triggers dramatic gene expression changes in the endpoint tumors. Future studies could focus on profiling tumor vessels at earlier cancer developmental stage.

3. It could be simply explained by the limited experimental replicates (# of mice) we included in the study. Substantial variations were observed between individual tumors in terms of tumor burden and vessel density, which may serve to mask subtle differences in gene changes between groups.

Taken together, we believe pharmacological manipulation, which enables more precise signaling kinetic control, would be a better tool to profile primary signaling event. Given tumor heterogeneity, more experimental replicates as well as multiple tumor types should be utilized to draw a conclusion.

Finding druggable targets on tumor blood vessels will require them to be better characterized. RiboTag technique can be a great tool to generate cell-specific gene expression signature to understand tumor development, metastasis and therapeutic response.

Reference

Ahmad, I., Balasubramanian, S., Del Debbio, C. B., Parameswaran, S., Katz, A. R., Toris, C., & Fariss, R. N. (2011). Regulation of ocular angiogenesis by Notch signaling: implications in neovascular age-related macular degeneration. *Invest Ophthalmol Vis Sci, 52*(6), 2868-2878. doi:10.1167/iovs.10-6608

Alford, S. K., Wang, Y., Feng, Y., Longmore, G. D., & Elbert, D. L. (2010). Prediction of sphingosine 1-phosphate-stimulated endothelial cell migration rates using biochemical measurements. *Ann Biomed Eng, 38*(8), 2775-2790. doi:10.1007/s10439-010-0014-6

Artavanis-Tsakonas, S., Rand, M. D., & Lake, R. J. (1999). Notch signaling: cell fate control and signal integration in development. *Science, 284*(5415), 770-776.

Bailis, W., Yashiro-Ohtani, Y., Fang, T. C., Hatton, R. D., Weaver, C. T., Artis, D., & Pear, W. S. (2013). Notch simultaneously orchestrates multiple helper T cell programs independently of cytokine signals. *Immunity, 39*(1), 148-159. doi:10.1016/j.immuni.2013.07.006

Bailis, W., Yashiro-Ohtani, Y., & Pear, W. S. (2014). Identifying direct Notch transcriptional targets using the GSI-washout assay. *Methods Mol Biol, 1187*, 247-254. doi:10.1007/978-1-4939-1139-4_19

Ben-Zvi, A., Lacoste, B., Kur, E., Andreone, B. J., Mayshar, Y., Yan, H., & Gu, C. (2014). Mfsd2a is critical for the formation and function of the blood-brain barrier. *Nature, 509*(7501), 507-511. doi:10.1038/nature13324

Benedito, R., Roca, C., Sorensen, I., Adams, S., Gossler, A., Fruttiger, M., & Adams, R. H. (2009). The notch ligands Dll4 and Jagged1 have opposing effects on angiogenesis. *Cell, 137*(6), 1124-1135. doi:10.1016/j.cell.2009.03.025

Bergers, G., & Hanahan, D. (2008). Modes of resistance to anti-angiogenic therapy. *Nat Rev Cancer, 8*(8), 592-603. doi:10.1038/nrc2442

Borggrefe, T., & Oswald, F. (2009). The Notch signaling pathway: transcriptional regulation at Notch target genes. *Cell Mol Life Sci, 66*(10), 1631-1646. doi:10.1007/s00018-009-8668-7

Bray, S. J. (2006). Notch signalling: a simple pathway becomes complex. *Nat Rev Mol Cell Biol, 7*(9), 678-689. doi:10.1038/nrm2009

Calo, E., & Wysocka, J. (2013). Modification of enhancer chromatin: what, how, and why? *Mol Cell, 49*(5), 825-837. doi:10.1016/j.molcel.2013.01.038

Carmeliet, P. (2003). Angiogenesis in health and disease. *Nat Med, 9*(6), 653-660. doi:10.1038/nm0603-653

Castel, D., Mourikis, P., Bartels, S. J., Brinkman, A. B., Tajbakhsh, S., & Stunnenberg, H. G. (2013). Dynamic binding of RBPJ is determined by Notch signaling status. *Genes Dev, 27*(9), 1059-1071. doi:10.1101/gad.211912.112

Chang, A. C., Fu, Y., Garside, V. C., Niessen, K., Chang, L., Fuller, M., . . . Karsan, A. (2011). Notch initiates the endothelial-to-mesenchymal transition in the atrioventricular canal through autocrine activation of soluble guanylyl cyclase. *Dev Cell, 21*(2), 288-300. doi:10.1016/j.devcel.2011.06.022

Chardin, P. (2006). Function and regulation of Rnd proteins. *Nat Rev Mol Cell Biol, 7*(1), 54-62. doi:10.1038/nrm1788

Creyghton, M. P., Cheng, A. W., Welstead, G. G., Kooistra, T., Carey, B. W., Steine, E. J., . . . Jaenisch, R. (2010). Histone H3K27ac separates active from poised enhancers and predicts developmental state. *Proc Natl Acad Sci U S A, 107*(50), 21931-21936. doi:10.1073/pnas.1016071107

Cui, H., Wang, Y., Huang, H., Yu, W., Bai, M., Zhang, L., . . . Liu, M. (2014). GPR126 protein regulates developmental and pathological angiogenesis through modulation of VEGFR2 receptor signaling. *J Biol Chem, 289*(50), 34871-34885. doi:10.1074/jbc.M114.571000

del Alamo, D., Rouault, H., & Schweisguth, F. (2011). Mechanism and significance of cis-inhibition in Notch signalling. *Curr Biol, 21*(1), R40-47. doi:10.1016/j.cub.2010.10.034

Dovey, H. F., John, V., Anderson, J. P., Chen, L. Z., de Saint Andrieu, P., Fang, L. Y., . . . Audia, J. E. (2001). Functional gamma-secretase inhibitors reduce beta-amyloid peptide levels in brain. *J Neurochem, 76*(1), 173-181.

Duarte, A., Hirashima, M., Benedito, R., Trindade, A., Diniz, P., Bekman, E., . . . Rossant, J. (2004). Dosage-sensitive requirement for mouse Dll4 in artery development. *Genes Dev, 18*(20), 2474-2478. doi:10.1101/gad.1239004

Ebos, J. M., Lee, C. R., & Kerbel, R. S. (2009). Tumor and host-mediated pathways of resistance and disease progression in response to antiangiogenic therapy. *Clin Cancer Res, 15*(16), 5020-5025. doi:10.1158/1078-0432.CCR-09-0095

Eerola, I., Boon, L. M., Mulliken, J. B., Burrows, P. E., Dompmartin, A., Watanabe, S., . . . Vikkula, M. (2003). Capillary malformation-arteriovenous malformation, a new clinical and genetic disorder caused by RASA1 mutations. *Am J Hum Genet, 73*(6), 1240-1249. doi:10.1086/379793

Fang, T. C., Yashiro-Ohtani, Y., Del Bianco, C., Knoblock, D. M., Blacklow, S. C., & Pear, W. S. (2007). Notch directly regulates Gata3 expression during T helper 2 cell differentiation. *Immunity, 27*(1), 100-110. doi:10.1016/j.immuni.2007.04.018

Felsenfeld, G., & Groudine, M. (2003). Controlling the double helix. *Nature, 421*(6921), 448-453. doi:10.1038/nature01411

Fischer, A., Schumacher, N., Maier, M., Sendtner, M., & Gessler, M. (2004). The Notch target genes Hey1 and Hey2 are required for embryonic vascular development. *Genes Dev, 18*(8), 901-911. doi:10.1101/gad.291004

Fiuza, U. M., & Arias, A. M. (2007). Cell and molecular biology of Notch. *J Endocrinol, 194*(3), 459-474. doi:10.1677/JOE-07-0242

Foster, R., Hu, K. Q., Lu, Y., Nolan, K. M., Thissen, J., & Settleman, J. (1996). Identification of a novel human Rho protein with unusual properties: GTPase deficiency and in vivo farnesylation. *Mol Cell Biol, 16*(6), 2689-2699.

Fouillade, C., Baron-Menguy, C., Domenga-Denier, V., Thibault, C., Takamiya, K., Huganir, R., & Joutel, A. (2013). Transcriptome analysis for Notch3 target genes identifies Grip2 as a novel regulator of myogenic response in the

cerebrovasculature. *Arterioscler Thromb Vasc Biol, 33*(1), 76-86. doi:10.1161/ATVBAHA.112.251736

Frank, S. B., Schulz, V. V., & Miranti, C. K. (2017). A streamlined method for the design and cloning of shRNAs into an optimized Dox-inducible lentiviral vector. *BMC Biotechnol, 17*(1), 24. doi:10.1186/s12896-017-0341-x

Funahashi, Y., Shawber, C. J., Vorontchikhina, M., Sharma, A., Outtz, H. H., & Kitajewski, J. (2010). Notch regulates the angiogenic response via induction of VEGFR-1. *J Angiogenes Res, 2*(1), 3. doi:10.1186/2040-2384-2-3

Gale, N. W., Dominguez, M. G., Noguera, I., Pan, L., Hughes, V., Valenzuela, D. M., . . . Yancopoulos, G. D. (2004). Haploinsufficiency of delta-like 4 ligand results in embryonic lethality due to major defects in arterial and vascular development. *Proc Natl Acad Sci U S A, 101*(45), 15949-15954. doi:10.1073/pnas.0407290101

Goda, T., Takagi, C., & Ueno, N. (2009). Xenopus Rnd1 and Rnd3 GTP-binding proteins are expressed under the control of segmentation clock and required for somite formation. *Dev Dyn, 238*(11), 2867-2876. doi:10.1002/dvdy.22099

Gonzalez, C., Sims, J. S., Hornstein, N., Mela, A., Garcia, F., Lei, L., . . . Sims, P. A. (2014). Ribosome profiling reveals a cell-type-specific translational landscape in brain tumors. *J Neurosci, 34*(33), 10924-10936. doi:10.1523/JNEUROSCI.0084-14.2014

Gottesbuhren, U., Garg, R., Riou, P., McColl, B., Brayson, D., & Ridley, A. J. (2013). Rnd3 induces stress fibres in endothelial cells through RhoB. *Biol Open, 2*(2), 210-216. doi:10.1242/bio.20123574

Greenwald, I. S., Sternberg, P. W., & Horvitz, H. R. (1983). The lin-12 locus specifies cell fates in Caenorhabditis elegans. *Cell, 34*(2), 435-444.

Guarani, V., Deflorian, G., Franco, C. A., Kruger, M., Phng, L. K., Bentley, K., . . . Potente, M. (2011). Acetylation-dependent regulation of endothelial Notch signalling by the SIRT1 deacetylase. *Nature, 473*(7346), 234-238. doi:10.1038/nature09917

Guasch, R. M., Scambler, P., Jones, G. E., & Ridley, A. J. (1998). RhoE regulates actin cytoskeleton organization and cell migration. *Mol Cell Biol, 18*(8), 4761-4771.

Gupta-Rossi, N., Le Bail, O., Gonen, H., Brou, C., Logeat, F., Six, E., . . . Israel, A. (2001). Functional interaction between SEL-10, an F-box protein, and the nuclear form of activated Notch1 receptor. *J Biol Chem, 276*(37), 34371-34378. doi:10.1074/jbc.M101343200

Haapasalo, A., & Kovacs, D. M. (2011). The many substrates of presenilin/gamma-secretase. *J Alzheimers Dis, 25*(1), 3-28. doi:10.3233/JAD-2011-101065

Hambleton, S., Valeyev, N. V., Muranyi, A., Knott, V., Werner, J. M., McMichael, A. J., . . . Downing, A. K. (2004). Structural and functional properties of the human notch-1 ligand binding region. *Structure, 12*(12), 2173-2183. doi:10.1016/j.str.2004.09.012

Harb, R., Whiteus, C., Freitas, C., & Grutzendler, J. (2013). In vivo imaging of cerebral microvascular plasticity from birth to death. *J Cereb Blood Flow Metab, 33*(1), 146-156. doi:10.1038/jcbfm.2012.152

Harrington, L. S., Sainson, R. C., Williams, C. K., Taylor, J. M., Shi, W., Li, J. L., & Harris, A. L. (2008). Regulation of multiple angiogenic pathways by Dll4 and Notch in human umbilical vein endothelial cells. *Microvasc Res, 75*(2), 144-154. doi:10.1016/j.mvr.2007.06.006

Hass, M. R., Liow, H. H., Chen, X., Sharma, A., Inoue, Y. U., Inoue, T., . . . Kopan, R. (2015). SpDamID: Marking DNA Bound by Protein Complexes Identifies Notch-Dimer Responsive Enhancers. *Mol Cell, 59*(4), 685-697. doi:10.1016/j.molcel.2015.07.008

Heintzman, N. D., Stuart, R. K., Hon, G., Fu, Y., Ching, C. W., Hawkins, R. D., . . . Ren, B. (2007). Distinct and predictive chromatin signatures of transcriptional promoters and enhancers in the human genome. *Nat Genet, 39*(3), 311-318. doi:10.1038/ng1966

Heinz, S., Romanoski, C. E., Benner, C., & Glass, C. K. (2015). The selection and function of cell type-specific enhancers. *Nat Rev Mol Cell Biol, 16*(3), 144-154. doi:10.1038/nrm3949

Hellstrom, M., Phng, L. K., Hofmann, J. J., Wallgard, E., Coultas, L., Lindblom, P., . . . Betsholtz, C. (2007). Dll4 signalling through Notch1 regulates formation of tip cells during angiogenesis. *Nature, 445*(7129), 776-780. doi:10.1038/nature05571

Heng, J. I., Nguyen, L., Castro, D. S., Zimmer, C., Wildner, H., Armant, O., . . . Guillemot, F. (2008). Neurogenin 2 controls cortical neuron migration through regulation of Rnd2. *Nature, 455*(7209), 114-118. doi:10.1038/nature07198

Hoey, T., Yen, W. C., Axelrod, F., Basi, J., Donigian, L., Dylla, S., . . . Gurney, A. (2009). DLL4 blockade inhibits tumor growth and reduces tumor-initiating cell frequency. *Cell Stem Cell, 5*(2), 168-177. doi:10.1016/j.stem.2009.05.019

Hofmann, J. J., & Luisa Iruela-Arispe, M. (2007). Notch expression patterns in the retina: An eye on receptor-ligand distribution during angiogenesis. *Gene Expr Patterns, 7*(4), 461-470. doi:10.1016/j.modgep.2006.11.002

Ishikawa, Y., Katoh, H., & Negishi, M. (2006). Small GTPase Rnd1 is involved in neuronal activity-dependent dendritic development in hippocampal neurons. *Neurosci Lett, 400*(3), 218-223. doi:10.1016/j.neulet.2006.02.064

Iso, T., Hamamori, Y., & Kedes, L. (2003). Notch signaling in vascular development. *Arterioscler Thromb Vasc Biol, 23*(4), 543-553. doi:10.1161/01.ATV.0000060892.81529.8F

Iso, T., Kedes, L., & Hamamori, Y. (2003). HES and HERP families: multiple effectors of the Notch signaling pathway. *J Cell Physiol, 194*(3), 237-255. doi:10.1002/jcp.10208

Iso, T., Maeno, T., Oike, Y., Yamazaki, M., Doi, H., Arai, M., & Kurabayashi, M. (2006). Dll4-selective Notch signaling induces ephrinB2 gene expression in endothelial cells. *Biochem Biophys Res Commun, 341*(3), 708-714. doi:10.1016/j.bbrc.2006.01.020

Jaffe, E. A., Nachman, R. L., Becker, C. G., & Minick, C. R. (1973). Culture of human endothelial cells derived from umbilical veins. Identification by morphologic and immunologic criteria. *J Clin Invest, 52*(11), 2745-2756. doi:10.1172/JCI107470

Jain, R. K. (2005). Normalization of tumor vasculature: an emerging concept in antiangiogenic therapy. *Science, 307*(5706), 58-62. doi:10.1126/science.1104819

Jakobsson, L., Franco, C. A., Bentley, K., Collins, R. T., Ponsioen, B., Aspalter, I. M., . . . Gerhardt, H. (2010). Endothelial cells dynamically compete for the tip cell position during angiogenic sprouting. *Nat Cell Biol, 12*(10), 943-953. doi:10.1038/ncb2103

Jeong, H. W., Hernandez-Rodriguez, B., Kim, J., Kim, K. P., Enriquez-Gasca, R., Yoon, J., . . . Adams, R. H. (2017). Transcriptional regulation of endothelial cell behavior during sprouting angiogenesis. *Nat Commun, 8*(1), 726. doi:10.1038/s41467-017-00738-7

Kangsamaksin, T., Murtomaki, A., Kofler, N. M., Cuervo, H., Chaudhri, R. A., Tattersall, I. W., . . . Kitajewski, J. (2015). NOTCH decoys that selectively block DLL/NOTCH or JAG/NOTCH disrupt angiogenesis by unique mechanisms to inhibit tumor growth. *Cancer Discov, 5*(2), 182-197. doi:10.1158/2159-8290.CD-14-0650

Katoh, M., & Katoh, M. (2007). WNT antagonist, DKK2, is a Notch signaling target in intestinal stem cells: augmentation of a negative regulation system for canonical WNT signaling pathway by the Notch-DKK2 signaling loop in primates. *Int J Mol Med, 19*(1), 197-201.

Keene, M. A., Corces, V., Lowenhaupt, K., & Elgin, S. C. (1981). DNase I hypersensitive sites in Drosophila chromatin occur at the 5' ends of regions of transcription. *Proc Natl Acad Sci U S A, 78*(1), 143-146.

Krebs, L. T., Shutter, J. R., Tanigaki, K., Honjo, T., Stark, K. L., & Gridley, T. (2004). Haploinsufficient lethality and formation of arteriovenous malformations in Notch pathway mutants. *Genes Dev, 18*(20), 2469-2473. doi:10.1101/gad.1239204

Krejci, A., & Bray, S. (2007). Notch activation stimulates transient and selective binding of Su(H)/CSL to target enhancers. *Genes Dev, 21*(11), 1322-1327. doi:10.1101/gad.424607

Lamar, E., Deblandre, G., Wettstein, D., Gawantka, V., Pollet, N., Niehrs, C., & Kintner, C. (2001). Nrarp is a novel intracellular component of the Notch signaling pathway. *Genes Dev, 15*(15), 1885-1899. doi:10.1101/gad.908101

Larrivee, B., Freitas, C., Trombe, M., Lv, X., Delafarge, B., Yuan, L., . . . Eichmann, A. (2007). Activation of the UNC5B receptor by Netrin-1 inhibits sprouting angiogenesis. *Genes Dev, 21*(19), 2433-2447. doi:10.1101/gad.437807

LeBon, L., Lee, T. V., Sprinzak, D., Jafar-Nejad, H., & Elowitz, M. B. (2014). Fringe proteins modulate Notch-ligand cis and trans interactions to specify signaling states. *Elife, 3*, e02950. doi:10.7554/eLife.02950

Lesiak, A. J., Brodsky, M., & Neumaier, J. F. (2015). RiboTag is a flexible tool for measuring the translational state of targeted cells in heterogeneous cell cultures. *Biotechniques, 58*(6), 308-317. doi:10.2144/000114299

Lever, J., Kryzwinski, M., & Altman, N. (2017). Principal component analysis. *Nature Methods,* 14,641-642

Li, J. L., Sainson, R. C., Shi, W., Leek, R., Harrington, L. S., Preusser, M., . . . Harris, A. L. (2007). Delta-like 4 Notch ligand regulates tumor angiogenesis, improves tumor vascular function, and promotes tumor growth in vivo. *Cancer Res, 67*(23), 11244-11253. doi:10.1158/0008-5472.CAN-07-0969

Liefke, R., Oswald, F., Alvarado, C., Ferres-Marco, D., Mittler, G., Rodriguez, P., . . . Borggrefe, T. (2010). Histone demethylase KDM5A is an integral part of the core Notch-RBP-J repressor complex. *Genes Dev, 24*(6), 590-601. doi:10.1101/gad.563210

Lin, X., Liu, B., Yang, X., Yue, X., Diao, L., Wang, J., & Chang, J. (2013). Genetic deletion of Rnd3 results in aqueductal stenosis leading to hydrocephalus through up-regulation of Notch signaling. *Proc Natl Acad Sci U S A, 110*(20), 8236-8241. doi:10.1073/pnas.1219995110

Lobov, I. B., Renard, R. A., Papadopoulos, N., Gale, N. W., Thurston, G., Yancopoulos, G. D., & Wiegand, S. J. (2007). Delta-like ligand 4 (Dll4) is induced by VEGF as a negative regulator of angiogenic sprouting. *Proc Natl Acad Sci U S A, 104*(9), 3219-3224. doi:10.1073/pnas.0611206104

Lu, X., Le Noble, F., Yuan, L., Jiang, Q., De Lafarge, B., Sugiyama, D., . . . Eichmann, A. (2004). The netrin receptor UNC5B mediates guidance events controlling morphogenesis of the vascular system. *Nature, 432*(7014), 179-186. doi:10.1038/nature03080

Mailhos, C., Modlich, U., Lewis, J., Harris, A., Bicknell, R., & Ish-Horowicz, D. (2001). Delta4, an endothelial specific notch ligand expressed at sites of physiological and tumor angiogenesis. *Differentiation, 69*(2-3), 135-144. doi:10.1046/j.1432-0436.2001.690207.x

Margolis, B., & Skolnik, E. Y. (1994). Activation of Ras by receptor tyrosine kinases. *J Am Soc Nephrol, 5*(6), 1288-1299.

McElhinny, A. S., Li, J. L., & Wu, L. (2008). Mastermind-like transcriptional co-activators: emerging roles in regulating cross talk among multiple signaling pathways. *Oncogene, 27*(38), 5138-5147. doi:10.1038/onc.2008.228

Mittal, K., Ebos, J., & Rini, B. (2014). Angiogenesis and the tumor microenvironment: vascular endothelial growth factor and beyond. *Semin Oncol, 41*(2), 235-251. doi:10.1053/j.seminoncol.2014.02.007

Mohr, O. L. (1919). Character Changes Caused by Mutation of an Entire Region of a Chromosome in Drosophila. *Genetics, 4*(3), 275-282.

Nagy, J. A., Chang, S. H., Dvorak, A. M., & Dvorak, H. F. (2009). Why are tumour blood vessels abnormal and why is it important to know? *Br J Cancer, 100*(6), 865-869. doi:10.1038/sj.bjc.6604929

Nakatsu, M. N., Davis, J., & Hughes, C. C. (2007). Optimized fibrin gel bead assay for the study of angiogenesis. *J Vis Exp*(3), 186. doi:10.3791/186

Nakatsu, M. N., & Hughes, C. C. (2008). An optimized three-dimensional in vitro model for the analysis of angiogenesis. *Methods Enzymol, 443*, 65-82. doi:10.1016/S0076-6879(08)02004-1

Nam, Y., Weng, A. P., Aster, J. C., & Blacklow, S. C. (2003). Structural requirements for assembly of the CSL.intracellular Notch1.Mastermind-like 1 transcriptional activation complex. *J Biol Chem, 278*(23), 21232-21239. doi:10.1074/jbc.M301567200

Niessen, K., Fu, Y., Chang, L., Hoodless, P. A., McFadden, D., & Karsan, A. (2008). Slug is a direct Notch target required for initiation of cardiac cushion cellularization. *J Cell Biol, 182*(2), 315-325. doi:10.1083/jcb.200710067

Nobes, C. D., Lauritzen, I., Mattei, M. G., Paris, S., Hall, A., & Chardin, P. (1998). A new member of the Rho family, Rnd1, promotes disassembly of actin filament structures and loss of cell adhesion. *J Cell Biol, 141*(1), 187-197.

Noguera-Troise, I., Daly, C., Papadopoulos, N. J., Coetzee, S., Boland, P., Gale, N. W., . . . Thurston, G. (2006). Blockade of Dll4 inhibits tumour growth by promoting non-productive angiogenesis. *Nature, 444*(7122), 1032-1037. doi:10.1038/nature05355

Okada, T., Sinha, S., Esposito, I., Schiavon, G., Lopez-Lago, M. A., Su, W., . . . Giancotti, F. G. (2015). The Rho GTPase Rnd1 suppresses mammary tumorigenesis and EMT by restraining Ras-MAPK signalling. *Nat Cell Biol, 17*(1), 81-94. doi:10.1038/ncb3082

Pacary, E., Heng, J., Azzarelli, R., Riou, P., Castro, D., Lebel-Potter, M., . . . Guillemot, F. (2011). Proneural transcription factors regulate different steps of cortical neuron migration through Rnd-mediated inhibition of RhoA signaling. *Neuron, 69*(6), 1069-1084. doi:10.1016/j.neuron.2011.02.018

Paez-Ribes, M., Allen, E., Hudock, J., Takeda, T., Okuyama, H., Vinals, F., . . . Casanovas, O. (2009). Antiangiogenic therapy elicits malignant progression of tumors to increased local invasion and distant metastasis. *Cancer Cell, 15*(3), 220-231. doi:10.1016/j.ccr.2009.01.027

Palomero, T., Lim, W. K., Odom, D. T., Sulis, M. L., Real, P. J., Margolin, A., . . . Ferrando, A. A. (2006). NOTCH1 directly regulates c-MYC and activates a feed-forward-loop transcriptional network promoting leukemic cell growth. *Proc Natl Acad Sci U S A, 103*(48), 18261-18266. doi:10.1073/pnas.0606108103

Palomero, T., McKenna, K., J, O. N., Galinsky, I., Stone, R., Suzukawa, K., . . . Ferrando, A. A. (2006). Activating mutations in NOTCH1 in acute myeloid leukemia and lineage switch leukemias. *Leukemia, 20*(11), 1963-1966. doi:10.1038/sj.leu.2404409

Patel, N. S., Li, J. L., Generali, D., Poulsom, R., Cranston, D. W., & Harris, A. L. (2005). Up-regulation of delta-like 4 ligand in human tumor vasculature and the role of basal expression in endothelial cell function. *Cancer Res, 65*(19), 8690-8697. doi:10.1158/0008-5472.CAN-05-1208

Pelton, J. C., Wright, C. E., Leitges, M., & Bautch, V. L. (2014). Multiple endothelial cells constitute the tip of developing blood vessels and polarize to promote lumen formation. *Development, 141*(21), 4121-4126. doi:10.1242/dev.110296

Penton, A. L., Leonard, L. D., & Spinner, N. B. (2012). Notch signaling in human development and disease. *Semin Cell Dev Biol, 23*(4), 450-457. doi:10.1016/j.semcdb.2012.01.010

Phng, L. K., Potente, M., Leslie, J. D., Babbage, J., Nyqvist, D., Lobov, I., . . . Gerhardt, H. (2009). Nrarp coordinates endothelial Notch and Wnt signaling to control vessel density in angiogenesis. *Dev Cell, 16*(1), 70-82. doi:10.1016/j.devcel.2008.12.009

Potente, M., Gerhardt, H., & Carmeliet, P. (2011). Basic and therapeutic aspects of angiogenesis. *Cell, 146*(6), 873-887. doi:10.1016/j.cell.2011.08.039

Rand, M. D., Grimm, L. M., Artavanis-Tsakonas, S., Patriub, V., Blacklow, S. C., Sklar, J., & Aster, J. C. (2000). Calcium depletion dissociates and activates heterodimeric notch receptors. *Mol Cell Biol, 20*(5), 1825-1835.

Redmond, L., & Ghosh, A. (2001). The role of Notch and Rho GTPase signaling in the control of dendritic development. *Curr Opin Neurobiol, 11*(1), 111-117.

Ridgway, J., Zhang, G., Wu, Y., Stawicki, S., Liang, W. C., Chanthery, Y., . . . Yan, M. (2006). Inhibition of Dll4 signalling inhibits tumour growth by deregulating angiogenesis. *Nature, 444*(7122), 1083-1087. doi:10.1038/nature05313

Riou, P., Villalonga, P., & Ridley, A. J. (2010). Rnd proteins: multifunctional regulators of the cytoskeleton and cell cycle progression. *Bioessays, 32*(11), 986-992. doi:10.1002/bies.201000060

Risau, W., & Flamme, I. (1995). Vasculogenesis. *Annu Rev Cell Dev Biol, 11*, 73-91. doi:10.1146/annurev.cb.11.110195.000445

Rojas, M., Yao, S., & Lin, Y. Z. (1996). Controlling epidermal growth factor (EGF)-stimulated Ras activation in intact cells by a cell-permeable peptide mimicking phosphorylated EGF receptor. *J Biol Chem, 271*(44), 27456-27461.

Ronchini, C., & Capobianco, A. J. (2001). Induction of cyclin D1 transcription and CDK2 activity by Notch(ic): implication for cell cycle disruption in transformation by Notch(ic). *Mol Cell Biol, 21*(17), 5925-5934.

Rosenbloom, K. R., Dreszer, T. R., Pheasant, M., Barber, G. P., Meyer, L. R., Pohl, A., . . . Kent, W. J. (2010). ENCODE whole-genome data in the UCSC Genome Browser. *Nucleic Acids Res, 38*(Database issue), D620-625. doi:10.1093/nar/gkp961

Ruhrberg, C., & Bautch, V. L. (2013). Neurovascular development and links to disease. *Cell Mol Life Sci, 70*(10), 1675-1684. doi:10.1007/s00018-013-1277-5

Sanz, E., Evanoff, R., Quintana, A., Evans, E., Miller, J. A., Ko, C., . . . McKnight, G. S. (2013). RiboTag analysis of actively translated mRNAs in Sertoli and Leydig cells in vivo. *PLoS One, 8*(6), e66179. doi:10.1371/journal.pone.0066179

Sanz, E., Yang, L., Su, T., Morris, D. R., McKnight, G. S., & Amieux, P. S. (2009). Cell-type-specific isolation of ribosome-associated mRNA from complex tissues. *Proc Natl Acad Sci U S A, 106*(33), 13939-13944. doi:10.1073/pnas.0907143106

Shawber, C. J., Funahashi, Y., Francisco, E., Vorontchikhina, M., Kitamura, Y., Stowell, S. A., . . . Kitajewski, J. (2007). Notch alters VEGF responsiveness in human and murine endothelial cells by direct regulation of VEGFR-3 expression. *J Clin Invest, 117*(11), 3369-3382. doi:10.1172/JCI24311

Shawber, C. J., & Kitajewski, J. (2004). Notch function in the vasculature: insights from zebrafish, mouse and man. *Bioessays, 26*(3), 225-234. doi:10.1002/bies.20004

Shaye, D. D., & Greenwald, I. (2002). Endocytosis-mediated downregulation of LIN-12/Notch upon Ras activation in Caenorhabditis elegans. *Nature, 420*(6916), 686-690. doi:10.1038/nature01234

Shigeoka, T., Jung, H., Jung, J., Turner-Bridger, B., Ohk, J., Lin, J. Q., . . . Holt, C. E. (2016). Dynamic Axonal Translation in Developing and Mature Visual Circuits. *Cell, 166*(1), 181-192. doi:10.1016/j.cell.2016.05.029

Shojaei, F., Wu, X., Malik, A. K., Zhong, C., Baldwin, M. E., Schanz, S., . . . Ferrara, N. (2007). Tumor refractoriness to anti-VEGF treatment is mediated by CD11b+Gr1+ myeloid cells. *Nat Biotechnol, 25*(8), 911-920. doi:10.1038/nbt1323

Suchting, S., & Eichmann, A. (2009). Jagged gives endothelial tip cells an edge. *Cell, 137*(6), 988-990. doi:10.1016/j.cell.2009.05.024

Suchting, S., Freitas, C., le Noble, F., Benedito, R., Breant, C., Duarte, A., & Eichmann, A. (2007). The Notch ligand Delta-like 4 negatively regulates endothelial tip cell formation and vessel branching. *Proc Natl Acad Sci U S A, 104*(9), 3225-3230. doi:10.1073/pnas.0611177104

Suehiro, J., Kanki, Y., Makihara, C., Schadler, K., Miura, M., Manabe, Y., . . . Minami, T. (2014). Genome-wide approaches reveal functional vascular endothelial growth factor (VEGF)-inducible nuclear factor of activated T cells (NFAT) c1 binding to

angiogenesis-related genes in the endothelium. *J Biol Chem, 289*(42), 29044-29059. doi:10.1074/jbc.M114.555235

Sundaram, M. V. (2005). The love-hate relationship between Ras and Notch. *Genes Dev, 19*(16), 1825-1839. doi:10.1101/gad.1330605

Sundlisaeter, E., Edelmann, R. J., Hol, J., Sponheim, J., Kuchler, A. M., Weiss, M., . . . Haraldsen, G. (2012). The alarmin IL-33 is a notch target in quiescent endothelial cells. *Am J Pathol, 181*(3), 1099-1111. doi:10.1016/j.ajpath.2012.06.003

Takai, Y., Sasaki, T., & Matozaki, T. (2001). Small GTP-binding proteins. *Physiol Rev, 81*(1), 153-208. doi:10.1152/physrev.2001.81.1.153

Tata, M., Ruhrberg, C., & Fantin, A. (2015). Vascularisation of the central nervous system. *Mech Dev, 138 Pt 1*, 26-36. doi:10.1016/j.mod.2015.07.001

Taylor, P. C. (2002). VEGF and imaging of vessels in rheumatoid arthritis. *Arthritis Res, 4 Suppl 3*, S99-107. doi:10.1186/ar582

Teodorczyk, M., & Schmidt, M. H. H. (2014). Notching on Cancer's Door: Notch Signaling in Brain Tumors. *Front Oncol, 4*, 341. doi:10.3389/fonc.2014.00341

Tung, J. J., Tattersall, I. W., & Kitajewski, J. (2012). Tips, stalks, tubes: notch-mediated cell fate determination and mechanisms of tubulogenesis during angiogenesis. *Cold Spring Harb Perspect Med, 2*(2), a006601. doi:10.1101/cshperspect.a006601

Udan, R. S., Culver, J. C., & Dickinson, M. E. (2013). Understanding vascular development. *Wiley Interdiscip Rev Dev Biol, 2*(3), 327-346. doi:10.1002/wdev.91

Varnum-Finney, B., Wu, L., Yu, M., Brashem-Stein, C., Staats, S., Flowers, D., . . . Bernstein, I. D. (2000). Immobilization of Notch ligand, Delta-1, is required for induction of notch signaling. *J Cell Sci, 113 Pt 23*, 4313-4318.

Vasudevan, A., Long, J. E., Crandall, J. E., Rubenstein, J. L., & Bhide, P. G. (2008). Compartment-specific transcription factors orchestrate angiogenesis gradients in the embryonic brain. *Nat Neurosci, 11*(4), 429-439. doi:10.1038/nn2074

Walchli, T., Mateos, J. M., Weinman, O., Babic, D., Regli, L., Hoerstrup, S. P., . . . Vogel, J. (2015). Quantitative assessment of angiogenesis, perfused blood vessels and endothelial tip cells in the postnatal mouse brain. *Nat Protoc, 10*(1), 53-74. doi:10.1038/nprot.2015.002

Wang, H., Zang, C., Taing, L., Arnett, K. L., Wong, Y. J., Pear, W. S., . . . Aster, J. C. (2014). NOTCH1-RBPJ complexes drive target gene expression through dynamic interactions with superenhancers. *Proc Natl Acad Sci U S A, 111*(2), 705-710. doi:10.1073/pnas.1315023111

Wang, H., Zou, J., Zhao, B., Johannsen, E., Ashworth, T., Wong, H., . . . Aster, J. C. (2011). Genome-wide analysis reveals conserved and divergent features of Notch1/RBPJ binding in human and murine T-lymphoblastic leukemia cells. *Proc Natl Acad Sci U S A, 108*(36), 14908-14913. doi:10.1073/pnas.1109023108

Weis, S. M., & Cheresh, D. A. (2011). Tumor angiogenesis: molecular pathways and therapeutic targets. *Nat Med, 17*(11), 1359-1370. doi:10.1038/nm.2537

Weng, A. P., Millholland, J. M., Yashiro-Ohtani, Y., Arcangeli, M. L., Lau, A., Wai, C., . . . Aster, J. C. (2006). c-Myc is an important direct target of Notch1 in T-cell acute lymphoblastic leukemia/lymphoma. *Genes Dev, 20*(15), 2096-2109. doi:10.1101/gad.1450406

Wennerberg, K., Forget, M. A., Ellerbroek, S. M., Arthur, W. T., Burridge, K., Settleman, J., . . . Hansen, S. H. (2003). Rnd proteins function as RhoA antagonists by activating p190 RhoGAP. *Curr Biol, 13*(13), 1106-1115.

Woltje, K., Jabs, M., & Fischer, A. (2015). Serum induces transcription of Hey1 and Hey2 genes by Alk1 but not Notch signaling in endothelial cells. *PLoS One, 10*(3), e0120547. doi:10.1371/journal.pone.0120547

Wunnenberg-Stapleton, K., Blitz, I. L., Hashimoto, C., & Cho, K. W. (1999). Involvement of the small GTPases XRhoA and XRnd1 in cell adhesion and head formation in early Xenopus development. *Development, 126*(23), 5339-5351.

Yamamoto, N., Kosaka, H., Higashino, K., Morimoto, M., Yamashita, K., Tezuka, F., . . . Sairyo, K. (2018). Vertebral Lateral Notch as Optimal Entry Point for Lateral Mass Screwing Using Modified Roy-Camille Technique. *Asian Spine J, 12*(2), 272-276. doi:10.4184/asj.2018.12.2.272

Yan, M., Callahan, C. A., Beyer, J. C., Allamneni, K. P., Zhang, G., Ridgway, J. B., . . . Plowman, G. D. (2010). Chronic DLL4 blockade induces vascular neoplasms. *Nature, 463*(7282), E6-7. doi:10.1038/nature08751

Ye, X., Wang, Y., Cahill, H., Yu, M., Badea, T. C., Smallwood, P. M., . . . Nathans, J. (2009). Norrin, frizzled-4, and Lrp5 signaling in endothelial cells controls a genetic program for retinal vascularization. *Cell, 139*(2), 285-298. doi:10.1016/j.cell.2009.07.047

Yoshiura, S., Ohtsuka, T., Takenaka, Y., Nagahara, H., Yoshikawa, K., & Kageyama, R. (2007). Ultradian oscillations of Stat, Smad, and Hes1 expression in response to serum. *Proc Natl Acad Sci U S A, 104*(27), 11292-11297. doi:10.1073/pnas.0701837104

Zarkada, G., Heinolainen, K., Makinen, T., Kubota, Y., & Alitalo, K. (2015). VEGFR3 does not sustain retinal angiogenesis without VEGFR2. *Proc Natl Acad Sci U S A, 112*(3), 761-766. doi:10.1073/pnas.1423278112

Zhou, P., Zhang, Y., Ma, Q., Gu, F., Day, D. S., He, A., . . . Pu, W. T. (2013). Interrogating translational efficiency and lineage-specific transcriptomes using ribosome affinity purification. *Proc Natl Acad Sci U S A, 110*(38), 15395-15400. doi:10.1073/pnas.1304124110

Zhu, Z., Todorova, K., Lee, K. K., Wang, J., Kwon, E., Kehayov, I., . . . Mandinova, A. (2014). Small GTPase RhoE/Rnd3 is a critical regulator of Notch1 signaling. *Cancer Res, 74*(7), 2082-2093. doi:10.1158/0008-5472.CAN-12-0452

Ziyad, S., & Iruela-Arispe, M. L. (2011). Molecular mechanisms of tumor angiogenesis. *Genes Cancer, 2*(12), 1085-1096. doi:10.1177/1947601911432334

Zygmunt, M., Herr, F., Munstedt, K., Lang, U., & Liang, O. D. (2003). Angiogenesis and vasculogenesis in pregnancy. *Eur J Obstet Gynecol Reprod Biol, 110 Suppl 1*, S10-18.